Distribution of endogenous lipoproteins and sulfated proteoglycans in normal rabbit aorta and in atherosclerotic lesions induced by endothelial injury

by
Zorina S. Galis
Department of Pathology
McGill University
Montreal

A Thesis submitted to the Faculty of Graduate Studies and Research
in partial fulfilment of the requirements of the degree of
Doctor of Philosophy

ABSTRACT

The effects of an endothelial injury, produced by balloon catheterization of the aorta in normocholesterolemic rabbits, were studied by immunocytochemical and biochemical methods. Apolipoprotein B (apo B), as a marker for endogenous lipoproteins (LP), was detected by quantitative gold immunocytochemistry. In contrast to normal aortas, where apo B distribution was limited to the innermost regions, in previously injured aortas, apo B accumulated in advanced lesions developed under the regenerated endothelium, both in the extracellular space and inside foam cells, demonstrating the atherosclerotic nature of the lesions. In order to establish the putative role of chondroitin sulfate (CS) proteoglycans (PG), known for their great in vitro affinity for LP, the overall and ultrastructural distribution, as well as the biochemical properties of CS-PG molecules extracted from normal and injured aortas were examined. These analyses jointly suggested that the characteristic preferential distribution of large interstitial CS-PG in the intima of aorta could create a favorable environment for an increased interaction with the apo B-containing LP. By double immunocytochemistry, the frequent co-localization of apo B and CS-PG in the lesions, suggested that CS-PG might sequester LP and contribute to the formation of foam cells. Injury to the aortic endothelium can trigger the development of vascular lesions that contain the features of the human atherosclerotic lesions, including deposits of lipid derived from plasma LP, in normocholesterolemic conditions. The aortic sulfated PG appear to make an important contribution in the formation of apo B accumulation in injured arterial tissue.

ABREGÉ

Le projet concerne l'étude du rôle qu'une lésion de l'endothélium vasculaire peut jouer dans le développement de lésions athéromateuses. Les lésions sont obtenues expérimentalement chez le lapin suite à la cathéterisation de l'aorte. La distribution des lipoprotéines (LP) endogènes considérées athérogènes, detectées par un anticorps qui reconnaît l'apolipoprotéine B (apo B) de lapin, a été étudiée par immunocytochimie ultrastructurelle quantitative à l'or colloidal, dans des tissus provenant des aortes normales ou lésées. Dans les aortes normales, la distribution de l'apo B est restreinte à la couche endothéliale. Par contraste, dans les aortes lésées l'apo B est accumulée dans les lésions développées sous l'endothélium régénéré, autant dans l'espace intercellulaire que dans les cellules, confirmant leur nature athéromateuse. Les caractéristiques biochimiques et morphologiques des protéoglycanes (PG) contenant des chaînes de sulfate de chondroitine, qui interagissent avec grande affinité avec LP in vitro, et on suppose par conséquent qu'ils soient aussi responsables de leur immobilisation dans les lésions athéromateuses, ont été analysées dans des tissus provenant des aortes normales ou lésées. La distribution préférentielle de ce type de PG dans l'intima de l'aorte, influence sûrement les propriétés régionales de sa matrice extracellulaire, et est de nature à exagérer l'interaction avec les LP, conduisant à leur accumulation dans cette région. L'immunocytochimie en double marquage a révélé une intime relation entre l'apo B endogène et les PG contenant du sulfate de chondroitine dans les aortes lésées, qui suggère que les PG soient responsables de la séquestration de LP et la formation de cellules burées de lipide dans les lésions athéromateuses. L'altération de l'endothélium peut initier le développement des lésions qui contiennent les caractéristiques des plaques athéromateuses humaines, incluant l'accumulation des lipides provenant de LP sériques, même en présence de leur niveaux normaux. Les PG contenant du sulfate de chondroitine peuvent jouer un rôle important dans ce processus.

Abbreviations

Apo B = apolipoprotein B

CS = chondroitin sulfate

DS = dermatan sulfate

EC = endothelial cells

EM = electron microscope

GAG = glycosaminoglycan

HS = heparan sulfate

LM = light microscope

LP = lipoproteins

PG = proteoglycan(s)

SMC = smooth muscle cells

PROLOGUE

Strategy of research

This thesis is part of the interest, demonstrated over the years by the laboratory that I have joined for my PhD training in Pathology, in the role that proteoglycans might play in the development of the aortic lesions triggered by endothelial injury. The experimental, mechanical injury was induced using a balloon catheter for the selective deendothelialization of normocholesterolemic rabbit aorta.

I proposed to start my program by assessing the atherosclerotic nature of this type of vascular lesions. Since currently, a significant vascular accumulation of endogenous lipoproteins (LP) is considered to represent a hallmark of the atherosclerotic lesion, the detection of the endogenous apolipoprotein B (apo B), as a marker for native LP in injured aortas, was chosen. The long term effect that the injury had upon the normal aortic distribution of endogenous apo B was investigated by immunocytochemistry in normal, and balloon catheter-injured rabbit aortas. Several earlier studies have shown that the extracellular sulfated PG, particularly chondroitin sulfate (CS)-PG, have a high in vitro affinity for LP, and the fact that monocytes incubated in vitro with LP-PG complexes transform into foam cells. Consequently, it was inferred that the aortic PG could be involved in the in vivo sequestration and accumulation of LP in the atherosclerotic lesions. Therefore, I proceeded by investigating the distribution of sulfated PG within normal and injured aortas by immunocytochemical and biochemical methods. Finally, the in situ relation between the endogenous apo B and aortic CS-PG in the injured aortas was explored. These were detected in the lesions developed as a result of endothelial injury by double immunofluorescence and post-embedding immunocytochemistry using two sizes of colloidal gold conjugates.

Rationale of presentation

The candidate has the option of including as part of the thesis the text, or duplicated published text of an original paper or papers. I have chosen this option and I am required to include in the thesis the following regulations:

"- Manuscript-style theses must conform to all other requirements explained in the Guidelines Concerning Thesis Preparation
- Additional material (procedural and design data as well as description of equipment) must be provided in sufficient detail (eg. in appendices) to allow clear and precise judgement to be made of the importance and originality of the research reported.
- The thesis should be more than a mere collection of manuscripts published or to be published. It must include a general abstract, a full introduction and literature review and a final overall conclusion. Connecting texts which provide logical bridges between different manuscripts are usually desirable in the interest of cohesion. It is acceptable for these theses to include, as chapters, authentic copies of papers already published, provided these are duplicated clearly and bound as an integral part of the thesis. In such instances, connecting texts are mandatory and supplementary explanatory material is always necessary.
- While the inclusion of manuscripts co-authored by the candidate and others is acceptable, the candidate is required to make an explicit statement in the thesis of who contributed to such work and to what extent, and supervisors must attest to the accuracy of the claims at the Ph. D. Oral Defence. Since the task of the Examiners is made more difficult in these cases, it is in the candidate's interest to make the responsabilities of authors perfectly clear."

The following parts of this thesis have been previously submitted for publication, and were included as such:

Chapter 2: Distribution of endogenous apoprotein B-containing lipoproteins in normal and injured aortas of normocholesterolemic rabbits. (Galis et al., in press, Lab. Invest., may 1992).

Chapter 3: In situ ultrastructural characterization of chondroitin sulfate proteoglycans in normal rabbit aorta. (Galis et al., 1992, J Histochem Cytochem 40:251-263).

Chapter 5: Selective extraction and alternative glycosaminoglycan moiety analysis of the sulfated proteoglycans synthesized by rabbit aorta (Galis et al., in press, Anal Biochem).

Other chapters are in preparation for publication, and for uniformity have been presented in a similar independent form. Each has its own introduction, conclusions and references directly pertaining to the subject treated in detail in the respective section. A concise general introduction was also added, which for obvious reasons, did not attempt to review the huge amount of literature about various aspects of atherogenesis, but rather

aimed to correlate the subjects studied. Finally, the conclusions of various chapters were integrated at the end of the thesis. The present format was thought to facilitate the reading, although some overlap was inevitably created by this arrangement.

The experiments described in this thesis did not reproduce earlier works and represent original contributions to the field of atherosclerosis research. At the beginnning of my program I proposed the issues to be studied in my project and the experimental strategy to be employed. The work contained in this thesis was possible due to the colaboration with several people.

Dr. Sean Moore, my supervisor, has intially pointed out the most relevant aspects related to this model of atherosclerosis and afterwards has frequently discussed the results of my experiments. He also has looked at the histological specimens with me and guided my interpretation of the specimens.

Dr. Misbahuddin Alavi offered some advice regarding methods for glycosaminoglycan and lipoprotein isolation. He also provided me with a lot of literature on the subject and helped to get me integrated into the larger project that is under study in the lab.

Dr. Lucian Ghitescu from Départament d' Anatomie, Université de Montreal, has provided the protein A-gold probe and has taught me the technique of low temperature embedding for which I was allowed to use the facilities in their department. Together with him and Dr. Bendayan, form the same department, I have often discussed the problems related to electron microscope gold immunocytochemistry.

Dr. Zhihe Li has instructed me in the procedure of balloon catheterization and also assisted me with the surgical procedures.

I consider that the most important original aspects contained in this thesis are:
1. Although there have been several immunocytochemical studies on the distribution of endogenous lipoproteins, it is the first time that apolipoprotein B has been visualized at the ultrastructural level in normal aorta. The quantification of this distribution was also made for the first time.

2. The study on injured aortas has shown that endogenous lipoproteins accumulate solely as an effect of injury, and are not necessarily related to high levels of circulating LP.

3. CS-PG were detected for the first time by electron microscope immunocytochemistry using an antibody recognizing the saccaridic chains, and several cathegories of these molecules have been described in this thesis.

4. I have proposed a new method for the extraction and characterization of sulfated proteoglycans from aorta.

5. The changes in CS-PG as a result of endothelial injury were studied by ultrastructural post-embedding immunocytochemistry, a method that preserves their morphology very well.

6. The relationship between apoliprotein B and chondroitin sulfate proteoglycans was detected for the first time in situ, by double immunocytochemistry.

ACKNOWLEDGEMENTS

I wish to thank my supervisor, Dr. Sean Moore, who has recognized many years ago the importance of endothelial injury in the development of the vascular lesions, for giving me the opportunity to become acquainted with this model, and for guiding my efforts to investigate such an interesting hypothesis regarding atherogenesis. Thanks are due to the other members of the team, Dr. Misbahuddin Z. Alavi for his unrestricted, friendly support, and Dr. Zhihe Li for invaluable help with the surgical procedure of balloon catheterization. Drs. Moise Bendayan and Lucian Ghitescu, from the Departement d'Anatomie, Université de Montréal, generously allowed "the competition" to fully benefit from their extensive experience in gold immunocytochemistry. Several other people offered me kind advice: Drs. Serge Jothy, Istvan Huttner, and Edith Zorychta form the Department of Pathology, and Dr. James Hanley from the Department of Epidemiology and Biostatistics, McGill. The excellent help of Leng Tsao for microtomy, and Robert Sawka and Noemi Sebastiao for frozen section immunocytochemistry, deserves acknowledgement.

Last, but not least, I would like to thank my family for their understanding, especially my son, who was deprived of many hours of undivided attention, and I truly hope that with time, he will evolve from appreciating solely the length of this thesis, to what it represents in fact.

Table of contents

CHAPTER 1

INTRODUCTION

Atherogenesis is a puzzle over which pathologists have never ceased to be perplexed... There have been certain moments when some decided that it was the time to take a break and formulate the solution, but years have passed by, and we are still investigating it.

It so happens that some years after the publication of several exhaustive hypotheses regarding atherogenesis, this thesis and many others still are trying to add a few pieces to the great puzzle. Not everybody who lives long enough would be affected by cancer, but quite surely she/he would suffer from complications of atherosclerosis. The concepts regarding atherosclerosis have evolved from early descriptions of one main cause triggering a nicely ordered succession of events, to complicated plots in which various elements could conceivably act either as initiators, or effectors; and the hypotheses that place emphasis on endothelial injury or dysfunction (Gimbrone, 1986), caused by a wide variety of factors ranging from increased rate of cell death, hydrodynamic stress, viral infection, mechanical injury, and even hypercholesterolemia, have lately gained ground (Munro and Cotran, 1988; Haust, 1989; Battergay et al., 1990; Hajjar, 1991; Ross, 1991). Among them, the lipoproteins (LP) and the proteoglycans (PG) are a famous duo never quite caught in the act. There are of course, several good reasons which entitle the investigators to question the role of each of them, and of their relationship in the larger picture of atherosclerotic lesion development.

The LP containing apolipoprotein B (apo B), i.e. VLDL, IDL, LDL, and Lp(a), are considered atherogenic (Steinberg, 1987; Editorial, 1988). Their involvement in atherosclerosis has received serious support from many clinical observations and from experimental models. The discovery of the genetic deficiency affecting the LP receptor (Goldstein and Brown, 1974), leading to severe hyperlipoproteinemia and early atherosclerosis, has been a corner stone in atherosclerosis research. However, as opposed to the well characterized fibroblast receptor for apo B, it is interesting to note that the physiological mechanism by which plasma LP containing apo B enter the aortic wall is

still under investigation.

Many mass studies have related high levels of circulating LP to cardiovascular diseases secondary to atherosclerosis (Averbook et al., 1989; Zemel and Sowers, 1990; Stampfer et al., 1991). The accumulation of endogenous apo B, as a marker for LP, in human vascular lesions has been repeatedly described (Hoff et al, 1978; Bocan et al., 1988; Shekhonin et al., 1990; Smith, 1990), and has come to be regarded as a hallmark of atherosclerosis.

Several experimental models of atherosclerosis, in which hypercholesterolemia has been induced in various animal species by high cholesterol feeding, have been developed (White, ed., 1989). While in many animals a hypercholesterolemic diet inevitably raises the level of plasma cholesterol and determines the deposition of lipid in numerous organs, including blood vessels (Anitschkov and Chalatow, 1913; Altschul, 1950, McMillan et al., 1954), in humans, the relation between dietary habits, hypercholesterolemia and atherosclerosis is still controversial (Malenka and Baron, 1988; Palumbo, 1989; Stebhens, 1991). The aortic lesions that develop in the hypercholesterolemic models are composed almost entirely of lipid laden macrophages and reproduce the morphology of lesions found in individuals suffering from homozygous familial hypercholesterolemia.

In the experiments described further, a different type of vascular lesion was experimentally induced. The aortas of normocholesterolemic rabbits have been injured by selective deendothelialization with a balloon catheter, and then allowed to regenerate. Endothelial injury triggers healing of the aorta, which is in fact the final picture of an incredibly large spectrum of interconnected processes. As a consequence, in contrast with the rather simple morphology of the lesions induced in animals by hypercholesterolemia, in the injury model, the lesions consist of numerous smooth muscle cells (SMC), abundant extracellular matrix, inflammatory cells, calcification, extracellular and intracellular lipid (Moore, 1981), and therefore bear more resemblance to human atherosclerotic lesions. Interestingly enough, this type of endothelial injury determines the appearance of atherosclerosis-like lesions in species, such as rats, which are resistant to aggressive hypercholesterolemic diets.

The updated version of the "response-to-injury" hypothesis, regarding the

development of the atherosclerotic lesions, includes rounds of migratory and proliferative events involving inflammatory cells, especially monocytes/macrophages, and of the vascular SMC (Ross, 1991). All these cells are thought to participate actively in interactions inside the aortic wall, but the endothelium seems to play a key role by mediating the interactions of the blood vessel with the blood-borne cells (Gimbrone, 1981; Bevilacqua et al., 1987), and by regulating the proliferation of SMC (Clowes and Clowes, 1989).

In vivo, after the balloon catheterization of aorta in different species, the endothelium that regenerates has a different morphology (Huttner et al., 1985). The metabolism of the entire aortic wall covered by regenerated endothelium is modified (Hajjar et al., 1981). The lesions re-covered by endothelium show larger intimal thickening (Williams, 1991) than adjacent regions lacking an endothelial layer. Rabbit aortas injured by balloon catheterization synthesize altered patterns of GAG compositions (Alavi and Moore, 1985), and lipid accumulates without any dietary supplement (Moore, 1989). Other types of arterial injury have been described to have similar effects (Moore, 1967; Moore and Richardson, 1985; Richardson et al., 1989). In injured aortas, the correlation between the presence of a regenerated endothelium, an increased concentration of aortic PG, and the preferential development of lipid deposition, implies the existence of a close relationship between them. Many of these effects are likely to be modulated by the interaction between the endothelium and other vascular cells. It is known that the endothelial cells (EC) influence the proliferation and metabolism of SMC both in vitro, and in vivo (Clowes and Karnovsky, 1979; Karnovsky, 1981; Huttner et al., 1989; Campbell et al., 1990), and this relation takes new dimensions in pathologic conditions (Davies, 1986; Reidy, 1989).

EC injured by mechanical disruption release growth factors (Klagsbrun and Edelman, 1989; McNeil et al., 1989). As compared to the persistently deendothelialized regions, the areas covered by regenerated endothelium internalize and retain, over short time intervals, increased amounts of exogenous radiolabelled LP (Alavi et al., 1983; Falcone et al., 1984).

Further, it was found that, the endothelial injury produced by catheterization,

would worsen the accumulation of lipid in hypercholesterolemic animals (Minick, 1981). Initially, metabolic differences in the neointima have been proposed as the cause for the lipid accumulation in the regions covered by regenerated endothelium (Day et al., 1974; Hajjar et al., 1980).

The greatest support is currently received by the hypothesis that the lipid accumulates in injured aorta as a result of a direct sequestration of plasma LP, as seems to be the case with human atherosclerotic lesions. However, the presence of endogenous LP has not been demonstrated before in injured aortas.

Therefore, the first question that was investigated in the present project was whether atherosclerosis-like accumulations of endogenous apo B could occur solely as a result of the injury, i.e. in the conditions of normal levels of plasma LP. In addition to answering the basic question regarding the atherosclerotic nature of the catheter injury-induced lesions, by comparing the distribution of endogenous apo B in normal and injured aortas, it was possible to assess the sites most affected by the injury. The detection of apo B by ultrastructural immunocytochemistry allowed the visualization of its in situ interaction with the cells and the extracellular matrix of the aortic wall. In conjunction with a quantitative analysis of the labelling over various vascular compartments in different types of normal and injured aortic tissue, the factors that might contribute to the previously reported morphological differences, were revealed.

Early observations suggested that extracellular factors might be directly involved in the accumulation of LP in the atherosclerotic lesions (Duff, 1935), and the aortic sulfated proteoglycans (PG) appear to be major candidates (Berenson et al., 1985). Indeed, from the amorphous "ground substance" of the extracellular space, these molecules have finally emerged as playing key roles in essential physiological processes, such as cell regulation (Wight et al., 1989) and interaction with components of the interstitial matrix (Saunders and Bernfield, 1988), the synthesis and assembly of the extracellular matrix (Hamati et al., 1989; Ruoslahti, 1988), and cell migration (Kinsella and Wight, 1986).

The known members of the large PG family are numerous (Heinegard et al., 1985), and their number has continued to increase. This is partially explained by the

rather loose classification which assigns to this group, any protein that possesses glycosaminoglycan (GAG) moieties as side chains. As a result, miscellaneous molecules such as the large interstitial molecules of cartilage, a TGFß receptor, collagen type IX, the molecules of the neutrophil granules, are all PG.

The vascular sulfated PG have been classified into three main groups according to their preponderant type of saccharidic moieties. Although representing a small percentage of the total mass of the aortic tissue (2 - 5%) (Wight, 1989), they have been recently recognized as the main extracellular component of the normal aortic intima (Stary et al., 1992). Arterial PG received special attention due to their putative contribution in maintaining the viscoelastic, permeability, and thromboresistant properties of the arterial wall (Wight, 1989). Distinct classes of PG are synthesized in vitro by the cellular components of the arterial wall: endothelial cells produce mostly heparan sulfate (HS) PG, while smooth muscle cells and monocytes predominantly synthesize chondroitin sulfate (CS) PG, but the exact spectrum of PG molecules varies depending on the cell phenotype (Uhlin-Hansen et al., 1989; Merrilees et al., 1990) and the culture conditions (Vijayagopal et al., 1988).

Most important for the exercise of their functions and interactions, are their negatively charged, unbranched side GAG chains. This explains why, in the great majority of the early studies, the GAG were the focus of interest (Iverius, 1972, 1973; Srinivasan et al., 1972; Toledo and Mourao, 1980, Trelstad, 1985), and the relatively late recognition of the whole PG molecules, as the genuine components of the extracellular matrix. In one of these early studies, Iverius (1972) formulated the possible role that GAG could play in atherosclerosis. Srinivasan et al. (1972) reported the isolation of complexes containing LP and CS from the fatty streaks of human aorta. Toledo and Mourao (1980) have concluded, after investigating several species, that a high content of chondroitin-6-sulfate of aorta would favour vascular lipid deposition. The content in CS increases in human coronaries with age, and the aortic content is well correlated with the content in apo B (Yla-Herttuala et al., 1986, 1987). In experimental atherosclerosis, both hypercholesterolemia and endothelial injury reportedly increase the total content, and modify the GAG composition of the aorta (Alavi and Moore, 1985).

Many other pieces of evidence have accumulated since, showing that PG molecules containing sulfated moieties, interact in vitro with great affinity with the apo B-containing LP (Mourao et al., 1981; Radhakrishnamurthy et al., 1982; Camejo et al., 1983; Steele et al., 1987). The affinity of aortic PG for plasma LP was even proposed to be considered as an additional risk factor for atherosclerosis (Camejo et al., 1980). The interaction between these molecules is supposedly due to the ionic interaction between the anionic sulfated residues of the GAG moieties and the cationic amino acids of apo B. Several sulfated PG have been shown to bind apo B (Mourao and Bracamonte, 1984; Srinivasan et al., 1986), but the PG containing CS moieties were found to have the highest affinity for apo B-containing LP (Camejo et al., 1983). Although the LP binding is mediated through the GAG side chains of the PG molecules, the rest of the molecule is thought to be important as well, since the removal of the protein core was shown to inhibit the precipitation of LP (Vijayagopal et al., 1981; Steele et al., 1987).

A soluble fraction enriched in PG, extracted from the areas covered by regenerated endothelium in the balloon catheter-injured rabbit aorta, binds homologous normocholesterolemic LP with higher affinity than a matched preparation of normal rabbit aorta (Alavi et al., 1989). This effect was exacerbated when the aortic extracts were incubated in vitro with hypercholesterolemic LP (Alavi et al., 1991).

Previous in vitro experiments suggested that the aortic PG might be also involved in the process of foam cell formation. The macrophages are considered to be an important constituent of the atherosclerotic lesions, and together with SMC, to be the precursors of foam cells (Rosenfeld and Ross, 1990). Using a heterologous in vitro system, in which previously formed PG-LP complexes were fed to monocytes, Salisbury et al. (1985) reported that these were capable of inducing the formation of foam cells in culture. They hypothesized that the negative charge of the GAG moieties induced a non-specific pinocytosis, and recognized that this would be a plausible physiologic model of in vivo LP modification inside the arterial wall. Vijayagopal et al. (1985) also described the same phenomenon, but in contrast with the former group, they recently maintained (Vijayagopal et al., 1991) that pinocytosis was a minor pathway for the internalization of the LP-PG complexes. They presented new data suggesting that a receptor, distinct

from the acetylated-LDL receptor (Brown and Goldstein, 1983), might be involved in the transformation of macrophages into foam cells by LP-PG complexes. The recently described Lp(a) is not typically recognized by peritoneal macrophages, but if complexed with aortic PG, is avidly taken up, and determines values of cholesterol esterification higher than acetylated LDL (Kostner, 1989).

The vascular sulfated PG were also visualized in previous histochemical and immunohistochemical studies of human arteries, or of experimentally-induced lesions. Various dyes, that interact with the negatively charged GAG chains of the PG molecules, have been frequently used in combination with special enzymatic treatments in order to distinguish different sulfated GAG and map their distribution on light or electron microscope (Wight and Ross, 1975; Moore and Richardson, 1985; Scott, 1985; Volker et al.,1987). In general, the large chondroitinase-sensitive particles were found mostly in the "soluble" extracellular matrix, while the smaller granules, of which some were interpreted as representing dermatan sulfate, were detected in the company of collagen, and those presumably representing heparan sulfate, associated with the surface of vascular cells and elastin. The effect of injury upon the distribution of the sulfated PG in rabbit aorta was previously investigated on EM, using Ruthenium red for their staining (Richardson et al., 1989). Different antibodies were used to detect the distribution of certain vascular PG (Wight, 1989).

Taking into account that no single PG was undoubtedly recognized to be associated with the atherosclerotic lesions, while there is a rather general consensus to implicate the CS moieties as the most important partner in the interaction with LP, I decided to use an antibody which specifically recognizes these GAG chains, irrespective of the PG protein core, and study their in situ distribution in normal and injured aortas. This approach, supported also by biochemical analyses, supplied interesting data, illustrating the contribution of CS-PG to the local variations in the properties of the aortic extracellular matrix, likely pertaining to the special pathology of the aortic intima.

REFERENCES

Alavi, M.Z., Galis, Z., Li, Z., and Moore, S. (1991). Dietary alterations of plasma lipoproteins influence their interactions with proteoglycan enriched extracts from neointima of normal and injured aorta of rabbit. Clin Invest Med, 14:419-431.

Alavi, M.Z., Richardson, M., and Moore, S. (1989). The in vitro interactions between serum lipoproteins and proteoglycans of the neointima of rabbit aorta after a single balloon catheter injury. Am J Pathol, 134:287-292.

Alavi, M.Z., and Moore, S. (1985). Glycosaminoglycan composition and biosynthesis in the endothelium-covered neointima of de-endothelialized rabbit aorta. Exp Mol Pathol, 42:389-400.

Alavi M.Z., Dunnett, C.W., and Moore, S. (1983). Lipid composition of rabbit aortic wall following removal of endothelium by balloon catheter. Arteriosclerosis, 3:413-419.

Anitschkov, N., and Chalatow, S. (1913, translated version 1983). On experimental cholesterin steatosis and its significance in the origin of some pathological processes. Arteriosclerosis, 3:178-182.

Altschul, R. (1950). Selected studies on atherosclerosis. Springfield, Illinois, Charles C. Thomas Publ.

Averbook, A., Wilson S.E., and White, G.H. (1989). Epidemiology and anatomic distribution of atherosclerosis in man. In: White, R.W. (ed), Atherosclerosis and arteriosclerosis: human pathology and experimental animal methods and models. CRC Press, Inc., Boca Raton, Florida, pp. 17-49.

Battergay, E.J., Raines, E.W., Seifert, R.A., Bowen-Pope, D.F., and Ross, R. (1990). TGFß induces bimodal proliferation of connective tissue via complex control of an autocrine PDGF loop. Cell, 63:515-524.

Berenson GS, Radhakrishnamurthy B, Srinivasan SR, Vijayagopal P, Dalferes ER: Proteoglycans and potential mechanisms related to atherosclerosis. Am NY Acad Sci 454:69, 1985.

Berenson,G.S., Radhakrisnamurthy, B., Dalferes, E.R., Srinivasan, S.R. (1971). Carbohydrate macromolecules and atherosclerosis. Hum Pathol, 2:57-79.

Bevilacqua, M.P., Pober, J.S., Mendrick, D.L., Cotran, R.S., and Gimbrone, M.A. (1987). Identification of an inducible endothelial-leukocyte adhesion molecule. Proc Natl Acad Sci USA, 84:9238-9242.

Bihari-Varga, M., Gergely, J., and Gero, S. (1964). further investigations on complex formation in vitro between aortic mucopolysaccharides and ß-lipoproteins. J Atheroscl Res, 4:106-109.

Bocan, T.M.A., Brown, S.A., and Guyton, J.R. (1988). Human aortic fibrolipid lesions. Immunochemical localization of apolipoprotein B and apolipoprotein A. Arteriosclerosis, 8:499-508.

Brown, M.S., and Goldstein, J.L. (1983). Lipoprotein metabolism in the macrophages: Implications for cholesterol deposition in atherosclerosis. Ann Rev Biochem, 52:223-261.

Campbell, J.H., Horrigan, S., Merrilees, M., Campbell, G.R. (1990). Endothelial-smooth muscle cell interactions. In: Interactions between endothelium and other vascular structures and their abnormalities in diabetes. In: Molinati,G.M., Bar, R.S., Belfiore, F., and Porta, M. (eds.). Endothelial cell function in diabetic microangiopathy: Problems in

methodology and clinical aspects. Front Diabetes, Basel, Karger, 9, pp 108-117.

Campbell, G.R., Campbell, J.H., Manderson, J.A., Horrigan, S., and Rennick, R.E. (1988). Arterial smooth muscle. A multifunctional mesenchymal cell. Arch Pathol Lab Med, 112:977-086.

Camejo, G., Ponce, E., Lopez, F., Starosta, R., Hurt, E., and Romano, M. (1983). Partial structure of the active moiety of a lipoprotein complexing proteoglycan form human aorta. Atherosclerosis, 49:241-254.

Camejo, G., Lopez, A., Vegas, H., and Paoli, H. (1975). The participation of aortic proteins in the formation of complexes between low density lipoproteins and intima-media extracts. Atherosclerosis, 21:77-91.

Clowes, A.W., and Clowes, M.M. (1989). Inhibition of smooth muscle proliferation by heparin molecules. Transpl Proc, 21:3700-3701.

Clowes, A.W., and Karnovsky, M. (1977). Suppression by heparin of smooth muscle cell proliferation in injured arteries. Nature, 265:625-626.

Davies, P.F. (1986). Vascular cell interactions with special reference to the pathogenesis of atherosclerosis. Lab Invest, 55:5-24.

Day, A.J., Bell, F.P., Moore, S., and Friedman, R. (1974). Lipid composition and metabolism of thromboatherosclerotic lesions produced by continued endothelial damage in normal rabbits. Circ Res, 34:467-480.

Duff, L. (1935). Experimental cholesterol atherosclerosis and its relationship to human atherosclerosis. Arch Pathol Lab Med, 20:80-124, 259-304.

Editorial. (1988). Apolipoprotein-B and atherogenesis. Lancet, may 21:1141-1142.

Falcone, D.J., Hajjar, D.P., and Minick, C.R. (1984). Lipoprotein and albumin accumulation in reendothelialized and deendothelialized aorta. Am J Pathol, 114:112-120.

Fransson LA: Structure and function of cell associated proteoglycans. TIBS 12:406, 1987

Galis, Z.S., Ghitescu, L., Li, Z., Alavi, M.Z., and Moore, S. (in press). Distribution of endogenous apoprotein B-containing lipoproteins in normal and injured aortas of normocholesterolemic rabbits. Lab Invest, may 1992.

Galis, Z., Alavi, M.Z., and Moore, S. (1992). In situ ultrastructural characterization of chondroitin sulfate proteoglycans of normal rabbit aorta. J Histochem Cytochem, 40:251-263.

Gimbrone, M.A. Jr. (1986). Endothelial dysfunction and the pathogenesis of atherosclerosis. In: Fidge, N.H. and Nestel, P.J. (eds.), Atherosclerosis VII, Elsevier, Amsterdam, pp. 367-369.

Gimbrone, M.A. Jr. (1981) In: Moore, S. (ed.), Vascular injury and atherosclerosis. Marcel Dekker, New York, pp. 25-52.

Goldstein J.L., Basu, S.K., Brunschede, G.Y., and Brown, M.S. (1976). Release of low density lipoprotein from its cell surface receptor by sulfated glycosaminoglycans. Cell, 7:85-95.

Goldstein, J.L., and Brown, M.S. (1974). Binding and degradation of low density lipoproteins by cultured human fibroblasts. J Biol Chem,, 249:5153-5162.

Hajjar, D.P. (1991). Viral pathogenesis of atherosclerosis: Impact of molecular mimicry

and viral genes. Am J Pathol, 139:1195-1211.

Hajjar, D.P., Falcone, D.J., Fowler, S. and Minick, C.R. (1980). Endothelium modifies the altered metabolism of the injured aortic wall. Am J Pathol, 102:28-39.

Hamati, H.F., Britton, E.L., and Carey, D.J. (1989). Inhibition of proteoglycan synthesis alters extracellular matrix deposition, proliferation, and cytoskeletal organization of rat aortic smooth muscle cells in culture. J Cell Biol 108:2495-2505.

Haust, M.D. (1989). Recent concepts on the pathogenesis of atherosclerosis. CMAJ, 140:929.

Heinegard, D., Bjorne-Persson, A., Coster, l., Franzen, A., Gardell S., Malmstrom, A., Paulsson, M., Sandfalk, R., and Vogel, K. (1985). The core proteins of large and small interstitial proteoglycans from various connective tissues form distinct groups. Biochem J, 230:181-194.

Hoff, H.F., Heideman, C.L., Gaubatz, J.W., Scott, D.W., Titus,J.L., and Gotto, A.M. (1978). Correlation of apoprotein B retention with the structure of atherosclerotic plaques from human aortas. Lab Invest, 38:560-567.

Huttner, I., Kocher, O., and Gabbiani, G. (1989). Endothelial and smooth-muscle cells. In: Diseases of the arterial wall, Camilleri, J.P., Berry, C.L., Fiessinger, J.N., and Bariety, J. (eds.). Springer-Verlag, London, pp. 3-41.

Huttner, I., Walker, C., and Gabbiani, G. (1985). Aortic endothelial cell during regeneration. Remodelling of cell junctions, stress fibres, and stress fibre-membrane attachment domains. Lab Invest, 53:287-302.

Iverius, P.H. (1972) The interaction between human plasma lipoproteins and connective

tissue glycosaminoglycans. J Biol Chem, 247:2607-2613.

Iverius, P.H. (1973). Possible role of the glycosaminoglycan in the genesis of atherosclerosis. In Porter, R., Knight, J. (eds.), Atherogenesis: Initiating factors. Ciba Foundation Symposium 12. Amsterdam, Associated Scientific Publishers, pp. 185-196.

Joris, I., Zand, T., and Majno, G. (1982). Hydrodynamic injury of the endothelium in acute aortic stenosis

Karnovsky, M.J. (1981). Endothelial-vascular smooth muscle cell interactions. Rous-Whipple Award Lecture. Am J Pathol, 105:200-206.

Kinsella, M.G., and Wight, T.N. (1986). Modulation of sulfated proteoglycan synthesis by bovine aortic endothelial cells during migration. J Cell Biol, 102:679-687.

Klagsbrun, M., and Edelman, E.R. (1989). Biological and biochemical properties of fibroblast growth factors. Implications for the pathogenesis of atherosclerosis. Arteriosclerosis, 9:269-278.

Koo, E.W.Y., and Gotlieb, A.I. (1989). Endothelial stimulation of intimal cell proliferation in a porcine aortic organ culture. Am J Pathol, 134:497-503.

Kostner, G.M. (1989). Lipoprotein receptors and atherosclerosis. Biochem Soc Trans, 17:639-641.

Malenka, D., and Baron, J.A. (1988). Cholesterol and coronary heart disease. The importance of patient-specific attributable risk. Arch Intern Med, 148:2247-2252.

McMillan, G.C., Klatzo, I., and Duff, G.L. (1954). Histochemical and staining reactions of tissues and organs of cholesterol-fed rabbits. Lab Invest, 3:451-468.

McNeil, P.L., Muthukrishnan, L., Warder, E., and D'Amore, P. (1989). Growth factors are released by mechanically wounded endothelial cells. J Cell Biol, 109:811-822.

Merrilees, M.J., Campbell, J.H., Spanidis, E., and Campbell, G.R. (1990). Glycosaminoglycan synthesis by smooth muscle cells of differing phenotype and their response to endothelial cell conditioned medium. Atherosclerosis, 81:245-254.

Minick, C.R. (1981). Synergy of arterial injury and hypercholesterolemia in atherogenesis. In: Moore, S. (ed.), Vascular injury and atherosclerosis, Marcel- Dekker, New York, pp. 149-173.

Moore, S. (1989). Lipid accumulation in the vessel wall. In: Camilleri, J.P., Berry, C.L., Fiessinger, J.N., and Bariety, J. (eds.), Diseases of the arterial wall. Springer-Verlag, London, pp. 197-208.

Moore, S. and Richardson, M. (1985). Proteoglycan distribution in catheter-induced aortic lesions in normolipaemic rabbits. Atherosclerosis, 55:313-330.

Moore, S. (1981). Injury mechanisms and atherogenesis. In Moore, S. (ed.), Vascular injury and atherogenesis. New York, Marcel Dekker, pp. 131-148.

Moore, S. (1967). Hypertension and nephrosclerosis: A re-appraisal and a new theory of renal ischemia. Am Heart J, 74:730-732.

Mourao, P.A.S., and Bracamonte, C.A. (1984). the binding of human aortic glycosaminoglycans and proteoglycans to plasma low density lipoproteins. Atherosclerosis, 50:133-146.

Mourao, P.A.S., Pillai, S., and Di Ferrante, N. (1981). The binding of chondroitin 6-sulfate to plasma low density lipoprotein. Biochem Biophys Acta, 674:178-187.

Munro, J.M. and Cotran, R. (1988). The pathogenesis of atherosclerosis: atherogenesis and inflammation. Lab Invest, 58:249-261.

Oohira, A., Wight, T.N., and Bornstein, P. (1983). Sulfated proteoglycans synthesized by vascular endothelial cells in culture. J Biol Chem 258:2014-2021.

Palumbo, P.J. (1989). Editorial. Cholesterol lowering for all: A closer look. JAMA, 262:91-92.

Radhakrishnamurthy, B., Srinivasan, S.R., Eberle, K., Ruiz, H., Dalferes, E.R., Jr., Sharma, C., Berenson, G.S. (1988). Composition of proteoglycans synthesized by rabbit aortic explants in culture and the effect of experimental atherosclerosis. Biochim Biophys Acta, 964:231-243.

Radhakrishnamurthy, B., Srinivasan, S.R., Vijayagopal, P., Dalferes, E.R., Berenson, G.S. (1982). Mesenchymal injury and proteoglycans of arterial wall in atherosclerosis. In Varma, R.S., and Varma, R. (eds.), Glycosaminoglycans and proteoglycans in physiological and pathological processes of body systems. Basel, Krager, pp. 231-251.

Reidy, M.A. (1988). Endothelial regeneration. VIII. Interaction of smooth muscle cells with endothelial regrowth. Lab Invest, 59:36-43.

Richardson, M., Alavi, M.Z., and Moore, S (1989). Rabbit models of atherosclerosis. In White, R.A., ed. Atherosclerosis and arteriosclerosis: human pathology and experimental animal methods and models. Boca Raton, FL, CRC Press, pp. 163-234.

Rosenfeld, M.E., and Ross, R. (1990). Macrophage and smooth muscle cell proliferation in atherosclerotic lesions of WHHL and comparably hypercholesterolemic fat-fed rabbits. Arteriosclerosis, 10:680-687.

Ross, R. (1991). Polypeptide growth factors and atherosclerosis. Trends Cardiovasc Med, 1:277-282.

Ruoslahti, E. (1989). Proteoglycans in cell regulation. J Biol Chem, 264:13369-13372.

Ruoslahti, E. (1988). Structure and biology of proteoglycans. Ann Rev Cell Biol, 4:229-255.

Saunders, S., and Bernfield, M. (1988). Cell surface proteoglycan binds mouse mammary epithelial cells to fibronectin and behaves as a receptor for interstitial matrix. J Cell Biol, 106:423-430.

Salisbury, B.G.J., Falcone, D.J., and Minick, C.R. (1985). Insoluble low-density lipoprotein-proteoglycan complexes enhance cholesterol ester accumulation in macrophages. Am J Pathol, 120:6-11.

Scott, J.E. (1985). Proteoglycan histochemistry - a valuable tool for connective tissue biochemists. Collagen Relat Res 5:541-575.

Shekhonin, B.V., Tararak, G.P, Samokhin, G.P.,Mitkevich, A.V., Mazurov, A.V., Vinogradov, D.V., Vlasik, T.N., Kalantarov, G.F., and Koteliansky, V.E. (1990). Visualization of apo B, fibrinogen/fibrin, and fibronectin in the intima of normal human aorta and large arteries and during atherosclerosis. Atherosclerosis, 82:213-226.

Smith, E.B. (1990). Transport, interactions and retention of plasma proteins in the intima: the barrier function of the internal elastic lamina. Eur Heart J, 11 (suppl):72-81.

Smith, E.B., Keen, G.A., and Grant, A. (1990). Factors influencing the accumulation in fibrous plaques of lipid derived from low density lipoproteins. Atherosclerosis, 84:165-

171.

Srinivasan, Vijayagopal, P., Dalferes, E.R., Abbate, B., Radhakrishnamurthy, B., and Berenson, G.S. (1986). Low density lipoprotein retention by aortic tissue. Contribution of the extracellular matrix. Atherosclerosis, 62:201-208.

Srinivasan, S.R., Dolan, P., Radhakrishnamurthy, B., and Berenson, G.S. (1972). Isolation of lipoprotein-acid mucopolysaccharide complexes from fatty streaks of human aorta. Atherosclerosis, 16:95-104.

Srinivasan, S.R., Lopez, A., Radhakrishnamurthy, B., and Berenson, G.S. (1970). Complexing of serum pre-ß- and ß-lipoproteins and acid mucopolysaccharides. Atherosclerosis, 12:321-334.

Stampfer, M.J., Sacks, F.M., Salvini, S., Willett, W.C., and Hennekens. C.H. (1991). A prospective study of cholesterol, apolipoproteins, and the risk of myocardial infarction. New England J Med, 325:373-381.

Stary, H.C., Blankenhorn, D.H., Chandler, A.B., Glagov, S., Insull, W.Jr., Richardson, M., Rosenfeld, M.E., Schaffer, S.A., Schwartz, C.J., Wagner, W.D., Wissler, R.W. (1992). A definition of the intima of human arteries and of its atherosclerosis-prone regions. A report from the committee on vascular lesions of the Council on Atherosclerosis, American Heart Association. Arteriosclerosis and Thrombosis, 12:120-1343.

Stebhens, W.E. (1991). Reduction of serum cholesterol levels and regression of atherosclerosis. Pathology, 23:45-53.

Steele, R.H., Wagner, W.D., Rowe, H.A., and Edwards, I.J. (1987). Artery wall proteoglycan-plasma lipoprotein interaction: lipoprotein binding properties of extracted

proteoglycans. Atherosclerosis, 65:51-62.

Steinberg, D. (1987). Lipoproteins and the pathogenesis of atherosclerosis. Circulation, 76:508-514.

Toledo, O.M.S., and Mourao, P.A.S. (1980). Sulfated glycosaminoglycans in normal aortic wall of different mammals. Artery, 6:341-353.

Trelstad, R.L. (1985). Editorial. Glycosaminoglycans: Mortar, matrix, mentor. Lab Invest, 53:1-4.

Uhlin-Hansen, L., Eskeland, T., and Kolset, S. (1989). Modulation of the expression of chondroitin sulfate proteoglycan in stimulated human monocytes. J Biol Chem, 25:14916-14922.

Vijayagopal, P., Srinivasan, S.R., Radhakrisnamurthy, B., and Berenson, G.S. (1991). Studies on the mechanism of uptake of low density lipoprotein-proteoglycan complex in macrophages. Biochim Biophys Acta, 1092:291-297.

Vijayagopal, P., Srinivasan, S.R., Dalferes, E.R. Jr., Radhakrishnamurthy, B., and Berenson, G.S. (1988). Effect of low-density lipoproteins on the synthesis and secretion of proteoglycans by human endothelial cells in culture. Biochem J, 255:639-646.

Vijayagopal, P., Srinivasan, S.R., Jones, K.M., Radhakrisnamurthy, B., and Berenson, G.S. (1985). Complexes of low-density lipoproteins and arterial proteoglycan aggregates promote cholesteryl ester accumulation in mouse macrophages. Biochim Biophys Acta, 837:251-261.

Vijayagopal, P, Srinivasan, S.R., Radhakrishnamurthy, B., and Berenson, G.S. (1981). Interaction of serum lipoproteins and a proteoglycan from bovine aorta. J Biol Chem,

256:8234-8241.

Volker, W., Schmidt, A., and Buddecke, E. (1987). Mapping of proteoglycans in human arterial tissue. Eur J Cell Biol, 45:72-79.

Zemel P.C., and Sowers, J.R. (1990). Relation between lipids and atherosclerosis: Epidemiological evidence and clinical implications. Am J Cardiol, 66:7-12.

White, R.A. (1989) ed. Atherosclerosis and arteriosclerosis: Human pathology and experimental animal methods and models. CRC Press, Inc., Boca Raton, Florida.

Wight, T.N. (1989). Cell biology of arterial proteoglycans. Arteriosclerosis 9:1-20.

Wight, T.N., Curwen K.D., Litrenta, M.M., Alonso, D.R., and Minick, C.R. (1983). Effect of endothelium on glycosaminoglycan accumulation in injured rabbit aorta. Am J Pathol 113:156-164.

Wight TN, Ross R (1975). Proteoglycans in primate arteries. I. Ultrastructural localization and distribution in the intima. J Cell Biol 67:660-674.

Williams, S. (1991). Editorial. Regulation of intimal hyperplasia: Do endothelial cells participate ?. Lab Invest, 64:721-723.

Yla-Herttuala, S., Solakivi, T., Hirvonen, J., Laaksonen, Mottonen, M., Pesonen. E., Raekallio, J., Akerblom, H.K., and Nokkari, T. (1987). Glycosaminoglycans and apolipoproteins B and A-I in human aortas. Chemical and immunological analysis of lesion-free aortas from children and adults. Arteriosclerosis, 7:333-34.

Yla-Herttuala, S., Sumuvuori, H., Karkola, K., Mottonen, M., and Nikkari, T. (1986). Glycosaminoglycans in normal and atherosclerotic human coronary arteries. Lab Invest, 54:402-407.

CHAPTER 2

DISTRIBUTION OF ENDOGENOUS APOPROTEIN B-CONTAINING LIPOPROTEINS IN NORMAL AND INJURED AORTAS OF NORMOCHOLESTEROLEMIC RABBITS.

Zorina S. Galis, Lucian D. Ghitescu, Zhihe Li, Misbahuddin Z. Alavi, Sean Moore*

From: Department of Pathology, McGill University, and * Departement d'Anatomie, Université de Montréal, Montreal, Que, Canada

Address for correspondence: Zorina Galis, Department of Pathology, McGill University, 3775 University, Montreal, H3A 2B4, Que, Canada.

Short title: Endogenous apo B in aorta

2.1. ABSTRACT

The distribution of endogenous apolipoprotein B (apo B) was studied in both normal and balloon catheter-injured aortas of standard fed-rabbits. Using light and electron microscopy, the distribution within entire aortic walls and individual tissue compartments was investigated by immunocytochemistry using an antibody raised against rabbit apo B. The concentration of apo B across the vessel wall dropped sharply from the luminal front towards the media of the normal aortas. The strong superficial reaction was mainly due to a heavy, yet specific, labelling of endothelial cells. Significant concentrations of apo B were also detected within the innermost regions of the extracellular space. The characteristics associated with the labelling of the intimal layer suggested an intense uptake and transcellular transport of apo B by endothelial cells (EC). In contradistinction, normal smooth muscle cells (SMC) did not appear to be labelled. In the previously injured aortas, the same features of strong superficial apo B labelling were present in the areas covered by regenerated endothelial cells, but not in those persistently deendothelialized. The SMC of these regions appeared to show a low uptake of apo B. The increased concentrations of apo B in deeper interstitial areas of injured aortas, indicated the contribution of the extracellular matrix to apo B accumulation. This was especially prominent in the advanced lesions, selectively developed within neointima covered by regenerated endothelium. A rather uniform labelling pattern accompanying small lipid particle deposits, suggested a direct extracellular accumulation of circulating lipoproteins. Intensely labelled foam cells and irregularly distributed apo B within areas of cellular necrosis were detected as well. Injury-mediated responses of the cellular and extracellular aortic components can trigger the development of lipoprotein accumulations characteristic of atherosclerosis within aortas of normocholesterolemic animals.

Key words: apolipoprotein B, aorta, endothelium, endothelial injury, atherosclerosis

2.2. INTRODUCTION

Although major aspects of the structure and functions of lipoproteins (LP) are known, they remain a continuing subject of study, especially as potentially pathogenic factors (8,14,47). Lipids that accumulate within arterial vessel walls during atherogenesis are thought to be related to circulating LP - since LP accumulations have been repeatedly associated with human complicated atherosclerotic lesions (5,24). The details of this process are still not clearly understood, in spite of a rather long history of investigation (2,3). The new knowledge that we possess today in areas such as biochemistry, cellular and molecular biology, allows us to imagine an increasingly more complicated scenario of events that might lead to atherosclerosis. While traditionally accepted concepts begin to be challenged and reformulated (7,43), a rapidly growing number of new questions are raised. The obvious consequence is that, at present we have more questions than answers. The issue of finding the main causal factor(s) of this disease, has prompted investigators to propose several models, in which, by different experimental manipulations, atherosclerotic or atherosclerotic-like lesions could be induced in animals.

One important traditional line stresses the pivotal role played in vascular lipid deposition by dietary-perturbed compositions of serum LP and other fats, as well as by the presence of modified circulating molecules (39,47).

Another view, considers that the determining factors that we should look for, when studying atherogenesis, are related to the blood vessel wall itself. In this regard, the response of arterial endothelium to different stress factors is thought to be of crucial importance (19,22,33,36,37). The models rely on experimentally-induced morphological or functional endothelial injury obtained by using physical, chemical, or immunological challenges. A rather frequently used experimental approach has been to combine mechanical endothelial injury and a hypercholesterolemic diet in an effort to enhance their effects (32).

Vascular lipid accumulations have been described to occur following endothelial injury (12,34,42). In balloon catheter-injured aortas, over a short period of time, injected exogenous LP have been shown to be retained selectively in areas covered by the

regenerated endothelium (1,15). However the precise connection of endogenous LP with this type of vascular lesion and their relevance to lipid accumulation has not been investigated so far. We therefore decided to examine the effect of endothelial injury upon the normal aortic distribution of native LP that contain apolipoprotein B (apo B) and which are thought to be related to atherogenesis (14).

The distribution of endogenous apo B in normal or experimentally injured aortas of normocholesterolemic rabbits was compared. Light microscope (LM) immunocytochemistry revealed typical overall patterns, while by using electron microscope (EM) gold immunocytochemistry, apo B distribution could be studied in relation to different compartments of the normal and diseased aortic wall.

2.3. EXPERIMENTAL DESIGN

The distribution of endogenous apo B was studied in two groups of normocholesterolemic rabbits. The first group of animals was used as a source of normal aortic tissue, while the second provided the specimens on which the effects of a previous catheter-induced endothelial injury were evaluated. Normal tissue and characteristic areas that developed following balloon catheterization were processed for either light or electron microscope immunocytochemistry.

For this purpose, a polyclonal antibody to rabbit apo B was raised. Its specificity against lipoprotein fractions isolated from normal rabbit serum was characterized using immunoelectrophoresis, immunodotting, and Western blotting. The primary antibody followed by protein A - gold complexes were used to detect apo B, either adsorbed onto nitrocellulose membranes or present in tissue sections.

The overall apo B distribution on frozen sections of normal or injured aorta was assessed by LM, silver-enhanced, gold immunocytochemistry. For EM, the tissues were divided according to provenance and macroscopic appearance into several categories. They included: from control animals, normal aortic tissue; from injured animals, persistently deendothelialized areas, regions covered by regenerated endothelium, and areas of grossly thickened lesions of aorta. Small pieces derived from each type of aortic tissue were embedded at low temperature in Lowicryl K4M. This procedure was found to preserve apo B antigenicity very efficiently. Endogenous apo B was detected post-embedding, using protein A-gold EM immunocytochemistry.

The results of the immunocytochemical staining were eventually evaluated by morphometric analysis of the gold particle distribution as detected on EM.

2.4. RESULTS

Anti apo B antibody

Following the anti-serum fractionation procedure, the purity of the anti-apo B IgG fraction was confirmed by the profiles obtained in SDS-PAGE as described under "Methods". On immunoelectrophoresis, the isolated IgG fraction produced only the ß LP-specific precipitation ring when tested against whole rabbit serum. The comparative immunostaining intensity of dots derived from serum, VLDL, LDL, and HDL, adjusted to equivalent total protein concentrations (Fig. 1A), was in good agreement with their expected apo B content (31). Western blot staining (Fig. 1B) revealed the characteristic MW of apo B, confirming the specificity of this polyclonal antibody.

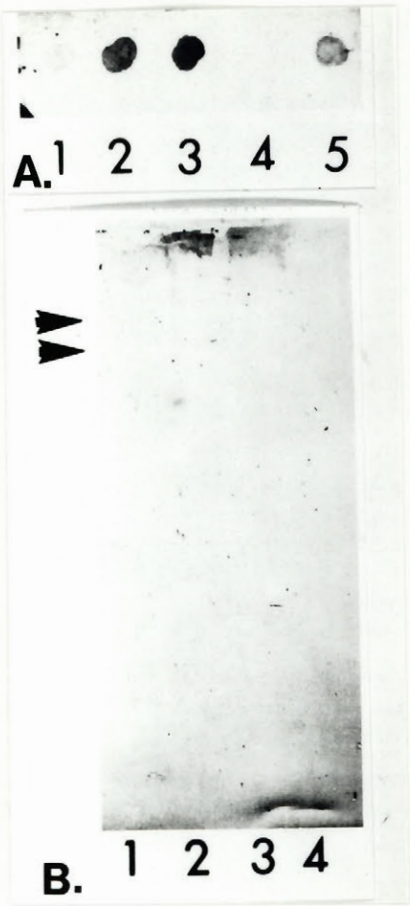

Fig. 1. Anti-apo B antibody specificity. The antigen (apo B) was detected with the polyclonal antibody, followed by protein A-gold. A. Dot blot. 1 μl aliquots derived from: serum (1); VLDL (2); LDL (3); HDL (4), brought to the same total protein concentration (15 μg/ml); and 1 μl of undiluted serum (5). B. Immunoblot. 3-8 % SDS-PAGE of rabbit serum and isolated lipoprotein fractions. Lanes: 1, serum; 2, VLDL; 3, LDL; 4, HDL. Arrowheads correspond to markers of MW = 180 kDa, and 116 kDa respectively.

Immunocytochemistry

The morphological features of specific arterial regions that develop as a result of balloon catheter-deendothelialization have been previously described by several investigators (11,15,25,42). Therefore, this report deals with the features of apo B immunocytochemical detection. The results have been grouped according to the provenance of tissue, e.g.: from normal aorta, or from deendothelialized, reendothelialized, or markedly thickened areas of injured aortas. Then, apo B localization has been described in relation to individual compartments of the investigated area, e.g.: endothelium, interstitial cells, extracellular matrix.

Normal animals - Normal aorta

Examining the immunostaining of frozen sections, an overall rapidly decreasing gradient of the reaction product from intima to media was detected (Fig. 2) . The strongest staining, indicating the highest concentration of endogenous apo B, was consistently detected over the luminal regions of the aortic wall. This fact was confirmed and detailed by the immunocytochemical analysis of apo B distribution at the EM level (Fig. 3).

Fig. 2. LM immunocytochemical detection of endogenous apo B distribution in normal rabbit aorta. Unstained frozen section processed by incubation with anti-apo B, followed by protein A-gold, and silver enhancement procedure. Innermost aortic layers give a very strong reaction, apo B concentration rapidly decreases towards the media. L = lumen. x 1,200; bar = 10 μm.

Fig. 3. EM immunocytochemical detection of apo B in normal rabbit aorta. Lowicryl-embedded tissue processed by protein A-gold immunocytochemistry. Many gold particles are found over the endothelial layer (E), and are also present in the subendothelial space, apparently excluded from areas occupied by elastin (el). Smooth muscle cells (SMC) do not appear to be labelled. L = lumen. x 20,780; bar = 500 nm.

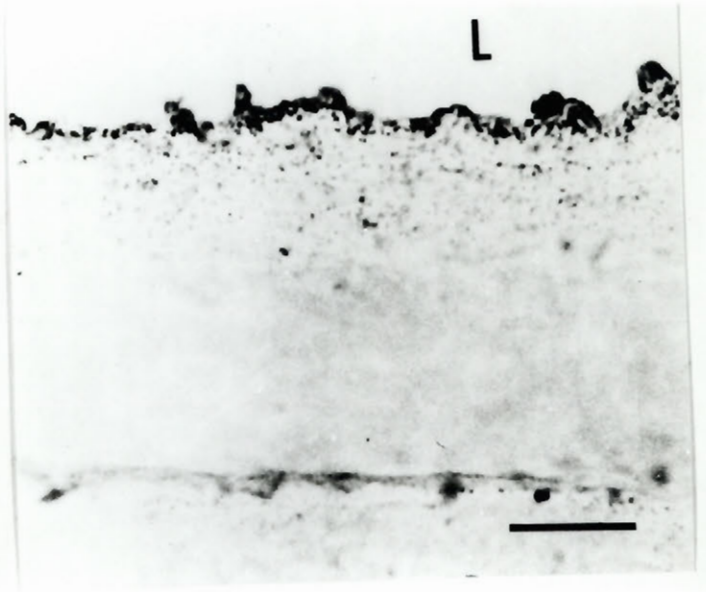
L

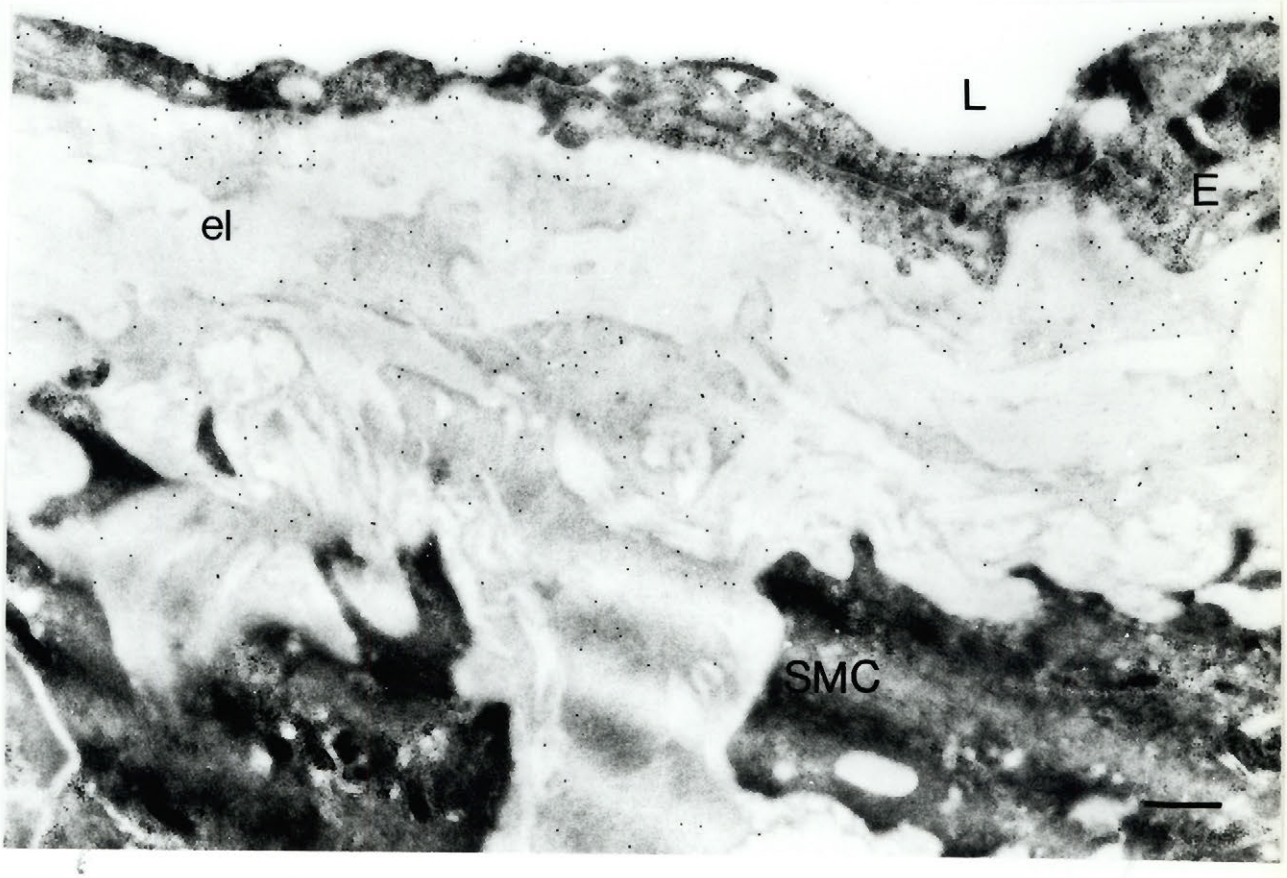
L
E
el
SMC

The endothelial cells of the intima were strongly labelled. On closer inspection (Fig. 4A), many gold particles were associated with the luminal surface of the EC. Numerous apo B containing vesicular structures were found on both luminal and abluminal fronts and intracellularly. Rarely, other larger intracellular structures supposedly representing multivesicular bodies or lysosomes, were labelled. An evaluation of the interendothelial junction labelling has shown that about 40 % of these compartments contained some gold particles (Fig. 5). These were frequently detected in the luminal segment of the interendothelial clefts, but were rarely found on the abluminal side of the stricture or towards the interstitial opening of the junctions. Many of the labelled junctions were associated with apo B containing vesicles closely apposed to or opening into the intercellular spaces (Fig. 5B).

In contradistinction with EC, the interstitial SMC of normal aorta were virtually devoid of apo B staining.

Fig. 4. Normal endothelium (E) of rabbit aorta. A. Numerous plasmalemmal vesicles contain endogenous apo B as detected by gold post embedding immunocytochemistry. B. Control. Comparable area of a successive thin section processed similarly, but primary antibody has been replaced by normal goat IgG. x 29,600; bar = 500 nm. L = lumen, n = nucleus.

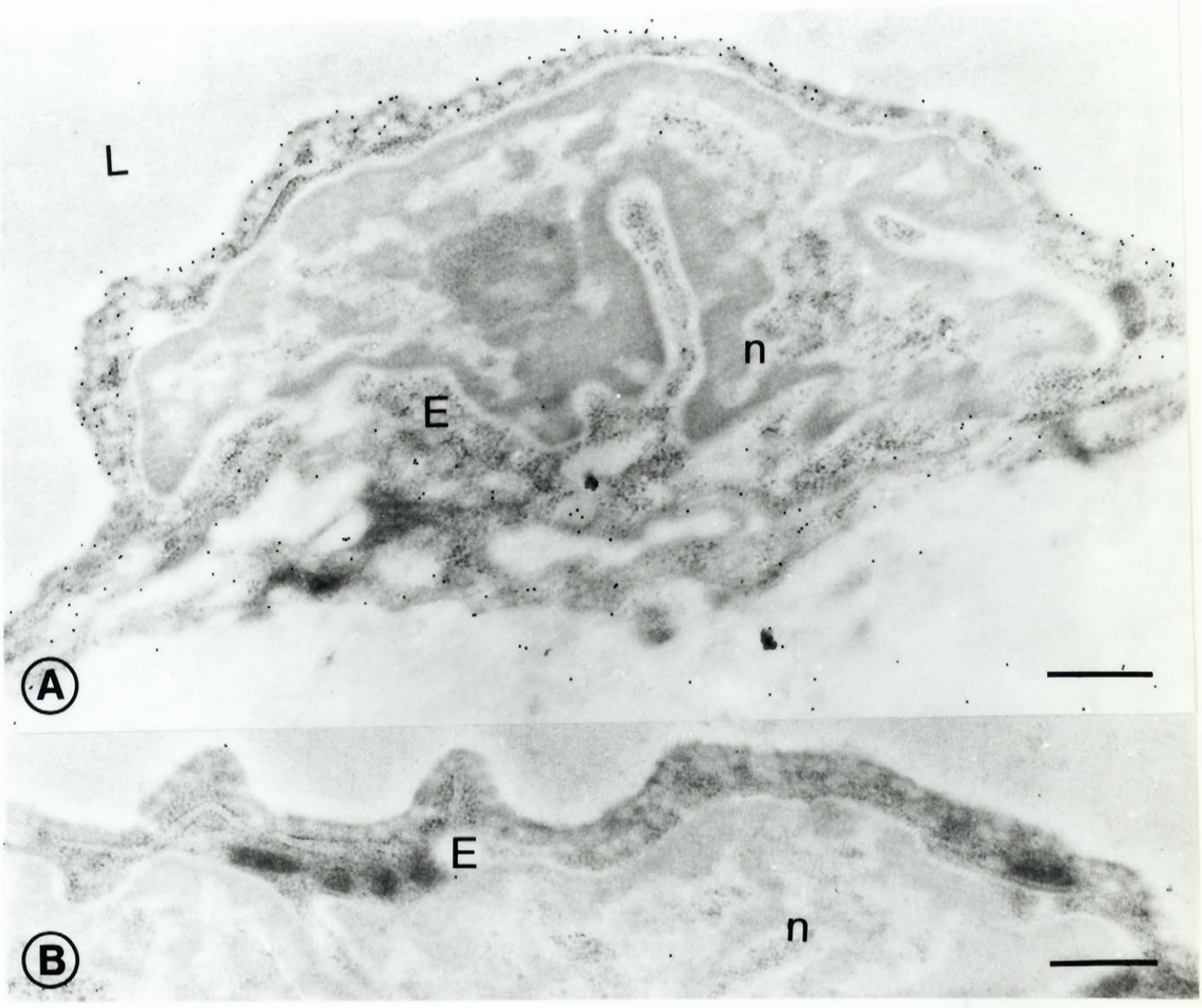
L
n
E
A
E
n
B

Fig. 5. Labelled endothelial junctions. Protein A-gold immunocytochemistry for detection of endogenous apo B. A. Gold particles contained in the luminal cleft of the junction. x 25,500. Bar = 500 nm. B. Apo B might cross the endothelial layer by being shuttled in plasmalemmal vesicles (arrowheads) or by following the junctional slits (open arrow heads). x 29,600. Bar = 500 nm. x 57,100. Bar = 250 nm.

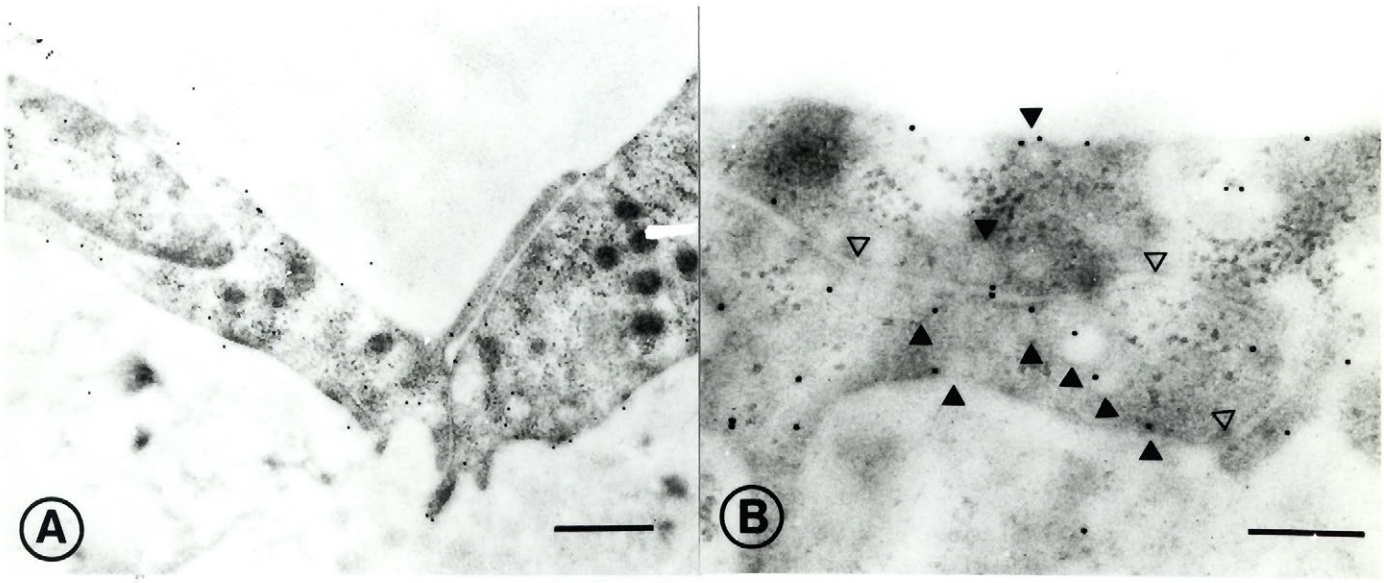
A
B

Intermediate levels of subendothelial apo B concentrations attenuated the otherwise striking difference between the high density of apo B within the endothelial layer and the faint overall staining of normal aorta. This arrangement was responsible for creating the general impression of an apo B gradient rapidly decreasing from intima to media. The gold particles appeared to be usually excluded from the areas of elastic fibres (as exemplified in Fig. 3); no other preferential pattern of extracellular distribution could be noticed. As implied above, the labelling of the extracellular matrix was uniformly very sparse in the deeper, successive, aortic layers. Overall the adventitia was weakly, but more variably stained. These variations could be related to the random occurrence of vasa vasorum. Whenever adventitial blood vessels were present in the sections, their profiles were intensely decorated with gold particles (Fig. 6).

Fig. 6. Vasa vasorum. Endogenous apo B detected by protein A-gold immunocytochemistry within lumen (L) and over the endothelium (E). e = erythrocyte. x 32,730; bar = 300 nm.


e
L
E

Injured animals - Deendothelialized areas

These regions were typically covered by several discontinuous layers of cells (Fig. 7), presumably derived from SMC which had migrated from the media (11) and proliferated in the intima (42). The hyperplastic SMC and rather abundant intervening extracellular matrix contributed to the increased width of the aortic wall.

The cells found on the luminal aspect of these aortic areas were weakly labelled for apo B (Fig. 7B). A similarly low intensity was detected within the superficial extracellular areas. The deeper interstitial space had visibly increased concentrations of apo B. Nevertheless, apo B staining suggested a discreet homogenous distribution, rather than an organized pattern.

The few foam cells found in some of the thin sections were intensely labelled by the anti-apo B antibody (Fig. 8). Gold particles were found on their plasma membrane and intracellularly, plasmalemmal vesicles appeared selectively labelled. Often, the apo B-positive vesicles were clustered, forming clearly distinct groups, while the large lipid inclusions of foam cells did not appear to be stained.

Fig. 7. Apo B EM immunocytochemistry in the deendothelialized areas of aorta. A. Image of smooth muscle cells that form interrupted layers on the luminal aspect of the vessel wall. x 6,230; bar = 2 μm. B. Higher magnification showing the scarce labelling (arrows) of luminal SMC which contrasts with the strong positive reaction over the endothelial cells covering the adjacent regions of injured aortas. L = lumen. x 42,800; bar = 750 nm.

Fig 8. Foam cell in deendothelialized area. Gold particles detecting native apo B on plasma membrane (arrowheads) and within vesicle clusters (arrows) consistently detected in this type of cell. x 36,230; bar = 400 nm.3

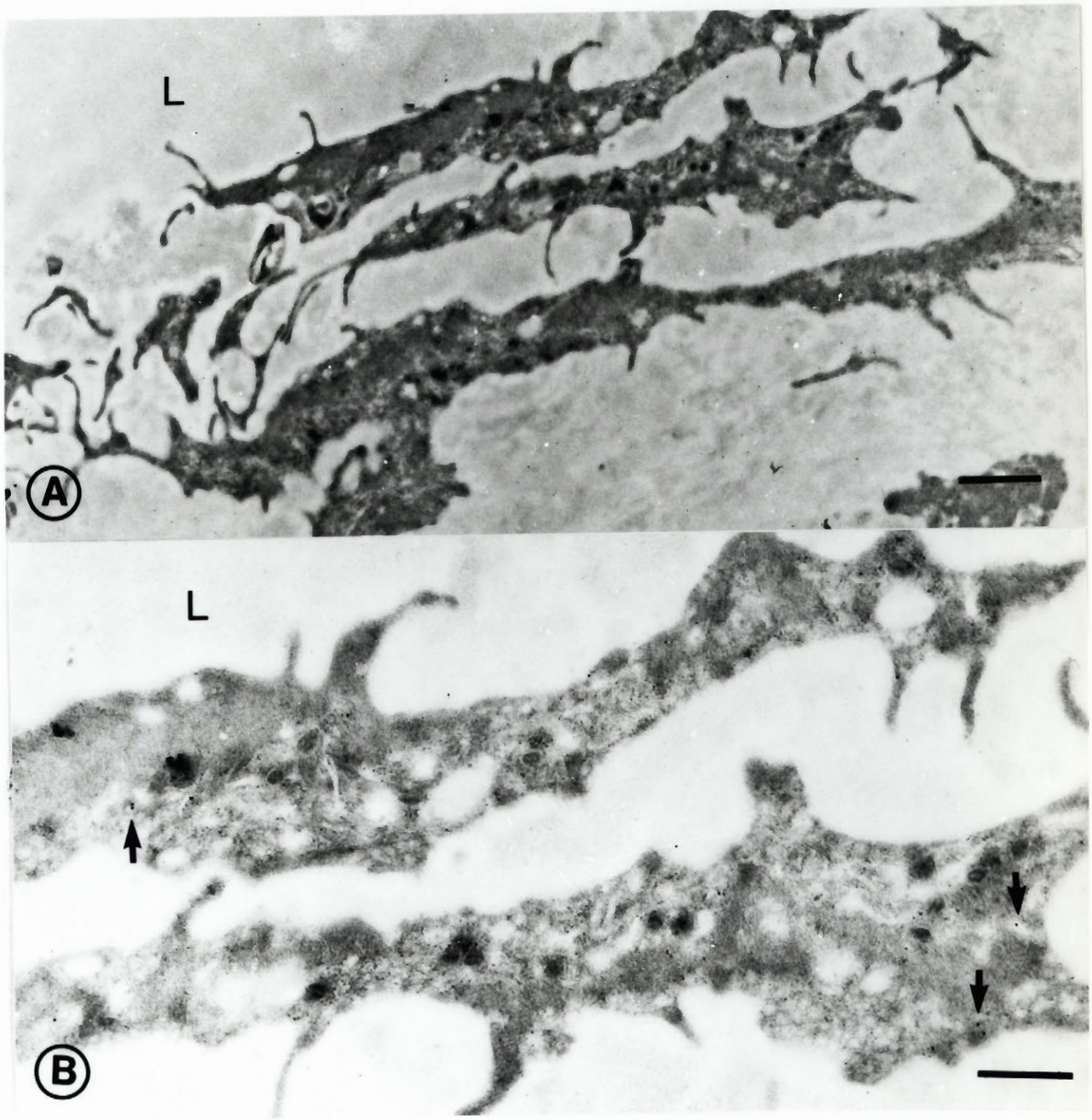
L
A
L
B

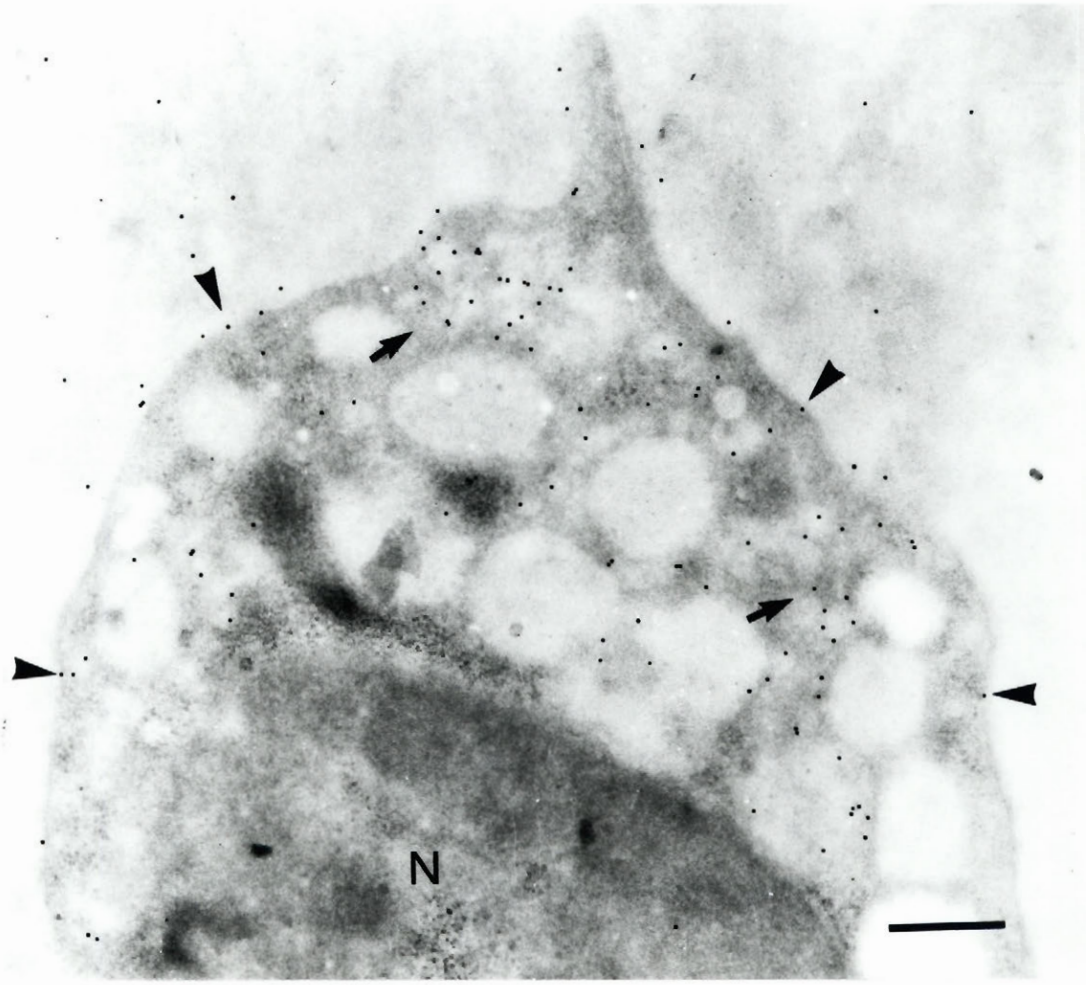
N

Areas covered by regenerated endothelium

Areas of endothelial regrowth, that on gross inspection did not present markedly elevated lesions, proved however to have microscopically detectable hyperplasia of the neointima. Covering the obviously wider acellular subendothelial space and neointima, the regenerated endothelium formed a continuous layer of cells with shapes varying from very plump to very elongated connected by typical elaborate junctions (25). These were the main morphological features at variance with the overall appearance of the normal aortic wall.

Like its normal counterpart, the new endothelium was highly stained for the presence of apo B-containing LP (Fig. 9). As in the case of normal EC, judging from the extent of vesicular vs junctional labelling, apo B appeared to follow mainly transcellular routes.

Gold particles associated with their surface, or inside SMC although few, could be repeatedly detected. The intensity of labelling was very low if compared to that of endothelial cells covering the same areas. The fact that SMC of these regions were labelled to a certain extent, represented however a different situation from the virtual lack of apo B detection in SMC of the normal aortic wall.

Within the extracellular matrix of the reendothelialized regions, the concentration of apo B was greater immediately beneath the regenerated endothelial layer - as it also was beneath normal endothelium. At variance with the normal aortas, the gold particle labelling was noticeable at extended depths of the interstitial space.

Fig. 9. Endogenous apo B distribution in areas covered by regenerated endothelium. Regenerated endothelium (RE) studded with numerous ribosomes is forming an apo B-positive continuous layer of cells. L = lumen. x 32,230; bar = 500 nm.

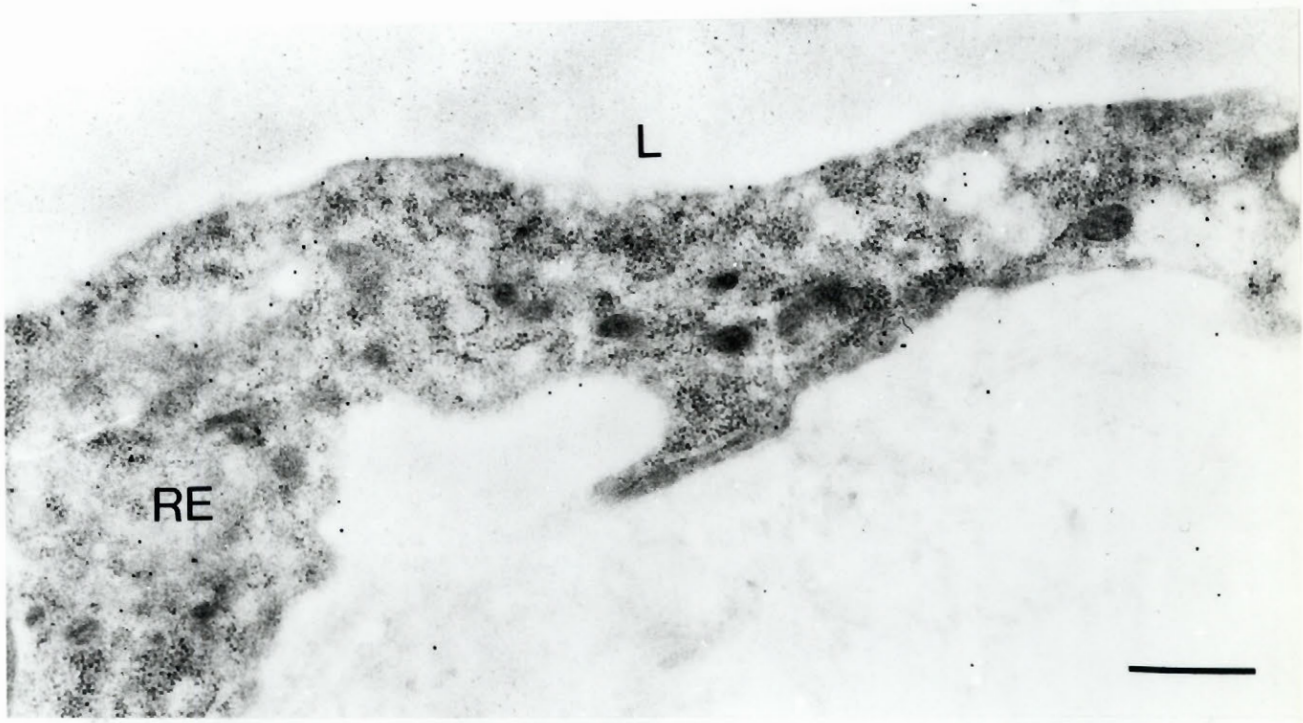
L
RE

Advanced lesions

As previously reported (34,42), the development of advanced vascular lesions occurred in intimal areas covered by regenerated endothelium.

These lesions could be selected due to their macroscopic presentation as marked yellowish thickening, sometimes having red streaks. Microscopically, they presented the characteristic components of complicated human atherosclerotic plaques. They included: pronounced smooth muscle cell proliferation, increased quantity and conspicuous morphologic changes of the extracellular matrix, foam cells, extracellular lipid accumulations, cholesterol crystals, superimposed thrombosis, haemorrhagic and necrotic cores.

Apo B concentration, as judged from the overall staining intensity of frozen sections cut from injured aortas, was highly enhanced in the thickened lesions (Fig. 10).

Fig. 10. LM immunocytochemical detection of apo B in a markedly thickened area of injured aorta. Frozen section sequentially incubated with anti-apo B antibody, and protein A-gold; followed by silver enhancement (no counterstain). Note the increased width of the vascular wall as compared to the normal aorta shown in Fig.2. The overall immunolabelling is greatly enhanced in this type of lesion. L = lumen. x 750; bar = 10 μm.

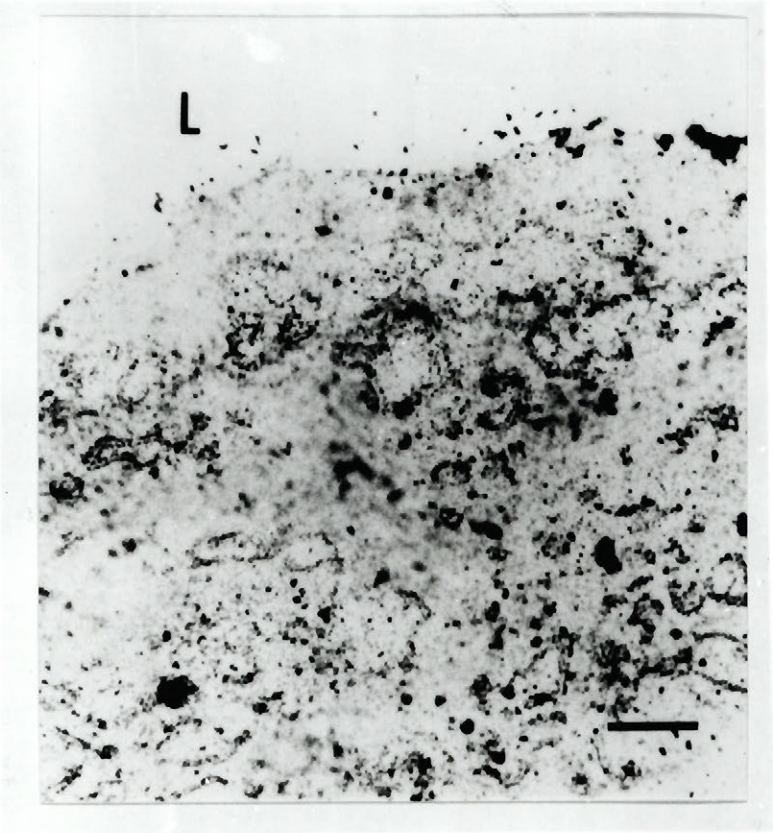
L

At the ultrastructural level, the pattern of staining proved to be related to both organized extracellular, and concentrated intracellular accumulations.

In the extracellular space, colloidal gold particles were associated with pale round-shaped structures (Fig. 11). Their location, shape, and size were consistent with the description of extracellular lipid vesicles found in human atherosclerotic plaques (10,20), and in the hypercholesterolemic rabbit model (18,45) where they have been called extracellular liposomes. Their clear cut ultrastructural identification was hampered since our preliminary experiments had shown that special EM procedures that enhance lipid preservation and visualization could not be used without loss of apo B antigenicity. Two main types of extracellular particles could be distinguished. The first consisted of rather uniform closely packed structures (Fig. 11A). Their round profiles were sometimes visible (as indicated by arrowheads), but more frequently were suggested by the disposition of the gold particles. Deeper inside the lesions, larger round structures were more loosely distributed, apparently enmeshed in the extracellular matrix (Fig. 11B). Apo B labelling was detected whenever these structures were distinguishable. Numerous cholesterol crystals were also present in these areas.

Fig. 11. EM detection of apo B extracellular accumulations in advanced lesions. A. The gold particles are associated with small uniform extracellular structures. Some round profiles are indicated (arrowheads). x 30,860; bar = 500 nm. B. Intense labelling of large (large arrowheads), and small (small arrowheads) extracellular liposomes and cholesterol clefts deeper inside the lesions. Inset. Control section, immunocytochemical staining with omission of the primary antibody. x 20,660; bars = 500 nm.

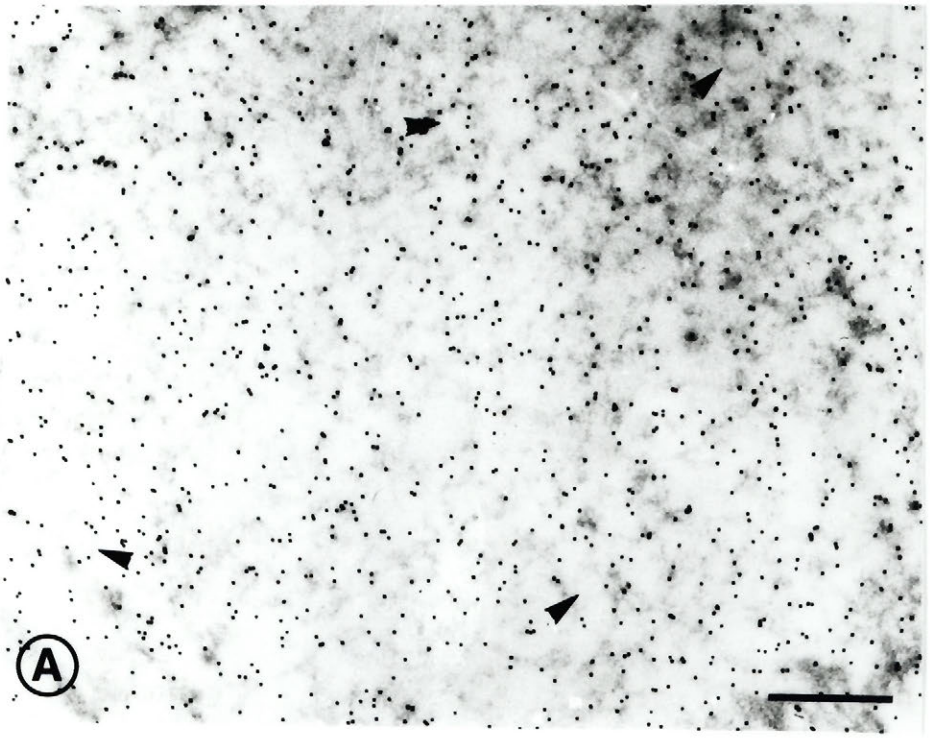
A

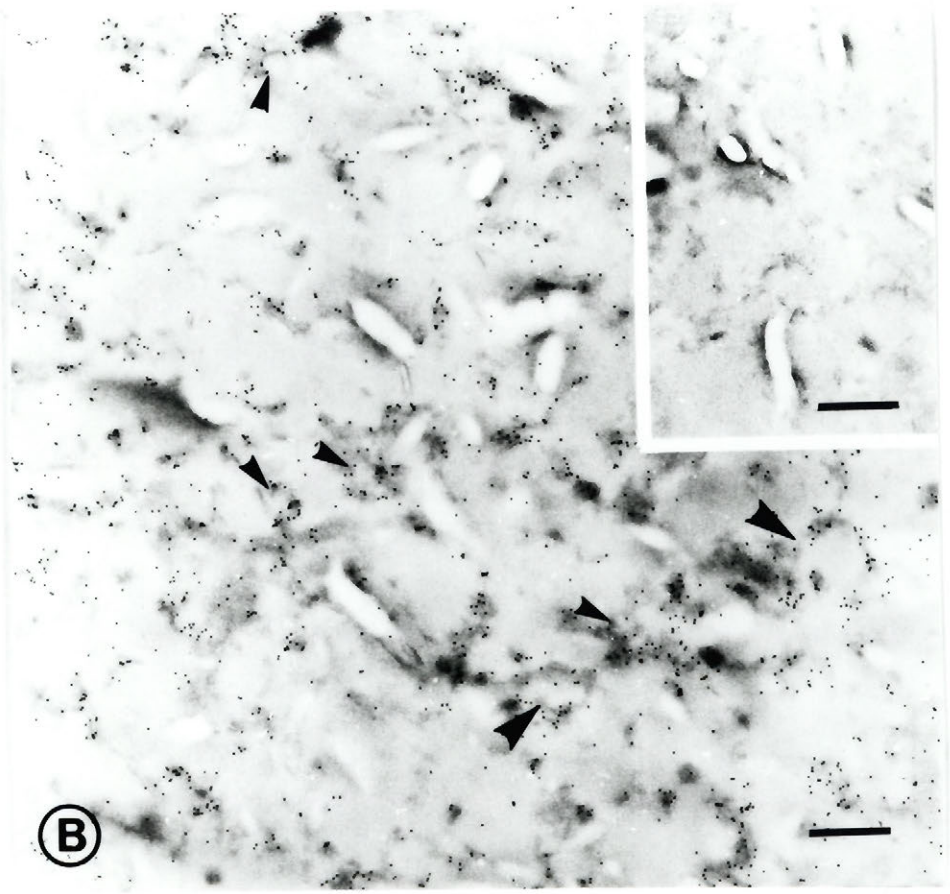
B

The interstitial cells were labelled to a significant extent. Some of the cells could be undoubtedly recognized as fat-laden SMC based on the abundance of contractile elements. The cellular origin of those completely loaded with lipid was more difficult to ascertain. The plasma membrane of foam cells was intensely decorated (Fig. 12), suggesting a sustained uptake of apo B. Concentrated accumulations of apo B were also visible intracellularly. A typical detail of the intracellular labelling is presented in Figure 13. The gold particles were seen to preferentially label the contour of intracellular structures with approximate diameters of 100 nm, apparently segregated from the large lipid inclusions of the foam cells.

Fig. 12. Endogenous apo B within foam cells (FC) of advanced lesions. Foam cells (FC) are decorated around their membrane and contain concentrated intracellular accumulations. x 12,000; bar = 1 μm.

Fig. 13. High magnification of typical intracellular accumulations. The highest concentrations of gold particles usually surrounds small vesicular structures (arrowheads), distinct from the large lipid inclusions of foam cells. ex = extracellular space, n = nucleus. x 44,460; bar = 250 nm.

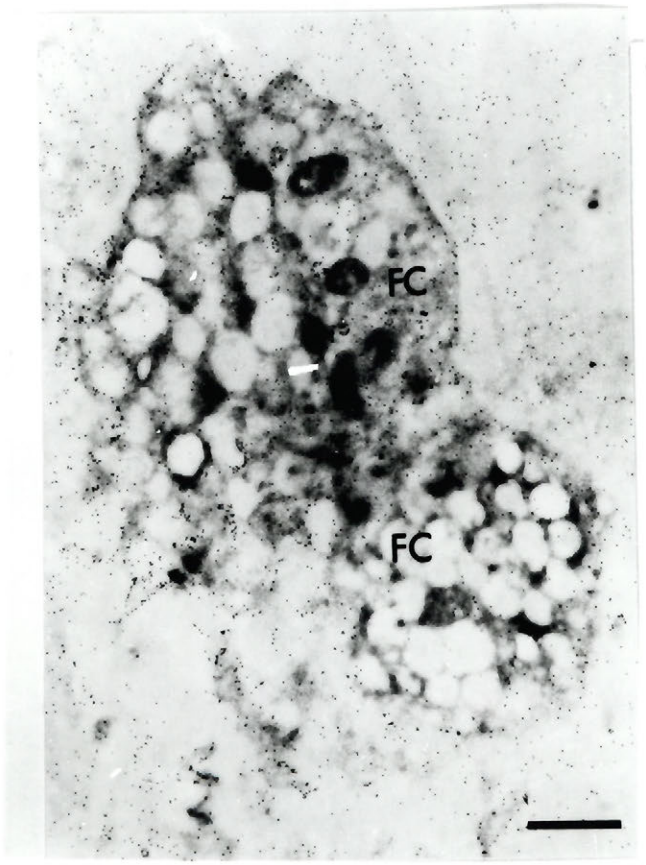
FC
FC


n
ex

Morphometric analysis

Gold labelling is presently considered to be the most suitable immunocytochemical technique for quantitation. The analysis of immunocytochemical staining could not however be expected to produce absolute estimates of apo B concentrations in different aortic tissues. It was merely intended to substantiate the visual impression and to provide grounds for a comparative evaluation of the labelling (Fig.14). Although affected by expected variations, the measurements were found to be consistent and the analysis of variance confirmed the visual impression of different values of apo B distribution within distinct morphological compartments of all types of examined aortic tissue ($p \leq 0.01$).

In the normal aortas, significant values of labelling were measured over the endothelial cells and in the subendothelial space. In the persistently deendothelialized areas, although low, the value of SMC labelling was found to be increased if compared with that measured on control specimens ($p=0.02$). Apo B density in the extracellular space was significantly increased deeper inside the arterial wall. In the areas covered by regenerated endothelium, the highest apo B concentration was measured over the endothelial cells. The labelling density immediately beneath regenerated endothelium was still higher than in the interstitial space, but the latter was nevertheless significant ($p=0.03$), suggesting an accumulation of apo B in these areas. The thick lesions had high densities of labelling associated with both the extracellular and intracellular space. Due to the fact that the normal appearance of cells was seriously modified by heavy lipid loading, we chose to calculate a single value for apo B cellular density. In the extracellular space, the two distinct morphological types of lipid accumulations also had different corresponding apo B densities ($p=0.009$).

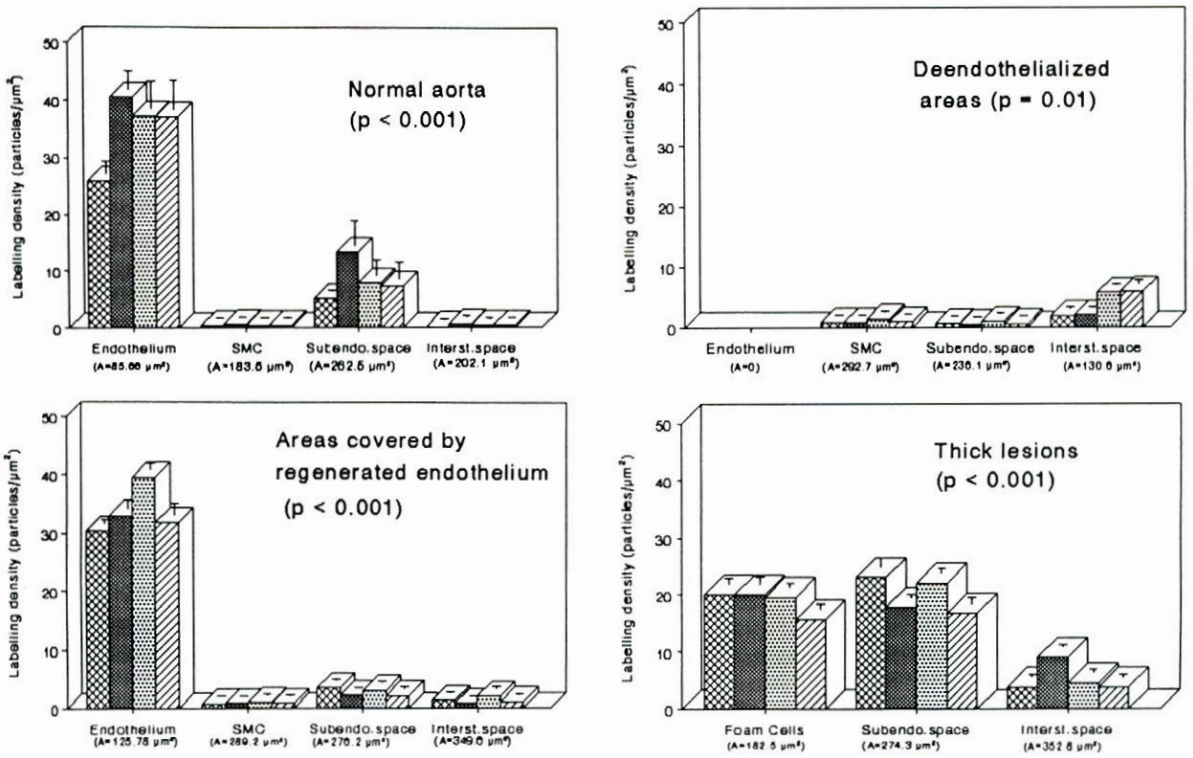

Fig. 14. Gold labelling densities in different compartments of four types of aortic tissue. Data were derived from the morphometric analysis of apo B detection by post embedding immunocytochemistry (p values, as calculated by one way ANOVA with repeated measures on one factor). Each column represents the mean labelling density over a morphological compartment obtained by averaging seven values measured in comparable areas of the same animal. Bars = S.E.M. A = area of real tissue measured for each compartment. In deendothelialized areas, "subendothelial space" represents the innermost extracellular space (see Methods). For the control specimen, gold particle density = 0.32 ± 0.16 μm^2 (A = 205.1 μm^2)

2.5. DISCUSSION

Data regarding the interaction between LP and components of the vascular wall have been mainly derived from previous biochemical studies employing labelled exogenous LP. LP were either injected, perfused through the vasculature, or incubated with cultured vascular cells (1,8,13,15,17,27,38,46). Exogenous LDL perfused in situ has been detected in an earlier electron microscopic study of the normal arterial endothelium (50). Due to obvious technical problems related to the inherent low levels of endogenous LP in experimental animals, either heterologous or homologous hypercholesterolemic sera have usually been used (1,15,46). As already recognized, while enabling the elegant monitoring of several parameters, this approach is associated with the inevitable pitfalls of modifying LP molecules during different experimental procedures or of using LP molecules intrinsically different from the native ones. In contrast, detection of endogenous molecules can produce an accurate, but static image of their native distributions.

2.5.1. LP detection in normal aortic wall

Most of the apolipoprotein was present in the intimal layer of the aorta, as previously reported from biochemical assays of normal human aortic tissue (49). The presence of endogenous apo B in normal aorta was detected by post-embedding immunocytochemistry and to the best of our knowledge, visualized for the first time at the ultrastructural level. The morphometric analysis of the EM specimens confirmed that significantly higher values of apo B concentrations were associated with EC. The extent of endothelial labelling seemed to indicate an intense uptake and/or transport of LP. Serum LP presumably interact with arterial endothelium in vivo by a double mechanism (45,48). One pathway is thought to rely on coated pits and vesicles, and to follow the principles of receptor-mediated endocytosis. The other, putatively the prevailing mechanism (46) of LP interaction with EC, was proposed to be responsible for the transcytosis of LP across the aortic endothelial layer (17,45,50). This process was postulated to be receptor-independent in the case of LP, and to rely on uncoated pits and

vesicles which escape the classic endocytic pathway. In our specimens, although numerous labelled vesicular structures were visible, the inherent low contrast of the embedding method made their classification debatable. Apo B detection seemed to be related most of the time to these structures of the endothelium but the contribution of the intercellular routes to apo B passage can not be ruled out, judging only from the static picture of labelling. Apo B-containing LP were detected within the luminal interendothelial clefts and could conceivably continue to diffuse through the junctions. The fact that gold particles were not typically detected at the abluminal openings was tentatively interpreted by us as a suggestion that in vivo transjunctional traffic might be less important for the passage of apo B-containing LP across the normal aortic endothelium.

In an isolated aorta system, perfused with radioactive LP (38) after internalization HDL exited through vasa vasorum in contradistinction with LDL which returned back into the lumen of aorta. This type of LDL interaction with aorta would be in concordance with the detection of high apo B concentrations over and immediately beneath the luminal endothelium. In our specimens, a similar pattern of endogenous apo B distribution was noticed to be also associated with the endothelial layer of the vasa vasorum, implying that this is also permeable to LDL and/or VLDL. However, since the labelling of the interstitial space in between the subendothelial regions of the intima and adventitia was insignificant, this could mean that these areas do not exchange apo B-containing LP, or do it in quantities well below those detectable in our system. Some other factors - probably of extracellular nature - could limit LP distribution within the aortic wall (49).

The densities measured over normal smooth muscle cells were at the level of non-specific binding. This result would sustain the assumption that, in normal conditions SMC may not be involved in significant apo B uptake.

2.5.2. Endogenous apo B in injured aortas

From the comparison of corresponding areas within normal or injured aortas, some possibly relevant differences may emerge. Although normal and regenerated endothelium appeared similarly labelled - and presumably making LP equally available

within their respective aortic walls - the fate of apo B seemed to be different. In injured aortas, the labelling of SMC from both deendothelialized and reendothelialized areas was significantly higher than that of normal SMC ($p=0.009$). When compared with the normal situation, the values of interstitial concentrations were increased in both deendothelialized ($p=0.05$) and regenerated endothelium-covered areas ($p=0.03$). These values were also higher than the cellular density of apo B measured over the SMC of the same regions.

Taking these results into consideration, high endogenous apo B densities within the intimal extracellular areas were associated with the existence of an endothelial layer, whether normal or regenerated. Alternatively, detection of apo B accumulations within deeper interstitial space of aortic wall, was consistently associated with injury, and could be dependent on injury-induced modifications of the extracellular space characteristics. Regions covered by regenerated endothelium were particularly prone to the development of full blown lesions, as detected within the thickened areas.

The modified interaction of LP with the injured vessel wall might arise as a result of several, possibly interconnected, processes. The mechanism of endothelial-dependent modification of serum LP, presumably increasing their atherogenicity as assessed in vitro (40), might also be triggered in pathologic conditions in vivo. The regenerated endothelium could influence the general metabolism of the injured arterial wall (21), or act as a "reverse" barrier for LP (11,33). The complete absence of endothelium did not produce an increase in apo B concentrations in the superficial area of the deendothelialized aortic wall, but - quite the contrary - was associated with a significant shift towards the preponderance in deeper extracellular areas, hinting at another putative mechanism of LP accumulation. Rather than being dependent on easy entry, LP might face a difficult "escape" from altered surroundings. The pattern of uniform apo B association with the extracellular lipid vesicles of advanced lesions, favours the mechanism of lipid accumulating directly from trapped interstitial lipoproteins, versus their possible liberation from intracellular deposits of necrotic cells found in the lipid cores. In such a case, modified aortic extracellular matrix could contribute directly to entrapment and/or formation of atherogenic LP complexes, and possibly modulate the

cellular affinity for LP (1,9,46,51). Detection of the ultrastructural characteristics of extracellular accumulations and association of apo B might add a helpful insight regarding the still debated origin of the extracellular lipid of atherosclerotic lesions (10,20).

2.5.3. Endothelial-injury model of atherosclerosis

The typical presence of apo B accumulations in human atherosclerotic lesions is an established fact (5,24). Intimal depositions of apo B have also been repeatedly detected in the lesions of hypercholesterolemic animals (16,45). Consequently, we consider that demonstration of endogenous apo B accumulation, occurring in lesions induced by endothelial injury, in normocholesterolemic animals permits new considerations regarding an alternative mechanism of lipid accumulation. The results support the idea that in vivo triggering of foam cell formation and massive extracellular lipid accumulations are not necessarily conditioned by the modifications induced by hypercholesterolemia, of either blood components, or arterial wall properties.

Regarding our model, we are aware that large endothelial denudations of arterial tissue areas are not thought to actually occur in the pathogenesis of human atherosclerosis. There are however several special situations when this type of injury may be induced in humans as a result of therapeutic interventions, that should therefore be critically examined (12). More over, repeated small areas of endothelial injury, might serve as the stimulus of the development of a neointima which accumulates lipid (33).

In our case, we used this procedure since it provides the opportunity to study the role of endothelium in LP distribution within the aortic wall. This model also has the capacity of triggering the complex cascade of interactions and events that accompany the in vivo healing of the vessel wall. Significant information revealed by this model (34,42) was that advanced lesions selectively develop in areas covered by regenerated endothelium. Even more significant was the fact that the large spectrum of characteristics found in human, fibrofatty, atherosclerotic lesions was detected. In our specimens, they included, besides foam cells, smooth muscle cell proliferation, lipid and apolipoprotein extracellular accumulations, a combination of features otherwise difficult to obtain in experimental models.

It seems important to again emphasise the fact that the aortic tissue has been derived from animals with low levels of serum cholesterol (27.6 $\pm$ 6.5 mg/dl, n=8). With models of dietary-induced atherosclerosis, the appearance of discrete morphological changes was reported to occur as early as two weeks, but these were accompanied by serum cholesterol levels of as much as ten times the normal value (44,45). This kind of dramatic increase in circulating cholesterol, was capable of rapidly inducing lipid accumulations in many organs and tissues, including aorta (2). In this respect, the vascular consequences of tremendous increases in circulating cholesterol such as those described in experimental hypercholesterolemia, could be attributed to a specific type of challenge to the vessel wall (36).

In the mechanical injury model that we used, neither the aortic wall properties nor the circulating LP were altered by hypercholesterolemia. The process of the vessel wall healing appeared able to modulate by itself the events leading to the development of characteristic atherosclerotic lesions. At this point, one can only speculate on the possible mechanisms involved. The cellular components of the vessel wall exert reciprocal influences by secretion of soluble factors, through modified extracellular matrix-dependent signalling, and by direct cell-to-cell communication (19,21,28,30,36,41,43,51).

Dysfunction or activation of endothelium and other vascular cellular components in response to strong or sustained stress factors, might result in a similar outcome (19,34,36). Several other lines of evidence including the well known specific location of atherosclerotic lesions could be also cited in favour of the idea that the main part in the atherogenesis scenario may be played by the blood vessel itself.

Observations regarding the detailed distribution of native apo B, as a marker for VLDL and LDL, in normal and injured aortas, have been obtained by immunocytochemistry. The use of EM gold immunocytochemistry offers the advantage of a greatly improved resolution of apo B detection and enabled us to perform a morphometric analysis of the

labelling. Lesions that developed in the injured aortas of normocholesterolemic animals presented the characteristics of atherosclerotic lesions, including extracellular and

intracellular deposits of apo B.

2.6. METHODS

Materials

SDS-PAGE molecular weight markers, normal goat IgG, and the cholesterol assay kit were from Sigma Chem Co (MO, USA), as were the other chemicals, unless otherwise stated. Protein A and DEAE-Sephacel were purchased from Pharmacia (Que, Canada). Nitrocellulose (NC) membrane was from BioRad (CA, USA). The 4F Fogarty balloon catheters were from Edward Lab Inc (CA, USA), Lowicryl K4M from JBS (Que, Canada), and O.C.T. compound was from Miles Inc (IN, USA).

Animal model

The procedure of catheter-induced deendothelialization was performed as previously described (1), on four New Zealand rabbits anaesthetized with sodium pentobarbital (20 mg/kg body weight). During this procedure, a Fogarty catheter introduced through the femoral artery, was subsequently inflated with 0.5 ml saline at the level of the thoracic aorta. By withdrawing the inflated catheter three times inside the aorta, the endothelium was selectively removed. Four matched control animals were subjected to a sham operation limited to surgical exposure of a femoral artery. All animals were allowed to recover for six months while receiving a standard rabbit chow diet (LC-51301, Ralston Purina Canada Inc.).

LP isolation and characterization

Rabbit blood of donor normal animals was collected on EDTA (1mg/ml final concentration). LP fractions were prepared from serum using the sequential flotation procedure of Hatch and Lees (23). VLDL (floating at d = 1.006 g/ml KBr), IDL (d = 1.006 - 1.019 g/ml), LDL (d = 1.019 - 1.065 g/ml), and HDL (d = 1.065 - 1.210 g/ml) were isolated and characterized. All cholesterol concentrations of sera and isolated LP fractions were assayed using an enzymatic test (Sigma), according to the manufacturer's procedure.

Protein concentrations were estimated by the Bradford method (6), using bovine serum albumin as a standard. Rabbit serum and LP protein compositions were analyzed by electrophoresis in 3-8 % discontinuous polyacrylamide gels in the presence of SDS (SDS-PAGE) (26).

Protein A-gold conjugate

Gold colloidal particles of 10 nm were prepared according to Muhlpfordt (35). The size and uniformity of gold particles were checked by measurements made on EM prints of gold sol samples spread on parlodion-coated grids.

The protein A-gold probes were obtained by stabilizing the gold sol with protein A and ultracentrifugation as described by Bendayan (4).

Antibody preparation and characterization

The anti-rabbit apo B serum was obtained by immunizing a goat against the LDL fraction isolated from normal rabbit serum. The goat serum was reprecipitated three times with a saturated solution of ammonium sulphate, in the ratio of 2:1 (vol/vol) for isolation of the IgG fraction. The third precipitate was selected based on immunodiffusion results, dialysed against 10 mM potassium phosphate buffer and fractionated by ion exchange chromatography on a DEAE-Sephacel column attached to a FPLC System (Pharmacia, Uppsala, Sweden). Protein compositions of consecutive peaks eluted by a 0-0.5 M NaCl gradient in starting buffer, were analyzed by SDS-PAGE, either in the presence or absence of 11 mM dithiothreitol (DTT). The antigen-recognizing capacity of ion-exchange fractions was tested by radial immunodiffusion against normal rabbit serum.

Anti-apo B specificity of the isolated IgG was investigated by immunoelectrophoresis, immunodotting, and Western blotting.

Immunodots and Western blotting

For immunodotting, rabbit serum and each of its isolated LP fractions, were adjusted to the same protein concentration in 10 mM Na phosphate, pH 7.4, containing 8.5 g/l of NaCl (PBS). 1 μl aliquots from 15 μg protein/ml samples were applied as spots

onto a NC membrane.

For Western blotting, the LP fractions were delipidated prior to electrophoresis by an ethanol-ether extraction procedure (31). Equal quantities of total protein (50 μg) were applied to each lane. Solubilization was obtained by boiling for 5 min in dissociating sample buffer, containing 1% SDS and 11 mM DTT. Molecular weight (MW) markers were applied concomitantly. At the end of migration, the gel was subjected to electrophoretic transfer on NC membrane, using the NovaBlot dry system (Pharmacia - LKB, Canada), as recommended in the technical manual. Ethanol was omitted from the blotting buffer in order to enhance the transfer of high molecular weight proteins.

Subsequently, the same immunodetection procedure was used for either the dotted or electrophoretically-transferred proteins. The membranes were incubated in blocking buffer (PBS containing 1% BSA and 0.05% Tween 20) for 15 min at room temperature, then primary antibody from a 2.5 mg/ml stock solution was added to a final 1/100 dilution. After two hours, the non-specifically bound antibody was washed away by 3 x 5 min consecutive changes of blocking buffer supplemented with 1% gelatin. The membranes were incubated with protein A-gold diluted in the gelatin-supplemented blocking buffer for 20 min. Eventually, the membranes were dried after being extensively washed with several changes of PBS and distilled water.

Tissue preparation

30 min before sacrificing the animals, blood samples were drawn for cholesterol assay. Subsequently, 5 ml of 0.45% (wt/vol) Evans Blue in saline were injected in their marginal ear veins. This dye has been shown to stain areas of increased permeability in blood vessels (11), contributing to an easier delineation of the different regions of injured aorta. By this procedure, areas of regenerated endothelium, originating from the intercostal branches orifices, appear as white patches on the blue background representing areas devoid of endothelium (1,11,32).

After anaesthetizing the animals, the blood was flushed away by perfusing PBS at 37^0 C and physiologic pressure through cardiac puncture. The aortas were excised after

being fixed in situ for 10 min with 4% paraformaldehyde and 0.5% glutaraldehyde in 100 mM Na phosphate buffer pH 7.4. The tissue pieces were fixed overnight and further processed for either light or electron microscope immunocytochemistry.

For LM, transverse 5 μm frozen sections of either normal or injured aortas were cut from O.C.T. embedded tissues.

For EM, aortas were opened longitudinally and the tissue was divided according to macroscopic appearance into four categories. They included: from control animals, normal aortic tissue; from injured animals, "blue" areas representing deendothelialized tissue, "white" areas which were covered by regenerated endothelium, and markedly thickened lesions of aorta. Small pieces derived from each type of aortic tissue were embedded at low temperature in Lowicryl K4M (4) in order to enhance the preservation of antigenicity.

Thin sections were mounted on parlodion-coated nickel grids and used for post-embedding immunostaining.

Immunocytochemical staining

Essentially, the same immunostaining sequence was performed, both for LM and EM immunocytochemistry. Several concentrations of the primary antibody and protein A-gold were tested. The sections were reacted with the primary antibody, and then the primary antibody was detected by protein A-gold.

For LM immunocytochemistry, an additional step representing a silver enhancement reaction of the gold labelling was applied (29).

For thin section labelling, the protein A-gold post-embedding immunocytochemical technique (4) was used.

Routinely, during this procedure grids were sequentially:

- floated face-down for 10 min on 20 μl drops of 1% ovalbumin in PBS

- applied on drops of optimally diluted primary antibody and incubated 2 h in a moist chamber at room temperature.

- washed for 3 x 5 min with PBS

- incubated in the same manner with protein A-gold conjugate for 30 min
- washed for 3 x 5 min with distilled water

The sections were counterstained with uranyl acetate and lead citrate and examined on a Philips microscope at 60 kV.

Immunocytochemical controls

The specificity of the primary antibody was checked by its replacement with either an equal concentration of normal goat IgG or, with antigen-preadsorbed antibody. Specificity of protein A-gold labelling was tested by omitting the primary antibody from the staining procedure.

Morphometric analysis

For each animal, prints derived from several histological fields for each condition were magnified at x 44,460. The precise magnifications of micrographs were estimated from measurements made with a calibration grid (2160 lines/mm, Pelco Int, CA). The morphometric measurements were made with a Videoplan Image Processing System (Kontron Bild Analyse, Germany). The density of gold labelling, expressed as number of particles per μm^2 of real tissue, was calculated by dividing the number of gold particles found over a certain morphologic component to its corresponding area. For morphometric quantification, all samples were processed using identical dilutions of the primary antibody and protein A-gold.

Cellular areas containing nuclei were not included for measurements to reduce the variations in apo B concentration due to the inconsistent occurrence of these unlabelled structures. The intracellular areas occupied by large lipid inclusions have been subtracted from the total area of foam cells. Within the extracellular space, we arbitrarily defined the "subendothelial space" as extending down to 2.2 μm beneath the endothelial layer, the rest being operationally called "interstitial space". The same spatial delimitation was made in the deendothelialized areas, starting the measurement from the luminal front.

For each morphological compartment, seven values of labelling densities measured over multiple areas of the same animal were averaged (Fig. 14). Gold particle density on

control specimens incubated with normal goat IgG was used as reference for non-specific labelling. The data were analyzed using a SYSTAT software package (SYSTAT Inc., IL, USA). The homogeneity of group variances was checked using the Bartlett's test and the significance of differences between mean labelling values was verified by one way ANOVA with repeated measure on one factor. Individual comparisons were made by paired t-tests.

2.7. ACKNOWLEDGEMENTS

This work was supported by grants from the Medical Research Council of Canada (MRC MT - 10590) and Heart and Stroke Foundation, Quebec. Z. Galis is a recipient of FCAR (Fonds pour la Formation de Chercheurs et l'Aide à la Recherche) and Royal Victoria Research Institute Fellowships. L. Ghitescu receives a Medical Research Council of Canada Fellowship, and Z. Li a Max Binz Studentship from the McGill Graduate Faculty. M.Z. Alavi is a Medical Research Scholar of the Canadian Heart and Stroke Foundation.

We thank Drs. Jim Hanley and Istvan Huttner (from Dept. of Epidemiology & Biostatistics, and Pathology, McGill University, respectively) for advice regarding the statistical analysis and for helpful comments. The generous support of Dr. Moise Bendayan (Université de Montréal) is gratefully acknowledged. Leng Tsao and Robert Sawka provided excellent technical assistance.

2.8. REFERENCES

1. Alavi MZ, Moore S: Kinetics of low density lipoprotein interactions with rabbit aortic wall following balloon catheter deendothelialization. Arteriosclerosis 4:395, 1984

2. Altschul, R: Selected studies on atherosclerosis. Springfield, Illinois, Charles C. Thomas Publ., 1950

3. Anitschow N, Chalatow S: On experimental cholesterin steatosis and its significance in the origin of some pathological processes, translated version of 1913' original paper. Arteriosclerosis 3:178, 1983

4. Bendayan M: Protein A - gold electron microscopic immunocytochemistry: Methods, applications, and limitations. J Electron Microsc Tech 1:243, 1984

5. Bocan TMA, Brown SA, Guyton JR: Human aortic fibrolipid lesions. Immunocytochemical localization of apolipoprotein B and apolipoprotein A. Arteriosclerosis 8:499,1988

6. Bradford HM: A rapid and sensitive method for the quantitation of microgram quantities of protein utilizing the principle of protein-dye binding. Anal Biochem 72:248,1976

7. Brown MS, Goldstein JL: Plasma lipoproteins: Teaching old dogmas new tricks. Nature 330:132, 1987

8. Brown MS, Goldstein JL: Lipoprotein metabolism in the macrophage: implications for cholesterol deposition in atherosclerosis. Ann Review Biochem 52: 223, 1983

9. Camejo G: The interaction of lipids and lipoproteins with the intercellular matrix of arterial tissue: its possible role in atherogenesis. Adv Lipid Res 19:1, 1982

10. Chao FF, Blanchette-Mackie EJ, Chen YJ, Dickens BF, Berlin E, Amende LM, Skarlatos SI, Gamble W, Resau JH, Mergner WT, Kruth HS: Characterization of two unique cholesterol-rich lipid particles isolated from human atherosclerotic lesions. Am J Pathol 136:169, 1990

11. Clowes AW, Collazo RE, Karnowsky MJ: A morphologic and permeability study of luminal smooth muscle cells after arterial injury in the rat. Lab Invest 39:141, 1978

12. Cushing GL, Gaubatz JW, Nava ML, Burdick BJ, Bocan TMA, Guyton JR, Weilbaecher D, DeBakey ME, Lawrie GM, Morrisett JD: Quantitation and localization of apolipoproteins[a] and B in coronary artery bypass vein grafts resected at re-operation. Arteriosclerosis 9:593, 1989

13. Dory L, Sloop CH, Roheim PS: Interstitial fluid (peripheral lymph) lipoproteins. Meth Enzymol 129:660, 1986

14. Editorial: Apolipoprotein B and atherogenesis. Lancet 1:1141, 1988

15. Falcone DJ, Hajjar DP, Minick CR: Lipoprotein and albumin accumulation in reendothelialized and deendothelialized aorta. Am J Pathol 114:112, 1984

16. Feldman DL, Hoff HF, Gerrity RG: Immuno-histochemical localization of apoB in aortas of hypercholesterolemic swine. Preferential accumulation in lesion-prone areas. Arch Pathol Lab Med 108:817, 1984

17. Fogelman AM, Berliner JA, Van Lenten BJ, Navab M, Territo M: Lipoprotein receptors and endothelial cells. Sem Thromb Hemost 14:206, 1988

18. Frank JS, Fogelman AM: Ultrastructure of the intima in WHHL and cholesterol-fed rabbit aortas prepared by ultra-rapid freezing and freeze-etching. J Lipid Res 30:967, 1989

19. Gimbrone MA Jr: Endothelial dysfunction and the pathogenesis of atherosclerosis. In Atherosclerosis VII, edited by Fidge NH, Nestel PJ. p 367. Amsterdam, Elsevier, 1986

20. Guyton JR, Klemp KF: The lipid-rich core region of human atherosclerotic fibrous plaques. Prevalence of small lipid droplets and vesicles by electron microscopy. Am J Pathol 134:705, 1989

21. Hajjar DP, Falcone DJ, Fowler S, Minick CR: Endothelium modifies the altered metabolism of the injured aortic wall. Am J Pathol 102:28, 1981

22. Hansson GK, Jonasson L, Seifert PS, Stemme S: Immune mechanisms in atherosclerosis. Arteriosclerosis 9:567, 1989

23. Hatch FT, Lees RS: Practical method for plasma lipoprotein analysis. Adv Lipid Res 6:1, 1968

24. Hoff HF, Heideman CL, Gaubatz JW, Scott DW, Gotto AM: Detergent extraction

of tightly bound apo B from extracts of normal aortic intima and plaques. Exp Mol Pathol 28:290, 1978

25. Huttner I, Walker C, Gabbiani G: Aortic endothelial cell during regeneration. Remodeling of junctions, stress fibers, and stress fiber-membrane attachment domains. Lab Invest 53:287, 1985

26. Laemmli UK: Cleavage of structural proteins during the assembly of the head of bacteriophage T4. Nature 227:680, 1970

27. Langeler EG, Snelting-Havinga I, van Hinsbergh VWM: Passage of low density lipoproteins through monolayers of human arterial endothelial cells. Arteriosclerosis 9:550, 1989

28. Madri JA, Reidy MA, Kocher O, Bell L: Endothelial cell behaviour after denudation injury is modulated by transforming growth factor-B1 and fibronectin. Lab Invest 60:755, 1989

29. Manigley C, Roth J: Applications of immunocolloids in light microscopy. Use of photochemical silver staining in a simple and efficient double-staining technique. J Histochem Cytochem 33:1247, 1985

30. McNeil PL, Muthukrishnan L, Warder E, D'Amore PA: Growth factors are released by mechanically wounded endothelial cells. J Cell Biol 109:811, 1989

31. Mills GL, Lane PA, Wee PK: The chemical characterization of lipoproteins. In A guide book to lipoprotein technique. Laboratory techniques in biochemistry and molecular biology 14, edited by Burdon RH, van Knippenberg PH, p 221. Amsterdam, Elsevier, 1984

32. Minick CR, Stemerman MB, Insull W: Role of endothelium and hypercholesterolemia in intimal thickening and lipid accumulation. Am J Pathol 95:131, 1979

33. Moore S: Thrombosis and atherogenesis - The chicken and the egg. Ann NY Acad Sci 454:146, 1984

34. Moore S: Endothelial injury and atherosclerosis. Exp Mol Pathol 1979;31:182-190

35. Muhlpfordt H: The preparation of colloidal gold particles using tannic acid as an additional reducing agent. Experientia 38:1127, 1982

36. Munro MJ, Cotran RA: Biology of disease. Pathogenesis of atherosclerosis:

Atherogenesis and inflammation. Lab Invest 58:249, 1988

37. Nerem RM, Levesque MJ, Logan SA, Schwartz CJ, Sprague EA: Biologic responses of vascular endothelial cells to shear stress. In Atherosclerosis VIII, edited by Crepaldi G, Gotto AM, Manzato E, Baggio G, p 421. Amsterdam, Elsevier, 1989

38. Nordestgaard BG, Hjelms E, Stender S, Kjeldsen K: Different efflux pathways for high and low density lipoproteins from porcine aortic intima. Arteriosclerosis 10:477, 1990

39. Nordoy A, Goodnight SH: Dietary lipids and thrombosis. Relationship to atherosclerosis. Arteriosclerosis 10:149, 1990

40. Parthasarathy S, Quinn MT, Schwenke DC, Carew TE, Steinberg D: Oxidative modification of beta-very low density lipoprotein. Potential role in monocyte recruitment and foam cell formation. Arteriosclerosis 9:398, 1989

41. Pomerantz KB, Hajjar DP: Eicosanoids in regulation of arterial smooth muscle cell phenotype, proliferative capacity, and cholesterol metabolism. Arteriosclerosis 9:413, 1989

42. Richardson M, Alavi MZ, Moore S: Rabbit models of atherosclerosis. In Atherosclerosis and arteriosclerosis: Human pathology and experimental animal methods and models, edited by White RA, p 163. Florida, CRC Press, 1989

43. Ross R: The pathogenesis of atherosclerosis - An update. N Engl J Med 314:488, 1986

44. Schwenke DC, Carew TE: Initiation of atherosclerotic lesions in cholesterol-fed rabbits. Arteriosclerosis 9:895, 1989

45. Simionescu N: Prelesional changes of arterial endothelium in hyperlipoproteinemic atherogenesis. In Endothelial cell biology in health and disease, edited by Simionescu N, Simionescu M, p 385. New York and London, Plenum Press, 1988

46. Srinivasan SR, Vijayagopal P, Dalferes ER Jr, Abbate B, Radhakrishnamurthy B, Berenson GS: Low density lipoprotein retention by aortic tissue. Contribution of extracellular matrix. Atherosclerosis 62:201, 1986

47. Steinberg D: Lipoproteins and the pathogenesis of atherosclerosis. Circulation 3:508, 1987

48. Steinberg D, Pittman RC, Carew TE: Mechanisms involved in the uptake and degradation of low density lipoprotein by the artery wall in vivo. Ann NY Acad Sci 454:195, 1985

49. Thompson WD, Smith EB: Atherosclerosis and the coagulation system. J Pathol 159:97, 1989

50. Vasile E, Simionescu M, Simionescu N: Visualisation of the binding, endocytosis and transcytosis of low density lipoproteins in the arterial endothelium in situ. J Cell Biol 96:1677, 1983

51. Vijayagopal P, Srinivasan SR, Radhakrishnamurthy B, Berenson GS: Factors regulating the metabolism of low-density lipoprotein-proteoglycan complex in macrophages. Biochim Biophys Acta 1024:204, 1990

CHAPTER 3

IN SITU ULTRASTRUCTURAL CHARACTERIZATION OF CHONDROITIN SULFATE PROTEOGLYCANS IN NORMAL RABBIT AORTA

0022-1554/92/$3.30
The Journal of Histochemistry and Cytochemistry

Vol. 40, No. 2, pp. 251–263, 1992
Printed in U.S.A.

Original Article

In Situ Ultrastructural Characterization of Chondroitin Sulfate Proteoglycans in Normal Rabbit Aorta[1]

ZORINA S. GALIS,[2] MISBAHUDDIN Z. ALAVI, and SEAN MOORE

Department of Pathology, McGill University, Montreal, Quebec, Canada.

Received for publication May 7, 1991 and in revised form September 10 1991; accepted September 14, 1991 (1A2321).

We used a monoclonal antibody recognizing chondroitin sulfate (CS) to investigate by immunocytochemistry the characteristics displayed in situ by aortic proteoglycans (PG) containing CS side chains. The antibody specifically precipitated metabolically labeled PG from aortic extracts. Anti-CS specificity was also tested directly on tissue sections and was confirmed by the virtual abolition of immunolabeling on those previously digested with CS-specific enzymes. The overall CS-PG distribution assessed by light microscopy after embedding in Lowicryl KM4 by silver-enhanced immunogold recapitulated that obtained on frozen sections with immunoperoxidase. Extracellular concentrations of CS-PG were very high in the innermost regions of aorta and decreased in the media. The reaction was weak and diffuse in the adventitia. By electron microscopy, the detailed labeling of CS-PG discriminated patterns of organization at both the regional and the molecular level and enabled morphometric estimations. In relation to other components of the extracellular matrix, we found that CS-PG and elastin mutually excluded each other, while two types of CS-PG were differently associated with collagen within media or adventitia. The use of high-resolution immunodetection for the in situ characterization of aortic CS-PG could add specific information relevant to many biological processes in which these molecules have been implicated. (*J Histochem Cytochem 40:251–263, 1992*)

KEY WORDS: Chondroitin sulfate proteoglycans; Normal rabbit aorta; Gold immunocytochemistry; Extracellular matrix.

Introduction

Proteoglycans (PG) are ubiquitous molecules that comprise an extremely diverse family of both cell-associated and extracellular species (9,28). Their common classification as PG is based on their property of possessing one or several side chains of glycosaminoglycans (GAG) attached to a central protein core. The potentially limitless diversity of PG molecular composition and conformation is due to both particular proteins and types of GAG chains that may be combined in various proportions (12,21,25). Throughout the body, the biochemical diversity of PG is the basis of their functional versatility (11,13,29,36).

The arterial wall alone is known to produce several distinct PG that possess binding sites for other components of the extracellular matrix, such as hyaluronic acid (HA), fibronectin, laminin, and collagen (21,29,36). Consequently, aortic PG are considered important organizers of the tridimensional extracellular architecture, responsible among others for maintenance of the viscoelastic and permeability characteristics of the vessel wall. Several types of "large" and "small" CS-PG have been extracted from arterial tissue and cultured vascular cells or, alternatively, have been detected by histological and immunocytochemical techniques (14,16,18,22,25,35,36). It is worth mentioning that among several species included in comparative biochemical studies, rabbit aortas have been found to have the closest GAG composition to human aorta (1). Defining some of the normal characteristics of rabbit aorta has potential relevance for one of the most extensively used animal models of atherosclerosis (26). Particular forms of GAG composition, rather than those of whole PG molecules, have been previously investigated in relation to angiogenesis, cell adhesion, migration and differentiation, and aging and atherosclerosis (24,26,29, 36), and have often been found to be associated with alterations of the chondroitin sulfate content of normal arterial tissue.

We investigated those aortic PG of normal rabbit aorta that contain CS by using an antibody to CS moieties. The preservation of the in situ PG distribution, as well as of their relation to other elements of the extracellular matrix, was facilitated by the use of immunocytochemistry. In an attempt to gain a more detailed insight into CS-PG organization, a monoclonal antibody recognizing small epitopes on their lateral chains was used in conjunction with the high resolution of EM immunogold.

Materials and Methods

Protein A and protein A–Sepharose were from Pharmacia (Uppsala, Sweden).

[1] Supported by grants from the Medical Research Council of Canada and the Heart and Stroke Foundation of Quebec. ZSG receives fellowships from Fonds pour la Formation de Chercheurs et Aide à la Recherche and the Royal Victoria Research Institute.

[2] Correspondence to: Zorina Galis, Dept. of Pathology, McGill University, 3775 University, Montreal, Quebec, Canada H3A 2B4.

Anti-chondroitin sulfate monoclonal antibodies, anti-mouse IgM (μ-chain specific) conjugated with 10-nm colloidal gold particles, chondroitinase ABC (EC 4.2.2.4), chondroitinase AC (EC 4.2.2.5), and hyaluronidase type X (EC 3.2.1.36) were from Sigma (St Louis, MO). Unlabeled rabbit anti-mouse Ig and the avidin–biotin immunocytochemical system were purchased from Dakopatts (Glostrup, Denmark), $Na_2{}^{35}SO_4$ and Cytoscint scintillation cocktail were from ICN Biomedicals Canada (Quebec, Canada), and OCT embedding medium for frozen sections was from Miles (Elkhart, IN).

Anti-CS Antibodies

The monoclonal antibodies have been previously described (2) as being IgM species that recognize the repetitive disaccharidic units of CS chains type A and C, but not of CS B (dermatan sulfate). Both CS A and CS C species are designated in the text as CS for the sake of simplicity. We tested the antibodies' capacity to immunoprecipitate CS-containing molecules from an extract of normal rabbit aorta.

Preparation and Characterization of the Aortic Extract

Aortas of five New Zealand rabbits killed by an overdose of sodium pentobarbital (60 mg/kg body weight), in accordance with the internal guidelines for care and use of laboratory animals, were quickly harvested under sterile conditions. For metabolic labeling of sulfated PG (24), the intimal–medial layers peeled off each aorta were separately incubated for 2, 4, 6, 8, or 12 hr with 1 mCi ^{35}S in 10 ml sterile Hank's balanced salt solution (HBSS) + 10% rabbit serum at 37°C and in a controlled gaseous atmosphere (95% O_2 + 5% CO_2). Tissue was washed with three changes of cold HBSS and low-speed centrifugation and was gently homogenized. A soluble aortic fraction was obtained after ultracentrifugation for 60 min at 100,000 × g. The pellets were further extracted overnight at 4°C with 4 M guanidinium hydrochloride (GuHCl) in the presence of protease inhibitors under constant stirring (23), filtered, and re-centrifuged for 60 min at 100,000 × g. After the extensive dialysis of supernatants against distilled water, their GAG and protein contents were assayed using alcian blue (3) and amido black (32), respectively. Metabolically incorporated radioactivity was measured by liquid scintillation.

GAG Composition

Aortic extracts were digested overnight at 37°C with papain (25:1 protein/enzyme, w/w) in 50 mM Tris-HCl, pH 8.8, containing 10 mM EDTA and 10 mM cysteine hydrochloride. Further, samples were first precipitated with trichloroacetic acid (TCA) (6% final concentration) and then with absolute ethanol in the presence of Na-acetate-saturated solution (1:4:1, v/v/v). The second precipitate was vacuum-dried, re-suspended in distilled water, and analyzed for GAG composition by cellulose acetate electrophoresis in a Gelman Semi-micro apparatus, using 0.3 M Ca-acetate buffer, pH 8, 1 mA/cm, for 1.5 hr. A GAG standard mixture was simultaneously electrophoresed. The cellulose membrane was stained with alcian blue (3), then dried and exposed for autoradiography. The relative compositions of the total and the newly synthesized GAG were estimated on the alcian-stained cellulose membrane or X-ray film, respectively, using a Hoeffer GS-300 scanning densitometer equipped with GS-360 software.

PG Characterization

The 12-hr aortic incubate having the highest activity per μg protein was used for digestion with specific GAG enzymes and immunoprecipitation. Aliquots of 100 μl were incubated overnight at 37°C with either chondroitinase ABC (1 U/ml) in Tris-acetate buffer, pH 8.0, or hyaluronidase (170 U/ml) in NaCl-acetate buffer, pH 5.4 (30). For control, the enzyme was replaced by a corresponding volume of distilled water. Incubation was stopped by adding TCA to all samples. TCA-soluble radioactivity was comparatively assayed by liquid scintillation counting of the supernatants. Protein composition of the pellets was analyzed by SDS-PAGE.

Immunoprecipitation Procedure

Fifteen mg of protein A–Sepharose, 900 μl PBS (10 mM Na-phosphate, pH 7.2, 9 g/liter NaCl), and 100 μl anti-mouse Ig antibodies were incubated in duplicate for 4 hr at room temperature in Eppendorf tubes. The secondary antibody had to be used because of the low protein A affinity for mouse monoclonals. Unbound anti-mouse Ig was washed away by repeated centrifugation (three times for 5 min, 2500 rpm) of the Sepharose gel in PBS, using a Baxter Biofuge A (Canlab; Quebec, Canada).

Aortic extract (500 μl) was mixed with 100 μl of fivefold concentrated solubilizing buffer (1 ml 1.0 M Na-phosphate, pH 7.2, 0.9 g NaCl, 1 ml Triton X-100, 0.5 g Na-deoxycholate, 0.1 g Na-dodecyl sulfate (SDS), 0.2 g Na-azide, 40 mg Na-fluoride brought to 25 ml with distilled water) and incubated for 30 min at 37°C with 10 μl of anti-CS antibodies, by end-over-end continuous agitation.

The secondary antibody specifically bound to the protein A–Sepharose and the antigen–primary antibody mixture were incubated together overnight at 4°C, in the same end-over-end motion. A control tube lacking the primary antibody was similarly processed. The gel was washed with solubilizing buffer by centrifugation (four times for 5 min, 2500 rpm). Finally, the sedimented gel was solubilized along with other samples for SDS-PAGE.

SDS-PAGE

SDS-PAGE (15) was performed in a Protean II apparatus (Biorad; Richmond, CA), using a 16-cm long 5–15% gradient with a 3% stacking gel. The samples were solubilized by 5-min boiling in denaturing sample buffer containing 0.1% SDS and 11 mM dithiothreitol. Pre-stained molecular weight (MW) markers were concomitantly applied. At the end of the run, the gel was soaked in 1 M Na-salicylate for enhancement of autoradiography (5), dried, and exposed to an X-ray film at −70°C for 7 days.

Protein A–Gold Conjugate Preparation

Colloidal gold particles of 10 nm were stabilized with protein A (10). Protein A–gold complexes were separated by ultracentrifugation and diluted with PBS to a final concentration corresponding to an optical absorbance at 515 nm, $A_{515nm} = 0.5$.

Tissue Collection and Processing

Five New Zealand male rabbits were sacrificed with an overdose of sodium pentobarbital (60 mg/kg body weight). The aortas were excised, washed briefly with ice-cold PBS, and individually collected in cold fixative (4% formaldehyde and 0.5% glutaraldehyde in 100 mM Na-phosphate, pH 7.4). For immmunoperoxidase, 1–2-mm thick full-circumference segments were embedded in OCT and frozen at −70°C. For detection of CS post embedding, pieces of 1-mm^2 aortic tissue were cut, fixed overnight, and processed by low-temperature (−20°C) embedding in Lowicryl K4M (4). Semi-thin sections on formvar-coated glass slides and thin sections on nickel grids covered with parlodion were further submitted to gold immunostaining.

Immunoperoxidase Staining on Frozen Sections

Transverse frozen sections of 5 μm were collected on clean glass slides, air-dried for 30 min, fixed in acetone (4°C), and further dried overnight. The sections were placed for 10 min in 1% bovine serum albumin (BSA) dissolved in Tris buffer (50 mM Tris-HCl, pH 7.6) and incubated for 1 hr at 37°C with the anti-CS antibody (1:200 in Tris buffer + 0.1% BSA). Excess antibody was washed off with Tris buffer (twice for 10 min). The sections were incubated for 20 min with 1:500 biotinylated rabbit anti-mouse Ig at 37°C and then washed with Tris buffer (twice for 10 min). Ten μl avidin and 10 μl HRP, as supplied in the kit by the manufacturer, were mixed in 1 ml Tris buffer and applied over the sections (20 min). After two 10-min washes the enzymatic reaction was developed with diaminobenzidine (5 mg to 10 ml Tris buffer + 5 μl H_2O_2) and stopped with cold water. The sections were counterstained with Mayer's hematoxylin and then mounted with permount.

Gold Immunocytochemistry

We tested two separate sequences of immunoreagents based on detection with different gold probes. A three-step procedure had a sequence represented by anti-CS, anti-mouse Ig, and protein A–gold; the other was a two-step procedure using anti-CS followed by anti-mouse IgM–gold conjugate.

All incubations were performed at room temperature in a moist chamber. Immunoreagents were diluted in PBS. In our hands, the following dilutions were found optimal: 1:200 anti-CS, 1:30 anti-mouse Ig, and 1:5 anti-IgM–gold conjugate. Gold probes were microfuged just before use.

CS-PG Detection at LM by Silver-enhanced Immunogold on Semi-thin Sections. Ovalbumin (1%) was layered over the semi-thin sections for 10 min, and the excess was removed with filter paper. The sections were incubated with anti-CS antibody (2 hr). Unbound antibody was washed off with PBS (three times for 5 min). Sections were covered with the anti-mouse IgM–gold conjugate (A_{520nm} = 1) for 30 min and then washed with distilled water (three times for 5 min). Gold staining was enhanced for LM detection by the chemical development of gold particles with silver supplied as silver acetate (27).

CS-PG Detection on Thin Sections. The protein A–gold staining protocol was essentially the same as that described by Bendayan (4). The grids were floated onto drops of 1% ovalbumin for 10 min, then transformed onto the anti-CS antibody (2 hr). The grids were washed with PBS (three times for 5 min) and incubated with anti-mouse Ig (1 hr). The excess secondary antibodies were removed by three 5-min PBS washes. Grids were floated for 30 min on drops of protein A–gold and finally washed with distilled water (three times for 5 min).

A similar procedure was used to detect the antigen with anti-CS antibodies followed by anti-mouse IgM–gold conjugate.

Different methods were tried for thin section staining in an attempt to improve the inherent low contrast of the Lowicryl sections. The grids were stained for variable lengths of time with either 2% aqueous or 5% methanolic uranyl acetate (8), and Reynold's lead citrate.

Morphometric Evaluation

The distribution of the immunoperoxidase reaction product across the aortic wall was estimated with a Hoeffer scanning densitometer on 10 randomly taken LM prints presenting the entire thickness of aorta. The relative values of optical densities were computer-integated over successive equal intervals within the vessel wall. By plotting the average values vs the distance from the luminal front, one can estimate the relative distribution of the antigen across the section from the partition of the immunoperoxidase reaction.

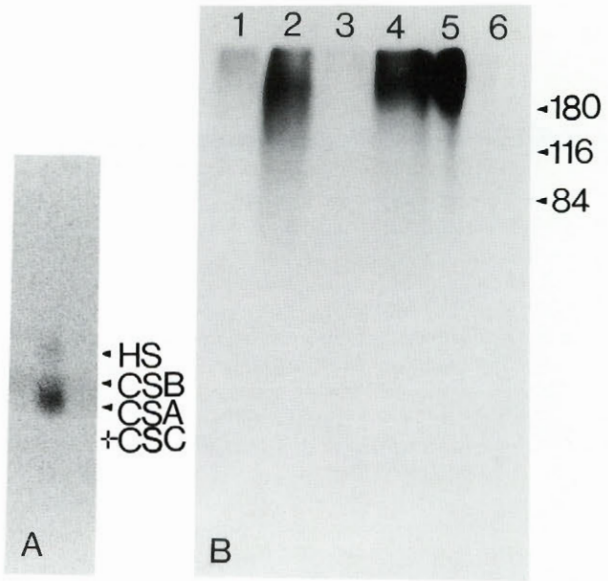

Figure 1. Autoradiographic image of (**A**) cellulose acetate and (**B**) SDS-PAGE electrophoresis of ^{35}S-labeled components extracted from normal rabbit aorta. (**A**) GAG moieties: heparan sulfate (HS), dermatan sulphate (CS B), CS A and CS C. (**B**) Sulfated PG in a 5–15% gradient gel: (1) Soluble aortic fraction; (2) GuHCl extract; (3) Same as 2 after digestion with chondroitinase ABC; (4) Same as 2 after digestion with hyaluronidase; (5) Immunoprecipitate of 2 obtained using anti-CS antibodies; (6) Control for immunoprecipitation. MW (KD) of markers run in parallel are indicated.

The morphometric analysis of the lengths of gold-labeled structures was performed on EM prints at × 44,460 magnification, using a videoplan processing system. The actual magnification was estimated by comparison with a calibration grid (2160 lines/mm; Pelco Int., Tustin, CA).

Immunocytochemical Controls

The specificity of CS-PG detection was tested with both first and second level immunocytochemical controls (17). They consisted of: (a) omission of the primary antibody, either alone or, in the case of the three-step procedure, also with the secondary antibody altogether; (b) use of pre-adsorbed primary antibodies; and (c) substitution of the primary antibodies with irrelevant monoclonal antibodies of the same Ig class.

As an additional way of checking the primary antibody specificity, the effects of previous selective enzymatic digestions of sections were evaluated. Grids were incubated for variable lengths of time at 37°C with either chondroitinase ABC or AC diluted with Tris-acetate buffer, pH 8 (30), to different specific activities.

Results

Biochemical Experiments

Chondroitinase ABC digestion increased TCA-soluble radioactivity of the extract from 45.1% to 92.6%. This susceptibility showed that ^{35}S was preferentially incorporated into CS moieties. The main sulfated GAG synthesized de novo by aortic explants were CS A and CS C (Figure 1A). The appropriateness of [^{35}S]-PG as a sample of normal aortic CS-PG was confirmed by the similarity be-

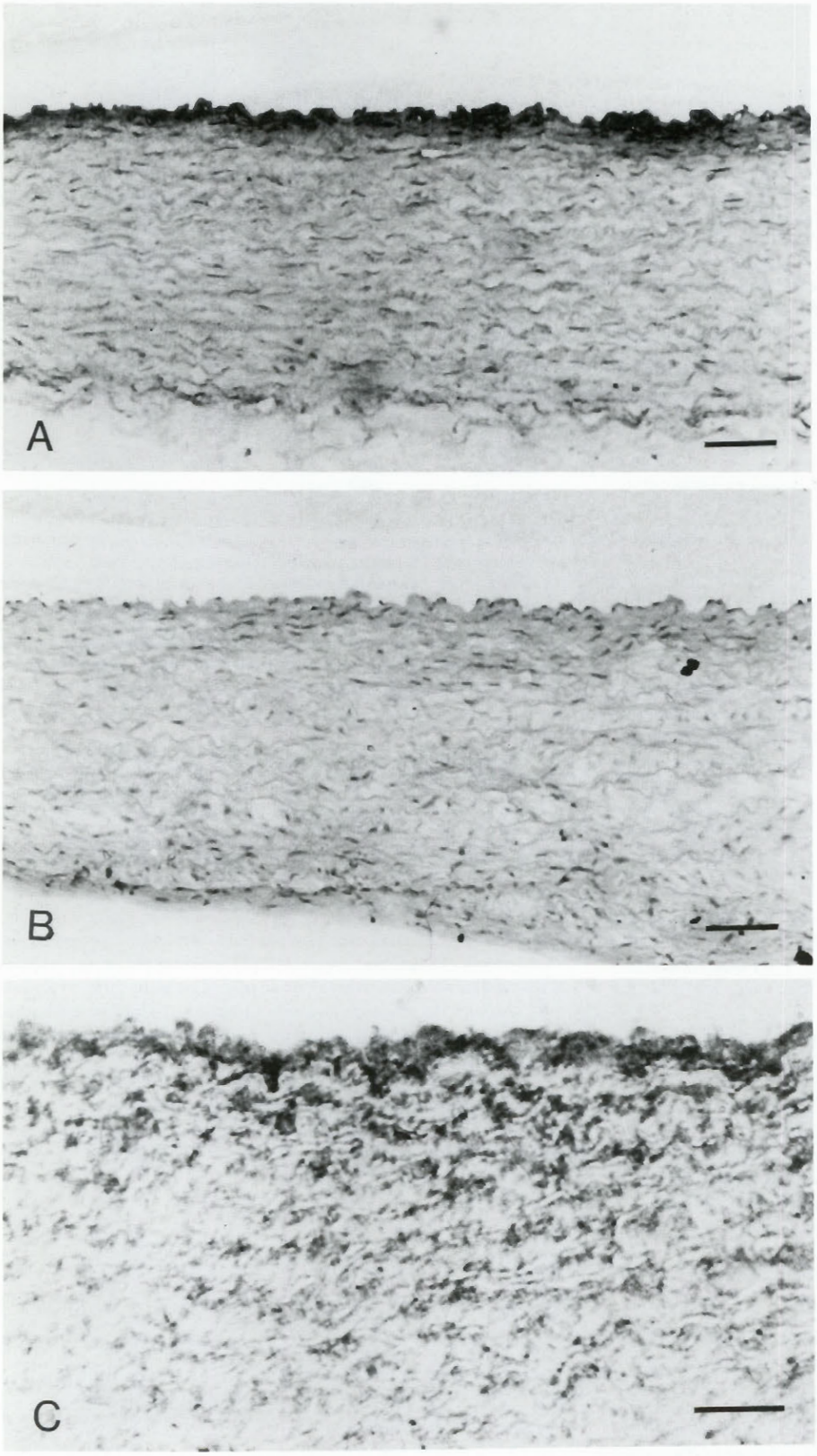

Figure 2. LM immunocytochemistry for CS-PG detection in normal rabbit aorta. The entire thickness of the aortic wall was positively stained. The highest labeling concentrations were found in the innermost regions of aortic wall. Frozen sections: (**A**) immunostaining with anti-CS, biotinylated secondary antibodies and avidin/HRP and (**B**) control similarly processed but with omission of primary antibody. Mayer's hematoxylin counterstain. (**C**) Silver-enhanced immunogold on Lowicryl K4M semi-thin section. Anti-CS, followed by anti-IgM–gold conjugate and silver development (no counterstain). The wavy pattern of labeling runs parallel to the aortic elastic laminae. Original magnifications: **A**,**B** × 500; **C** × 1250. Bars: **A**,**B** = 20 μm; **C** = 10 μm.

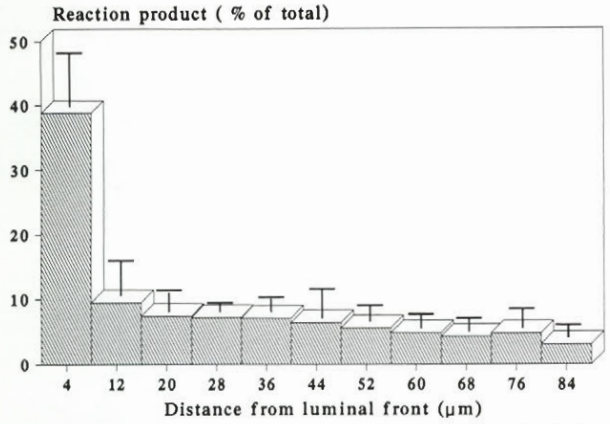

Figure 3. Densitometric evaluation of the CS-PG immunodetection in frozen sections of normal rabbit aorta. The columns represent % contribution to total staining of successive equal intervals across the aorta. Bars = SEM; n = 10.

tween the relative composition of newly synthesized and total aortic GAG (alcian stainable). SDS-PAGE autoradiography (Figure 1B) showed the typical track appearance of PG. PG with very high MW were contained in the soluble aortic fraction (Lane 1). TCA-precipitable (protein-associated) radioactivity of the GuHCl extract (Lane 2) was virtually eliminated by digestion with chondroitinase ABC (Lane 3). Hyaluronidase treatment had little effect on the absolute value of TCA-precipitable radioactivity (2.1% decrease), but determined its redistribution (Lane 4). This suggested a previous interaction of CS-PG with hyaluronic acid. ^{35}S-labeled PG were specifically precipitated from the rabbit aortic tissue extract by the anti-CS antibodies (Lane 5) used consequently for the detection of CS on aorta sections.

LM Immunocytochemistry

The general pattern of CS-PG distribution within the arterial wall was revealed by the specific labeling produced using the immunoperoxidase method on frozen sections (Figures 2A and 2B). The quantification of the enzymatic reaction product repartition (Figure 3) showed the major contribution of the innermost regions to the total content of CS in the rabbit aorta.

Silver-enhanced immunogold (Figure 2C) produced a similar distribution of labeling, which confirmed that the embedding procedure did not significantly affect CS-PG detection. The wavy pattern of the staining was parallel with the elastic laminae and its intensity was markedly increased towards the luminal aspect of the aorta, mostly in the intima and inner media. Under this superficial region of high CS-PG density the rest of the tunica media was more weakly labeled. Low concentrations of CS-PG were detected in the adventitia.

EM Gold Immunocytochemistry

The patchy appearance of labeling in the inner aorta and the small clusters scattered deeper within the medial layer could be distinguished even at the lowest magnifications, especially in the specimens processed by the three-step procedure and stained with aqueous uranyl acetate (Figure 4). Although the contrast of gold label was enhanced, the extracellular matrix ultrastructure was barely discernible. However, this could be clearly outlined by methanolic uranyl acetate staining of the thin sections. As a general rule of spatial distribution, throughout the aortic layers the CS-rich domains were inversely correlated with the areas occupied by elastin.

Controls

All immunocytochemical controls confirmed the specificity of labeling (Figure 5). Previous digestion of the sections with either chondroitinase ABC or AC considerably diminished the gold labeling, confirming once again the antibody specificity for the CS A and CS C moieties.

CS-PG Distribution

The extracellular spaces throughout the layers contained the great majority of the gold particles. Owing to the high resolution of labeling, we could undoubtedly detect three distinct types of CS-PG distributions, each consistently associated with a certain spatial position within the aortic wall.

In the innermost areas of aorta, the many labeled structures frequently appeared associated to form large extracellular networks of CS-PG (Figure 6A). Sometimes beneath the endothelium and especially around the first one or two rows of smooth muscle cells (SMC), prominent and almost confluent patches of closely packed gold particles contributed to very high levels of labeling.

The individual structures that appeared to be exposed at full length by sectioning were measured (as depicted by arrowheads in figure 6A). The mean value was estimated to be 153.8 ± 21.9 nm (n = 95).

In the medial layer (Figure 6B), most of the sparsely disposed, clustering associations of gold particles were found in the so called "soluble matrix" of the interstitial space. The mean length of several isolated interstitial clusters was 144.4 ± 24.7 nm (n = 64), not significantly different from that measured for the intimal structures. Apparently smaller CS-PG were consistently associated with the collagen bundles of the aortic media. Their maximal diagonal measurement averaged 58.4 ± 4.6 nm (n = 57). CS-PG were consistently excluded by the elastic lamellae and were detected solely at their periphery. Sporadic labeling appeared to follow lines parallel to the contour of SMC, presumably being associated with the external aspect of their basement membranes.

Individual straight lines or sometimes multiple tracks of consecutive gold particles (Figure 6) were frequently visible throughout the intima and media. For a tentative estimation of their lengths we selectively measured strings of gold particles that appeared linear. The mean value obtained from averaging track lengths from different areas was 65.1 ± 8.9 nm (n = 135).

In contradistinction to the previously described regions, within the adventitia the labeling of the interstitial space was very low. The difference was especially brought out by comparison of the space beneath the endothelial cells (EC) of vasa vasorum (Figure 7) and those forming the lumen of the aorta (see Figure 4). The

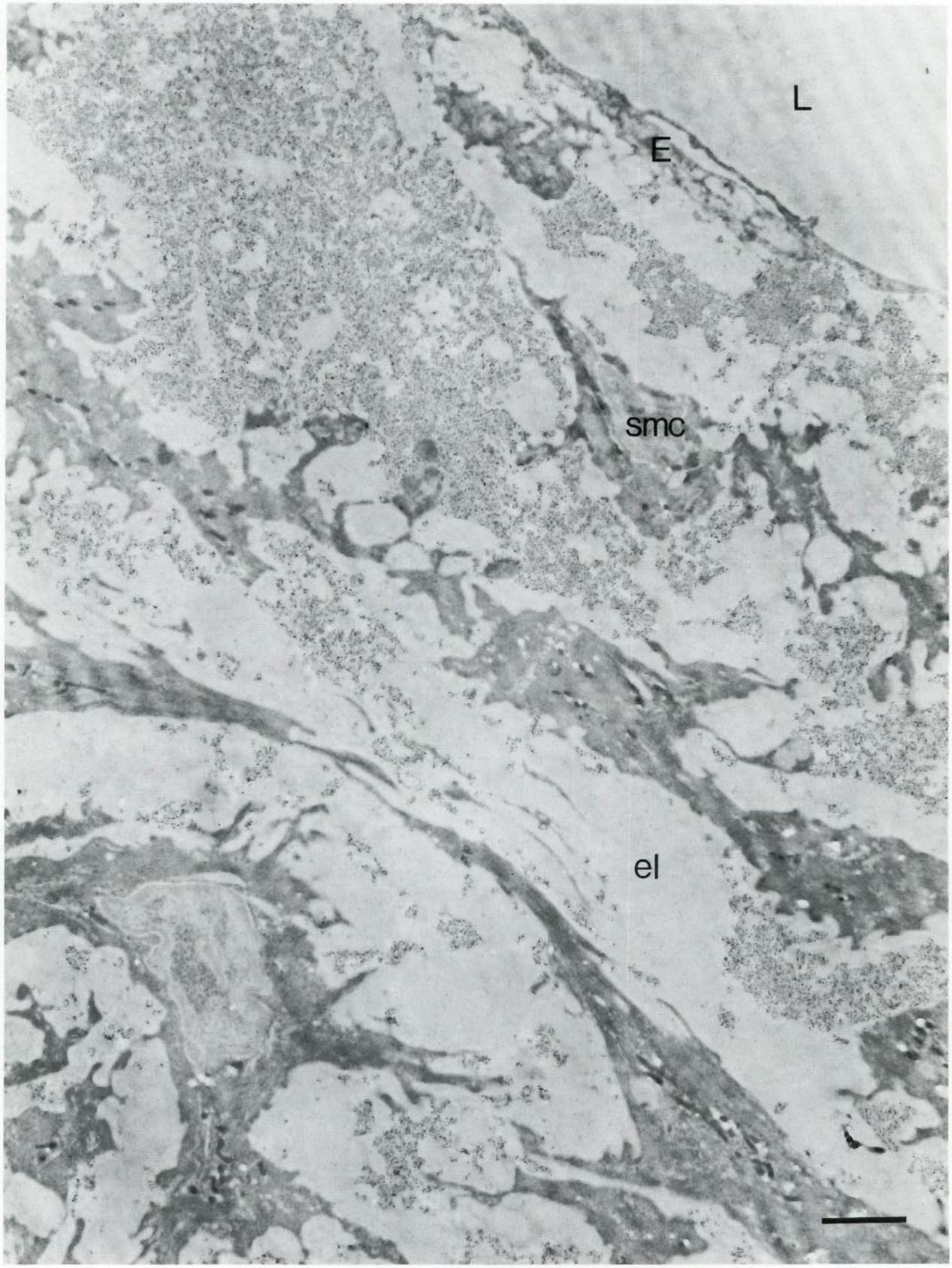
L
E
smc
el

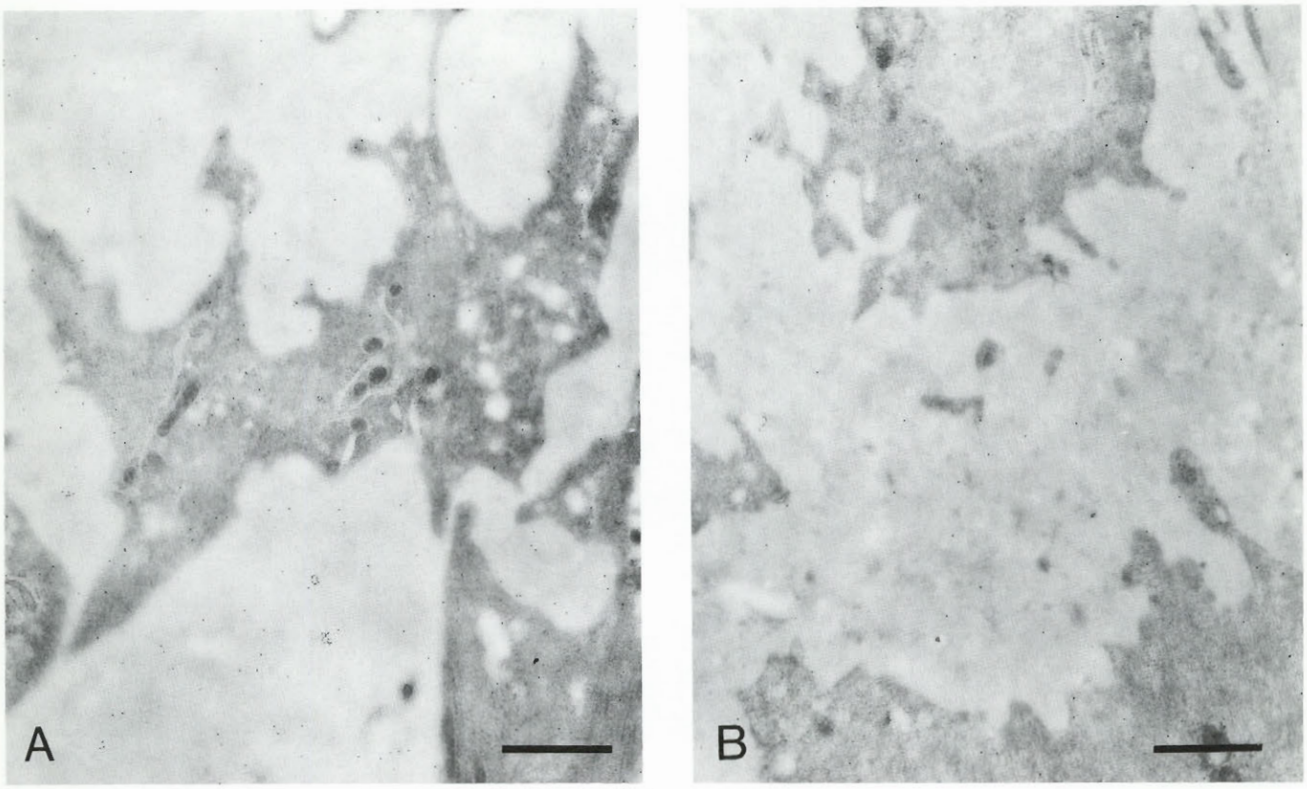

Figure 5. Controls for immunocytochemical detection of CS-PG. (**A**) Control of anti-CS antibody specificity. Section digested 4 hr with 0.8 U/ml chondroitinase ABC and subsequently processed by immunogold staining. (B) Control for gold labeling specificity, processed with omission of primary antibody. Original magnification × 13,640. Bars = 1 μm.

occurrence of CS moieties in the adventitia appeared largely dependent on the disposition of the large collagen bundles. Most evident was the consistent labeling of the fibril surface (Figure 7, inset) by individual gold particles.

Association of CS-PG with Other Elements of the Extracellular Matrix

Elastin. Gold labeling was consistently excluded from areas occupied by amorphous elastin. Nevertheless, CS-PG were found at the periphery of elastin fibers, probably in association with the microfibrillar component (Figure 8A).

Collagen. CS-PG were associated with collagen fibrils throughout the aorta. However, two different types of CS-containing structures could be discriminated (Figures 8A and 8B). The most widely distributed type was represented by clustering associations of CS wrapped around collagen fibrils, producing a "stuck on" appearance. The other type of labeling was characteristic for the large collagen bundles of the adventitia (Figure 8B). Presumably isolated CS epitopes, usually in close apposition with the surface of the collagen fibrils, were found. A preference for the gap region of collagen banding seemed to be suggested.

Fibrillar Components. The possible association of labeled CS-PG with extracellular fibrillar components was often noted (Figure 8B, inset). The longest fibrillar elements were visible mostly in the outer medial layer and adventitia. A possible identification with hyaluronic acid and fibronectin could be envisaged.

Discussion

Specific Considerations

The characteristics of CS-PG were examined by LM and EM immunocytochemistry in normal rabbit aorta. Since the great majority of aortic CS-PG were displayed in the interstitial space, the features of the extracellular distribution were preferentially followed.

Figure 4. Detection of aortic CS-PG using post-embedding protein A–gold EM immunocytochemistry. The dense labeling of the superficial layer is due to large, densely packed CS-PG accumulations beneath the endothelium (E) and surrounding the first layers of smooth muscle cells (smc). Deeper inside the media, CS-PG appear to be organized in interstitial clusters. Lowicryl section stained for 20 min with aqueous uranyl acetate and 30 sec lead citrate. L, lumen of aorta; el, elastin. Original magnification × 7500. Bar = 2 μm.

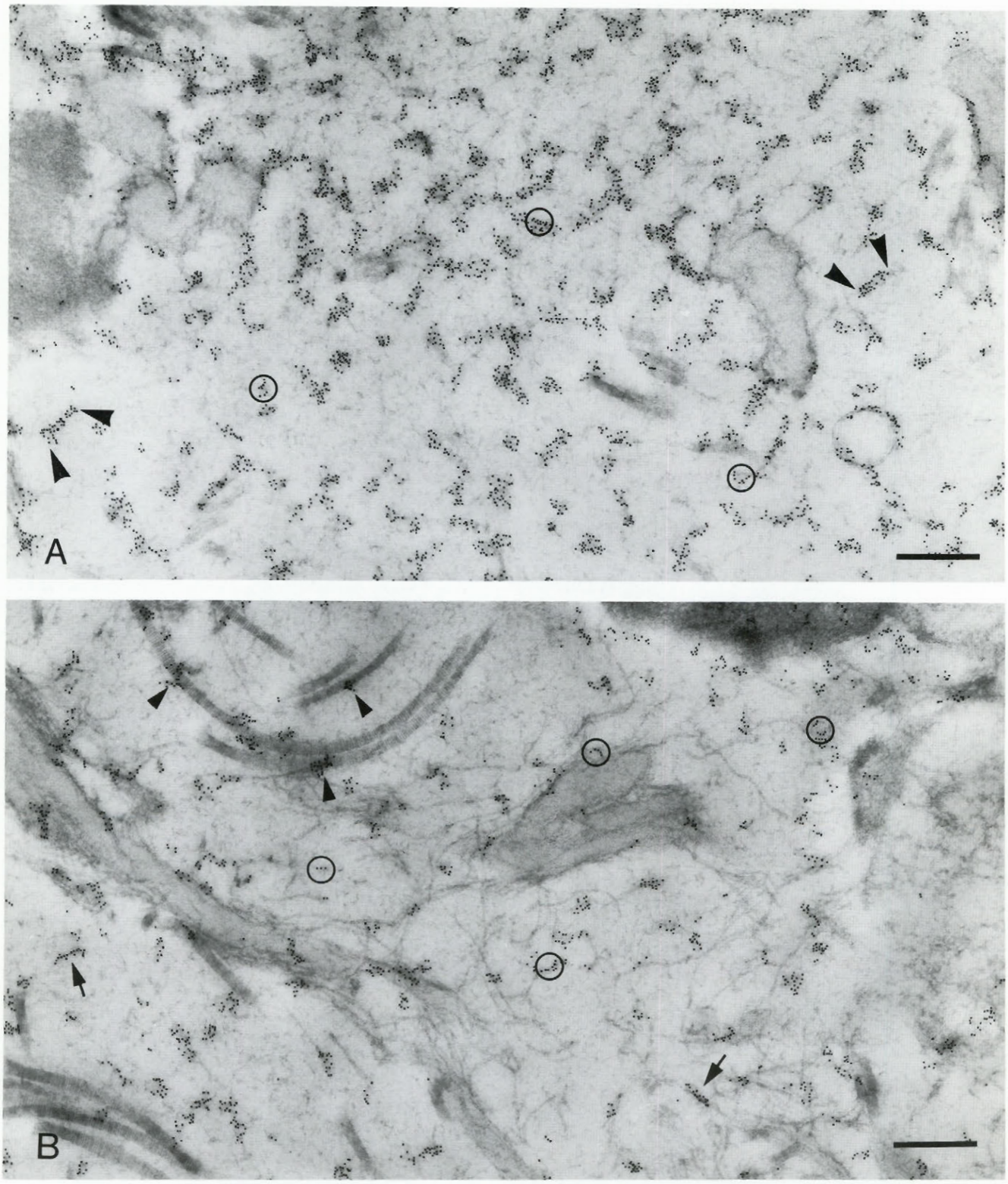

Figure 6. Characteristic patterns of CS-PG immunogold detection inside the aortic wall. (**A**) Region within the intima. In areas of high labeling concentration the formation of CS-PG molecular networks was suggested. The lengths of individual structures apparently exposed longitudinally were measured, as depicted by arrowheads. (**B**) Typical CS-PG of aortic media. The gold labeling detects scattered associations. CS-PG in the soluble interstitial matrix (arrows) and collagen-associated CS-PG (arrowheads). Examples of the many single or multiple linear tracks of gold particles are circled. Original magnification × 44,460. Bars = 0.3 μm.

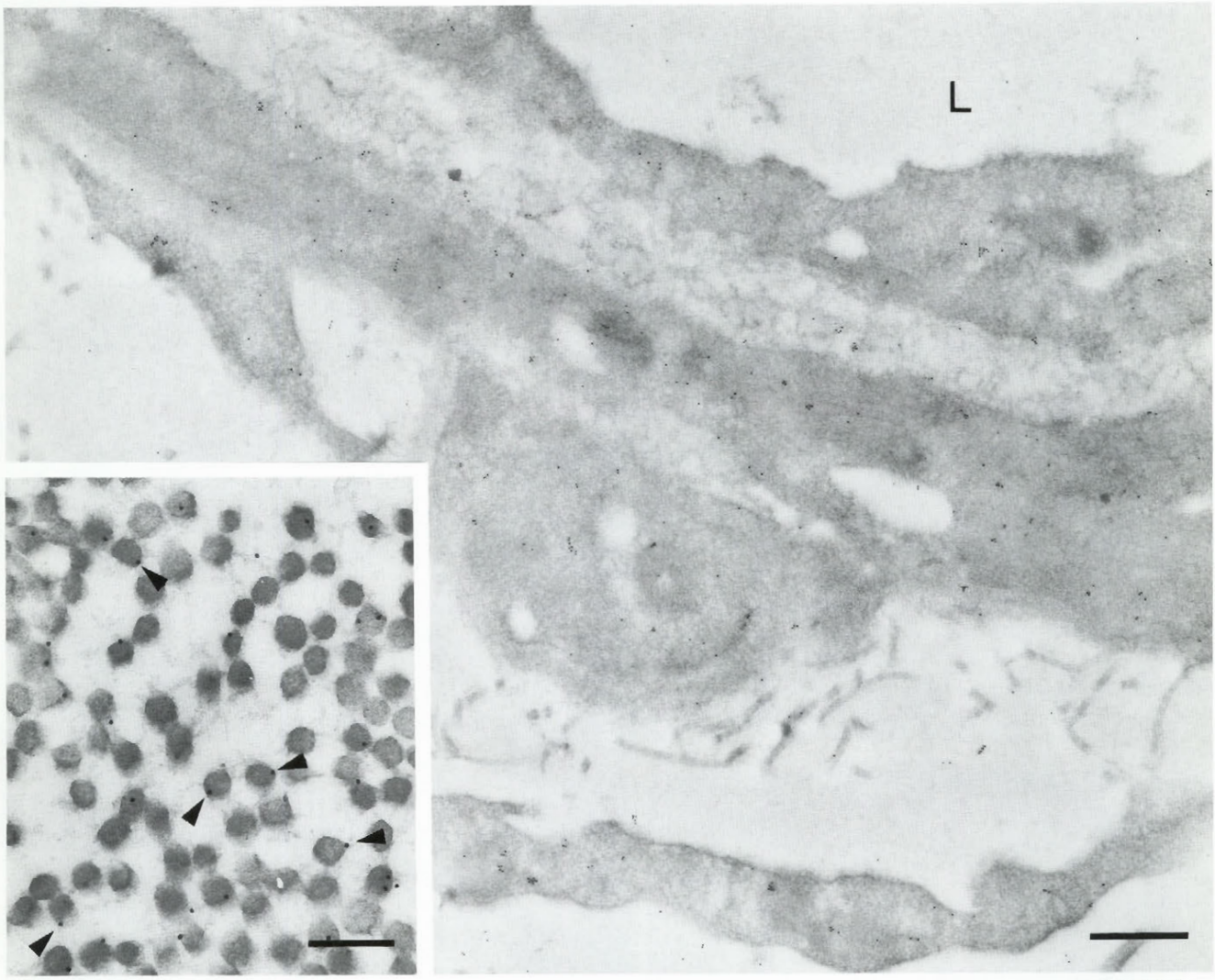

Figure 7. CS-PG in the adventitia of normal rabbit aorta, as detected by immunogold. Region surrounding vasa vasorum showing the rare extracellular labeling. E, endothelium. **(Inset)** Characteristic labeling of collagen bundles. Individual particles were typically detected in close association (arrowheads) with the surface of collagen fibrils cut in cross-section. L, lumen of aorta. Original magnification × 27,300; **inset** × 59,280. Bar = 0.5 μm; **inset** = 0.2 μm.

The in situ differential relation of CS-PG with collagen and the mutual exclusion with elastin were most evident.

The most obvious feature of CS-PG immunodetection at LM was the extremely high concentration displayed by the innermost regions. The densitometric analysis of CS distribution across the vessel wall estimated that around 40% of the total CS amount was accumulated in the inner tenth of the entire aorta thickness. This value might even be underestimated owing to the saturation of the immunoperoxidase staining. The CS-PG accumulation could be related both to a very active synthesis and to a special tendency of CS-PG to form large extracellular homophilic aggregates in this area. Both EC and SMC have the capacity of synthesizing different CS-PG in culture (6,22,25). In addition, EC-conditioned media could stimulate sulfate incorporation into PG synthesized by cultured SMC (20). The high concentration of CS-PG detected in the inner aorta might be related to a specific interaction between these cells. This would also explain why CS-PG were sparser deeper in the medial layer. However, the close apposition between endothelium and SMC had not produced detectable CS-PG accumulations around the arterioles of vasa vasorum. The possible site-specific interaction of EC and SMC could modulate the nature of perivascular CS-PG which, in turn, would significantly contribute to the differential properties of the blood vessels, such as permeability. Obviously, these effects would be easily missed by use of in vitro conditions.

The intima of the aorta is a vascular area preferentially affected by atherosclerosis. High concentrations of CS-PG, known to avidly bind lipoproteins, could create the proper environment for the development of typical lipid accumulations (24,26). The future ultrastructural investigation of changes that may occur in the normal distribution and/or organization of extracellular CS-PG during pathological processes could complement the more commonly used biochemical assays with relevant data.

The detailed gold labeling in the inner regions of aorta sug-

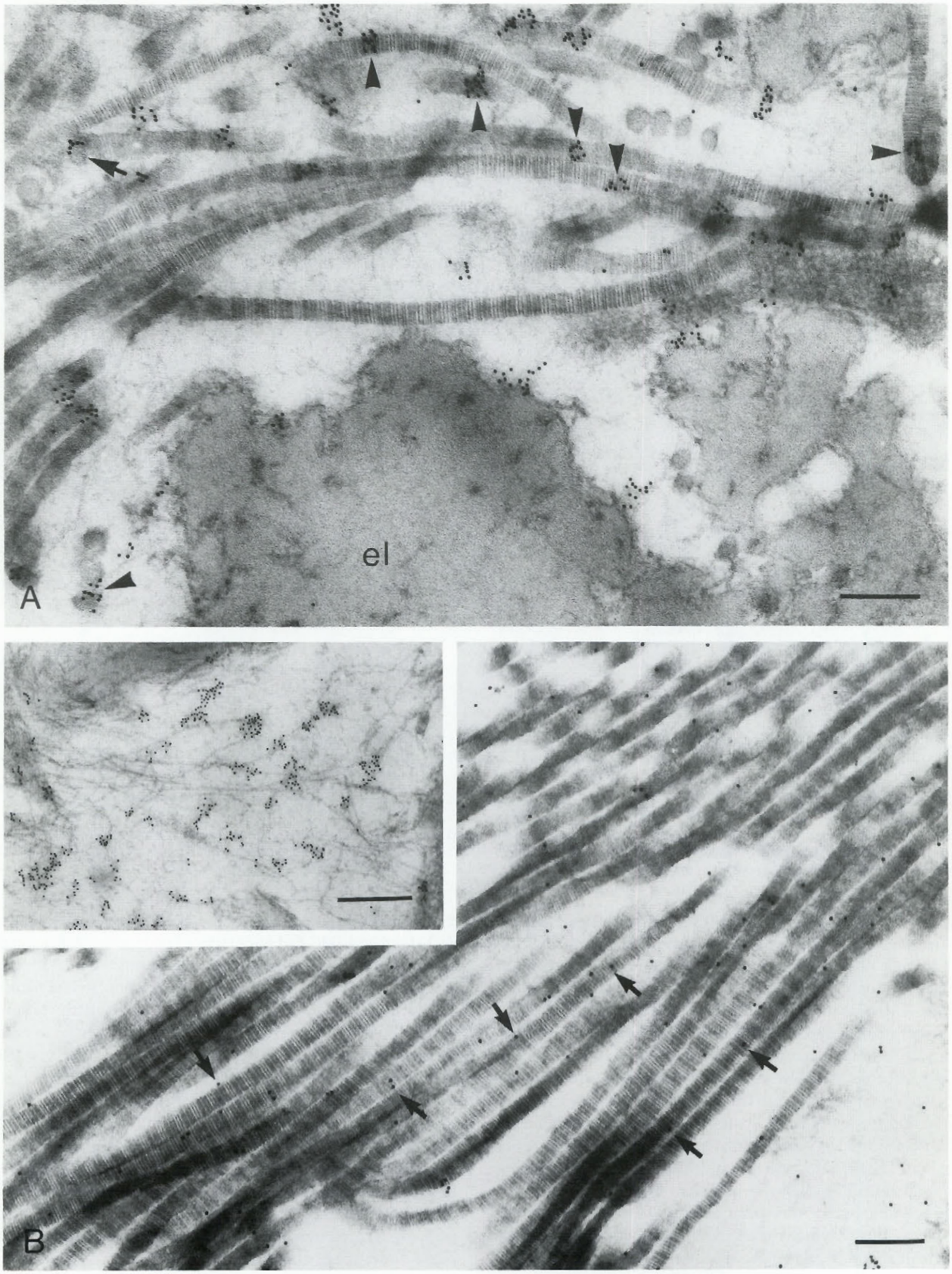
el
A
B

gested the presence of CS-PG capable of creating large molecular associations. An aggregating property has been described for the large CS-PG extracted from either bovine aorta or aortic cell cultures (12,19,21,22,36). These molecules possess specific binding domains for hyaluronic acid, and it was estimated that within the soluble matrix of the aorta approximately 10% of CS-PG interact with hyaluronic acid to form a bottle brush-like structure, well known from descriptions of cartilage PG (13,21).

In the medial layer of our specimens, CS-PG distribution had lower density. The large labeled structures, with length comparable to those measured in the intima, were detected in the interstitium either isolated or in the company of fibrillar components. In the media of human aorta, Volker et al. (35) described large precipitates produced by cuprolinic blue which, judging by their susceptibility to chondroitinase digestion and by their size, were thought to represent CS-PG aggregated with HA. A particular type of large CS-PG was also detected in the soluble matrix of the bovine aorta (16).

Apart from those CS-PG, tentatively identified as large aggregating CS-PG in the soluble extracellular matrix of the medial layer, smaller CS-PG were detected in association with collagen. The smaller sizes could either be genuine or caused by a visual effect of the molecule wrapping around the collagen fibrils. CS-PG accompanying the pericellular contour of the SMC basement membrane were also detected. Although heparan sulfate has been the traditionally acknowledged component of PG in the basement membranes, recently the presence of a CS-PG associated with these structures has also been reported (18). The low density of CS-PG found in this location might be responsible for their relatively late recognition.

The discrete distribution of gold particles along individual collagen fibrils in the adventitia suggested the presence of individual CS epitopes as components of a particular PG type. The features previously described in the literature for "small PG" interacting with collagen (9,12,25,29), such as biglycan and decorin, might be of relevance in this case. However, a definite immunocytochemical identification of the two types of collagen-associated CS-PG detected in our specimens would require the additional use of anti-protein core antibodies. Using a polyclonal antibody raised against a dermatan sulfate containing PG produced by human skin fibroblasts, a similar location was detected in human superficial femoral artery (36).

Although the low contrast of intracellular membranes inherent to Lowicryl embedding limited the resolution, it was possible to detect CS-PG within every type of vascular cell of rabbit aorta. This proved that in vivo all these cells contribute to the production of aortic CS-PG. The systematic use of antibodies specific to particular GAG moieties, in conjunction with an improved resolution of intracellular detail, might add some missing pieces of information regarding both normal and disturbed intracellular assembly of PG.

The EM morphometric evaluation of the individual labeling patterns was able to reveal that CS-containing structures of certain sizes were associated with different locations within the aorta. The consistency of the observations confirmed the feasibility of detecting different types of CS-PG. Moreover, taking into consideration that the embedded CS-PG would be expected to have apparent lengths smaller than those of flattened molecules, the dimensions inferred from the gold labeling were in good agreement with previous measurements made on extracted PG molecules, suggesting that it was actually able to detect features of the in situ molecular design of aortic CS-PG. For example, the large aortic PG capable of forming aggregates with hyaluronic acid, spread on grids and processed for EM by glycerol spraying/rotary shadowing (21), had been found to have protein cores of 237 ± 38 nm long, and 20–25 GAG side chains of 58 ± 24 nm. A small species with one or two GAG chains with lengths of 80 ± 25 nm has been also described. It therefore seems possible that in our system the frequent appearance of "beads on a string" is created by gold particles indirectly detecting several successive identical epitopes on CS chains.

Technical Considerations

The main problems that inevitably accompany procedures applied to the biochemical study of PG are related to selective PG extraction, alterations of their chemical composition and native structure, and disturbance of the in vivo interactions.

Previous histochemical and immunocytochemical studies have continuously added valuable information regarding the in situ distribution of different PG within the arterial wall. The most commonly used stains, ruthenium red, safranin O, alcian blue, and cuprolinic blue, interact strongly with the GAG chains of PG and, by producing the collapse of their molecular architecture, form either colored or electron-opaque aggregates (6,31,35,36). The otherwise straightforward staining procedures also have the disadvantage of limited penetration and, because of their rather broad specificity, require previous digestion of tissue with specific enzymes to distinguish among different GAG. As an alternative, several antibodies raised against PG molecules have been developed and used to detect their distribution in the arterial wall (1,7,16). Antibodies recognizing epitopes of the protein cores have been used to detect particular PG, but although capable of high specificity they may produce a relatively low labeling efficiency.

The use of antibodies capable of recognizing specific GAG moieties (2,33,34) creates the possibility of simultaneously detecting a family of several distinct PG that contain the same type of GAG. The high efficiency of labeling in our specimens was due to the intrinsic biochemical characteristics of the PG molecules: the high content of CS, the detection of CS chains in more than one type of PG, and the potential presence of several CS chains per PG molecule and of several antigenic epitopes per CS chain. In the three-

Figure 8. Patterns of aortic CS-PG in relation to other extracellular components by gold post-embedding EM immunocytochemistry. **(A)** Association with collagen and elastin in the media. CS-PG riding on collagen fibrils (arrowheads). The "stuck on" appearance was more evident with cross-sectioned fibrils (arrow). CS-PG were also found at the periphery of elastic lamellae (el), probably in relation to the microfibrillar component, but were excluded from the bulk of amorphous elastin. **(B)** Collagen bundle in the adventitia. Single gold particles punctuate the length of collagen fibrils, most often in the gap region (arrows). **(Inset)** CS-PG in association with long fibrillar extracellular structures. Original magnifications: **A** × 71,650; **B** × 57,920; **Inset** × 44,460. Bars: **A,B** = 0.2 μm; **Inset** = 0.3 μm.

vs two-step immunocytochemical procedure, the efficiency of detection and consequently the extent of labeling could be further increased both by the use of one additional immunoreagent and by the controlled preparation of protein A (10). In addition, the contrast of the labeled structures, due probably to superimposing more protein immunoreagent layers, outlined more clearly the differences between individual or associative CS-PG structures.

The complex ultrastructural details of PG and the antigenicity were optimally preserved by the procedure chosen for embedding. By using the immunostaining after embedding, CS-PG could be detected in the entire depth of the vessel wall. The limitation of using thin specimens, such as cell monolayers, vibratome sections, or peels of tissue, required to facilitate penetration of reagents in other procedures was therefore circumvented. The typically low contrast in Lowicryl K4M, related to the omission of commonly used EM-contrasting reagents to preserve antigenicity, could be overcome by appropriate staining of the thin sections.

Gold labeling increased the resolution of antigen detection and created the possibility of making dimensional estimates through EM morphometry. In fact, the protein A–gold technique has been previously employed to detect submolecular structures within extracted cartilage PG molecules (33). Limitations related to embedding, plane of exposure by sectioning, and additional contribution of immunoreagent size were expected to affect the morphometric analysis. The measurements made on specimens stained by the three-step immunocytochemical procedure yielded larger values, compatible with the amplification of detection. For example, in the aortic media the values obtained by two-step vs three-step procedures were: 144.4 ± 24.7 nm (n = 64) vs 264.5 ± 49.9 nm (n = 106) for isolated CS-PG, and 58.4 ± 4.6 nm (n = 57) vs 81.6 ± 14.6 nm (n = 40) for collagen-associated CS-PG. The fact that the dimensional relations between the average measurements of structures labeled by the two different sequences were consistent further supports the reliability of such estimations.

By the use of a high-resolution detection system, we have been able to distinguish patterns of regional CS-PG distribution within the normal aortic wall and to reveal some features of their molecular organization.

Acknowledgments

We wish to thank Dr M. Bendayan (Departement d'Anatomie, Université de Montréal) for his kind gift of the protein A–gold probe and for his constructive comments. The excellent technical assistance of Leng Tsao and Robert Sawka is gratefully acknowledged.

Literature Cited

1. Aikawa J, Munakata H, Isemura M, Ototani N, Yosizawa Z: Comparison of glycosaminoglycans from thoracic aortas of several mammals. Tohoku J Exp Med 143:107, 1984
2. Avnur Z, Geiger B: Immunocytochemical localization of native chondroitin-sulphate in tissues and cultured cells using specific monoclonal antibody. Cell 38:811, 1984
3. Bartold PM, Page RC: A microdetermination method for assaying glycosaminoglycans and proteoglycans. Anal Biochem 150:320, 1985
4. Bendayan M: Protein A–gold electron microscopic immunocytochemistry: methods, applications, and limitations. J Electron Microsc Tech 1:243, 1984
5. Chamberlain JP: Fluorographic detection of radioactivity in polyacrylamide gels with the water-soluble fluor, sodium salicylate. Anal Biochem 98:132, 1979
6. Chen K, Wight TN: Proteoglycans in arterial smooth muscle cell cultures: an ultrastructural histochemical analysis. J Histochem Cytochem 32:347, 1984
7. Couchman JR, Caterson B, Christner JE, Baker JR: Mapping by monoclonal antibody detection of glycosaminoglycans in connective tissues. Nature 307:650, 1984
8. Franc S, Garrone R, Bosch A, Franc JM: A routine method for contrasting elastin at the ultrastructural level. J Histochem Cytochem 32:251, 1984
9. Fransson LA: Structure and function of cell associated proteoglycans. Trends Biol Sci 12:406, 1987
10. Ghitescu L, Bendayan M: Immunolabeling efficiency of protein A–gold complexes. J Histochem Cytochem 38:1523, 1990
11. Hamati HF, Britton EL, Carey DJ: Inhibition of proteoglycan synthesis alters extracellular matrix deposition, proliferation, and cytoskeletal organization of rat aortic smooth muscle cells in culture. J Cell Biol 108:2495, 1989
12. Heinegard D, Hedbom E, Antonsson P, Oldberg A: Structural variability of large and small chondroitin sulphate/dermatan sulphate proteoglycans. Biochem Soc Trans 18:209, 1990
13. Heinegard D, Oldberg A: Structure and biology of cartilage and bone matrix macromolecules. FASEB J 3:2042, 1989
14. Kapoor R, Phelps CF, Coster L, Fransson LA: Bovine aortic chondroitin sulphate- and dermatan sulphate-containing proteoglycans. Isolation, fractionation and characterization. Biochem J 197:259, 1981
15. Laemmli UK: Cleavage of structural proteins during the assembly of the head of bacteriophage T_4. Nature 227:680, 1970
16. Lark MW, Yeo TK, Mar H, Lara S, Hellstrom I, Hellstrom KE, Wight TN: Arterial chondroitin sulphate proteoglycan: localization with a monoclonal antibody. J Histochem Cytochem 36:1211, 1988
17. Larsson LI: Methods for examining the specificity of antiserum/antibody interaction with tissue-bound antigen: controls. In Larsson LI, ed. Immunochemistry: theory and practice. Boca Raton, FL, CRC Press, 1988, 19
18. McCarthy KJ, Accavitti MA, Couchman JR: Immunological characterization of a basement membrane-specific chondroitin sulphate proteoglycan. J Cell Biol 109:3187, 1989
19. McMurtrey J, Radhakrishnamurthy B, Dalferes ER, Berenson GS, Gregory JD: Isolation of proteoglycan–hyaluronate complexes from bovine aorta. J Biol Chem 254:1621, 1979
20. Merrilees MJ, Campbell JH, Spanidis E, Campbell GR: Glycosaminoglycan synthesis by smooth muscle cells of differing phenotype and their response to endothelial cell conditioned medium. Atherosclerosis 81:245, 1990
21. Morgelin M, Paulsson M, Malmstrom A, Heinegard D: Shared and distinct structural features of interstitial proteoglycans from different bovine tissue revealed by electron microscopy. J Biol Chem 264:12080, 1989
22. Morita H, Takeuki T, Suzuki S, Maeda K, Yamada K, Eguchi G, Kimata K: Aortic endothelial cells synthesize a large chondroitin sulphate proteoglycan capable of binding to hyaluronate. Biochem J 265:61, 1990
23. Oegema TR, Hascall VC, Eisenstein R: Characterization of bovine aorta proteoglycan extracted with guanidine hydrochloride in the presence of protease inhibitors. J Biol Chem 254:1312, 1979
24. Radhakrishnamurthy B, Srinivasan SR, Eberle K, Ruiz H, Dalferres ER Jr, Sharma C, Berenson GS: Composition of proteoglycans synthesized by rabbit aortic explants in culture and the effect of experimental atherosclerosis. Biochim Biophys Acta 964:231, 1988

25. Rauch U, Glossl J, Kresse H: Comparison of small proteoglycans from skin fibroblast and vascular smooth-muscle cells. Biochem J 238:465, 1986

26. Richardson M, Alavi MZ, Moore S: Rabbit models of atherosclerosis. In White, RA, ed. Atherosclerosis and arteriosclerosis: human pathology and experimental animal methods and models. Boca Raton, FL, CRC Press, 1989, 163

27. Roth J: Post embedding labeling on Lowicryl K4M tissue sections. Detection and modifications of cellular components. In Tartakoff AM, ed. Methods in cell biology. Vol 31. Part A. New York, Academic Press, 1989, 513

28. Ruoslahti E: Proteoglycans in cell regulation. J Biol Chem 264:13369, 1989

29. Ruoslahti E: Structure and biology of proteoglycans. Annu Rev Cell Biol 4:229, 1988

30. Saito H, Yamagata T, Suzuki S: Enzymatic methods for the determination of small quantities of isomeric chondroitin sulfates. J Biol Chem 243:1536, 1968

31. Scott JE: Proteoglycan histochemistry—a valuable tool for connective tissue biochemists. Coll Relat Res 5:541, 1985

32. Schaffner W, Weissmann C: A rapid, sensitive, and specific method for the determination of protein in dilute solution. Anal Biochem 56:502, 1973

33. Sheehan JK, Ratcliffe A, Oates K, Hardingham TE: The detection of structures within proteoglycan molecules. Electron-microscopic immunolocalization with the use of protein A–gold. Biochem J 247:267, 1987

34. Sorell JM, Mahmoodian F, Schaffer IA, Davis B, Caterson B: Identification of monoclonal antibodies that recognize novel epitopes in native chondroitin/dermatan sulfate glycosaminoglycan chains: their use in mapping functionally distinct domains of human skin. J Histochem Cytochem 38:393, 1990

35. Volker W, Schmidt A, Buddecke E: Mapping of proteoglycans in human arterial tissue. Eur J Cell Biol 45:72, 1987

36. Wight TN: Cell biology of arterial proteoglycans. Arteriosclerosis 9:1, 1989

CHAPTER 4

IMMUNOCYTOCHEMICAL DETECTION OF CHONDROITIN SULFATE PROTEOGLYCANS IN RABBIT AORTAS INJURED BY BALLOON-CATHETERIZATION

4.1. INTRODUCTION

The components of the extracellular matrix, particularly various types of proteoglycans (PG), have a very complex relationship with cell regulation (Ruoslahti, 1989; Carey, 1991). Changes of the vascular PG in atherosclerosis might be related to many processes (Wight, 1989), since the quantity and composition of their glycosaminoglycan (GAG) moieties were found to be modulated in vitro by cell migration (Kinsella and Wight, 1986) or phenotypic modulation by exposure to cell-conditioned medium (Campbell et al., 1990), to proliferation stimulators/inhibitors (Chen et al., 1987; Wight et al., 1989), and to monocyte-stimulating factors (Uhlin-Hansen et al., 1989). Deendothelialization in vitro (Merrilees and Scott, 1985), or in vivo (Alavi and Moore, 1985), and hypercholesterolemia (Radhakrishnamurthy et al., 1988) also affect the GAG composition of arterial PG. Most of these studies assayed the effect upon the synthesis of the GAG component of PG in different systems, and although it is difficult to compare the various absolute values reported, the results collectively pointed towards chondroitin sulfate (CS), as the most representative aortic GAG.

In addition to effects related to cell regulation, it was proposed that in atherogenesis PG might be responsible for the direct in vivo sequestration of plasma lipoproteins (LP) inside the arterial wall (Camejo, 1982; Iverius, 1973). This idea was based on detection of increased quantities of sulfated PG in the atherosclerotic lesions, as well as on the findings of numerous in vitro experiments that demonstrated a high affinity of LP for the aortic sulfated PG (Iverius, 1972). The CS moiety of PG was found to interact preferentially with the apolipoprotein B (apo B) component of LP (Camejo et al., 1983). Therefore, it is thought that PG could also form complexes with LP in situ, and two direct implications for the process of LP accumulation in the extracellular and intracellular space have been proposed. First, the movement of LP particles through the

interstitial space of the aortic wall could be physically restrained through interaction with PG, resulting in the immobilization of LP in the extracellular matrix of the aortic wall. Secondly, the association of LP with the PG molecules could modify the biochemical properties of the LP particles, or could mask parts of the apo B molecule, essential for the interaction with the apo B receptor, since the CS moiety and this receptor share common binding sites on the apo B molecules (Wight, 1989). Consequently, by potentially rendering the apo B-containing LP unrecognizable for the down-regulated receptor pathway, CS-PG could contribute to lipid loading and formation of foam cells. The latter hypothesis was verified in several heterologous in vitro systems (Salisbury et al., 1985, Vijayagopal et al., 1985), in which, by incubation with LP-PG complexes, peritoneal macrophages have been transformed into foam cells.

Several morphological studies described histochemical changes of the sulfated PG in human and experimentally-induced atherosclerosis (Wight and Ross, 1975; Richardson et al., 1982, Volker et al., 1989). Robbins et al. (1989) investigated by immunocytochemistry the distribution of various PG in the pigeon aorta, as a model of spontaneous and diet-induced atherosclerosis, and found also that CS is a major component of the vascular lesions.

Due to the many observations relating CS with the atherosclerotic process, we chose to investigate expressly those aortic PG that contain CS moieties in an injury type of atherosclerosis. For this purpose we used an immunocytochemical approach, which was previously found to allow the detection of the characteristics displayed in situ by the aortic CS-PG (Galis et al., 1992).

4.2. MATERIAL AND METHODS

The CS-PG were detected using a monoclonal antibody recognizing epitopes of the CS side chains of PG (Sigma Chem. Co., St. Louis, MO), and the following secondary antibodies: anti-mouse IgM coupled with FITC (BioCan, Mississauga, Ont), anti-mouse IgM (μ-chain specific) gold conjugate, 10 nm from Sigma; and an avidin-biotin immunocytochemical system (Dakopatts, Glostrup, Denmark). The tissue was embedded in OCT (Miles, Elkhart, IN) for frozen sections, or in Lowicryl K4M (J.B.

EM Services Inc., Dorval, Que) for gold post-embedding immunocytochemistry.

4.2.1. Specimen collection and processing. The procedure of balloon catheterization was described in detail previously (§2.6). Essentially, normocholesterolemic New Zealand rabbits were subjected to a selective deendothelialization using a balloon catheter, then allowed to recover for six months. At the time of sacrifice, from the harvested aortas, whole aortic rings were embedded in OCT for light microscope (LM) immunocytochemistry, the rest of the tissue was classified according to macroscopic appearance, fixed, and embedded in Lowicryl K4M for post-embedding electron microscope (EM)immunogold (Galis et al., 1992).

4.2.2. Immunoperoxidase. Frozen sections of 5 μm cut from injured aortas were stained by an immunoperoxidase procedure similar to that previously applied for the detection of CS-PG in normal aortas (ch. 3).

4.2.3. Detection of CS-PG by immunofluorescence. Frozen sections were collected on poly-L-lysine-coated glass slides, and allowed to dry overnight at room temperature. The sections were rehydrated for 10 min in 50 mM Tris-HCl, pH 7.61, then incubated at 37°C, for 30 min with 1/50 anti-CS in the same buffer. After 2 x 10 min rinses with Tris buffer, the bound anti-CS was detected by incubation with anti-mouse IgM coupled with FITC (1/100), at 37°C, for 30 min. The non-specifically bound antibody was washed off with 3 x 10 min Tris rinses, in the dark. In order to reduce the high intrinsic fluorescence of elastin, the sections were stained for 5 min with 0.3 % Eriochrome black T in PBS, then washed 3 x 5 min with PBS, and mounted with 90% glycerine in 50 mM Tris-HCl, pH 8.6. The specificity of the primary monoclonal antibody for the staining of the frozen sections was tested previously (Galis et al., 1992). For the secondary antibody, the control sections were processed for immunofluorescence without the primary antibody. The labelling of the sections was examined with a Leitz microscope equipped with a FITC filter. Successive sections were stained with Mayer's haematoxylin for further identification of morphological features.

4.2.4. EM immunocytochemistry. Thin sections of Lowicryl-embedded tissue were incubated with 1/200 anti-CS antibody, and then with the anti-mouse IgM/gold conjugate (ch. 3, Methods).

4.3. RESULTS

4.3.1. Immunocytochemical detection of CS-PG on LM

The most intensely stained layer of injured aortas was the aortic neointima (Fig. 1). This preferential location was consistent with the distribution of CS-PG in the normal aortic wall. However, the thickness of the neointima was greatly increased in the vascular lesions, therefore a high density of CS-PG was demonstrated over a much wider area.

In the medial layer of the injured aortas, the staining was distributed in strands parallel with the elastic laminae, as in the normal aorta.

The staining obtained by immunofluorescence was also obviously concentrated in the thickened intima of the regions which were covered by regenerated endothelium. The fluorescent labelling suggested that CS-PG created dense networks in these areas.

Fig. 1. LM detection of the CS-PG distribution in rabbit aorta, by immunoperoxidase (top), and immunofluorescence (bottom).

Normal (top left), and injured (top right) rabbit aorta. The highest density of the immunoperoxidase reaction is detected over the normal intima and respectively, over the thickened neointima of injured aorta. Section counterstained with Mayer's haematoxylin. L = lumen of aorta. Original magnification x 250.

Injured aorta. Control section, with omission of primary antibody (bottom left). Weak endogenous fluorescence due to elastin. (Bottom right). Detection of CS-PG by FITC-tagged antibody. The pattern of fluorescent labelling suggests the existence of extensive CS-PG lattices in the lesions. The position of the internal elastic lamina, was marked with arrowheads, to emphasise the thickness of the neointima. Eriochrome black counterstain. Original magnification x 400.

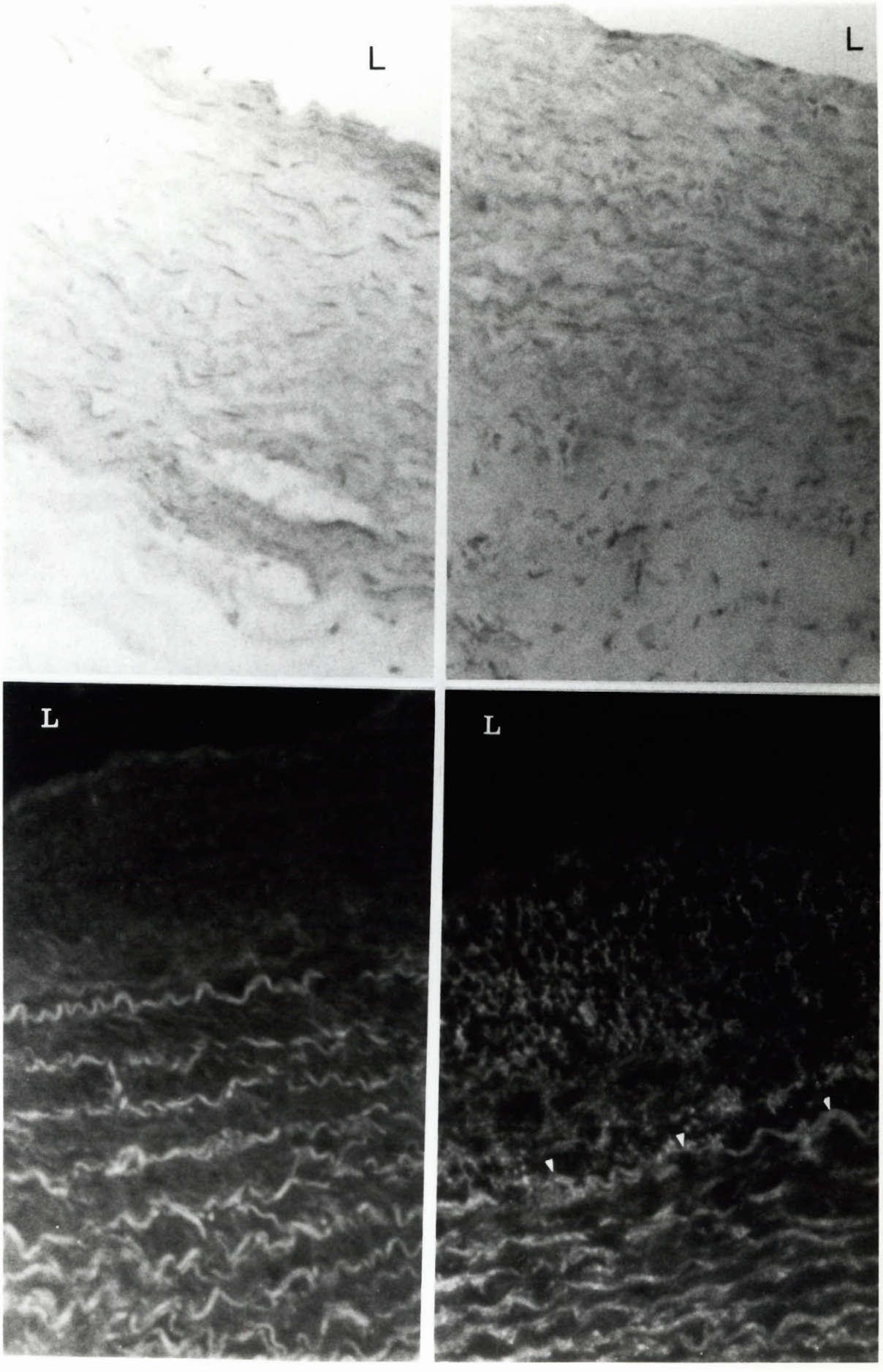
L
L
L
L

4.3.2. Ultrastructural detection of CS-PG

The hypercellularity of the intimal thickening was more pronounced in areas that were persistently deendothelialized than in the areas covered by a regenerated endothelium. These deendothelialized regions usually lacked inner interstitial clearings and typically, the CS-PG were very scarce (Fig. 2). The impression of crowding was enhanced by the extracellular matrix which was mostly fibrous and disorganized (Fig. 3). Deeper inside the non-endothelialized intima, the gold labelling was intense over a limited space above the internal elastic lamina. It was surprising to recognize in this location large interstitial clearings occupied by the CS-PG associations typical for the normal intima. Isolated lipid droplets, whose rims were decorated by gold particles were also detected (Fig. 4). The entire extracellular matrix was better organized than in the inner portion of the aortic wall.

Fig. 2. Persistently deendothelialized aorta. Rare extracellular CS-PG, indicated by arrowheads. SMC, smooth muscle cell, L = lumen of aorta. x 25,900. Bar = 500 nm.

Fig. 3. Disorganized extracellular matrix in the inner area of deendothelialized regions. Collagen-associated CS-PG. x 48,900. Bar = 300 nm.

Fig. 4. Extracellular space above internal elastic lamina (IEL). Interstitial clearing containing isolated lipid vesicles (arrows) rimmed by gold particles. A. x 30,000. Bar = 500 nm. B. Higher magnification of a similar area. Association of interstitial CS-PG with small, isolated lipid vesicles. x 41,500. Bar = 300 nm.

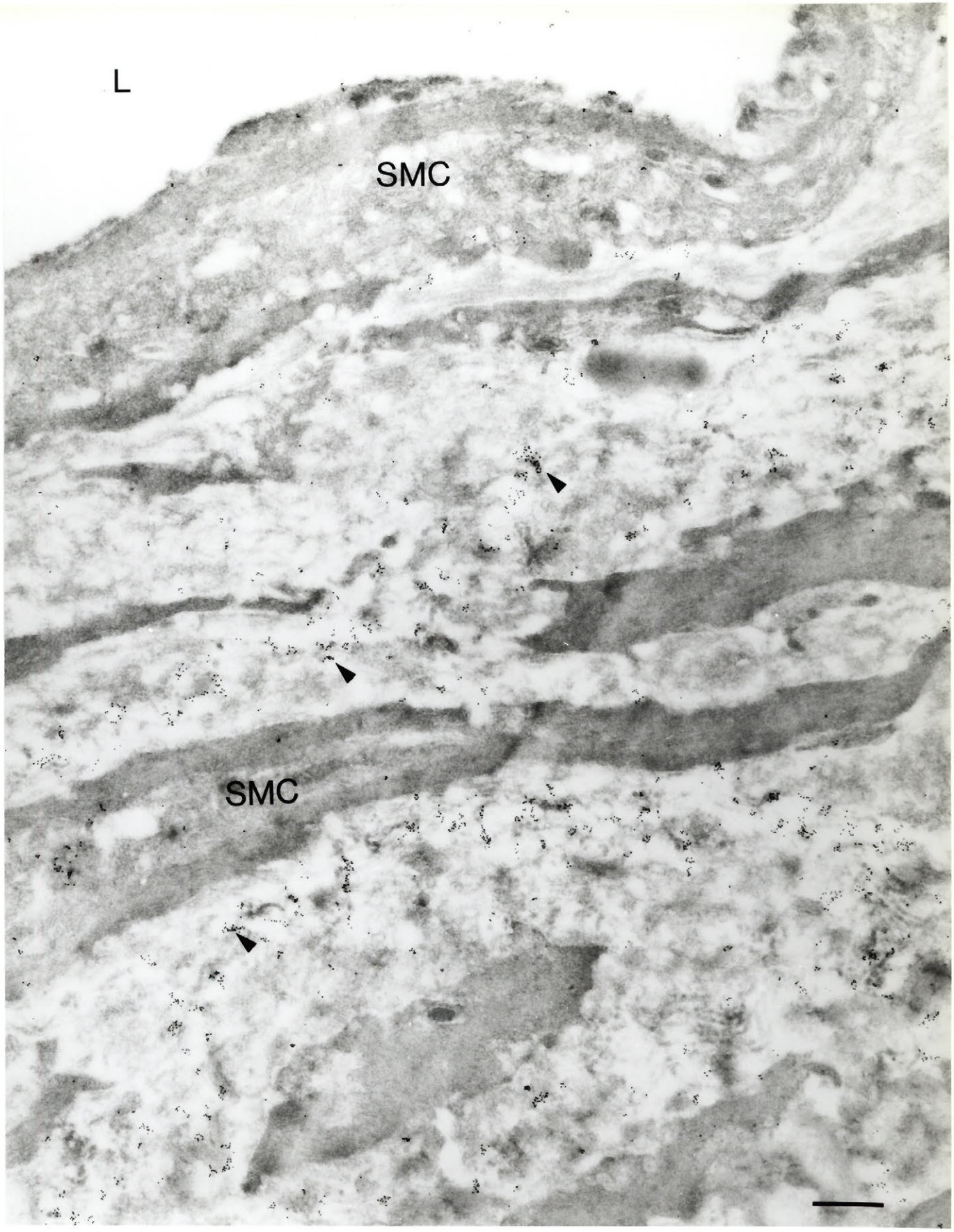
L
SMC
SMC

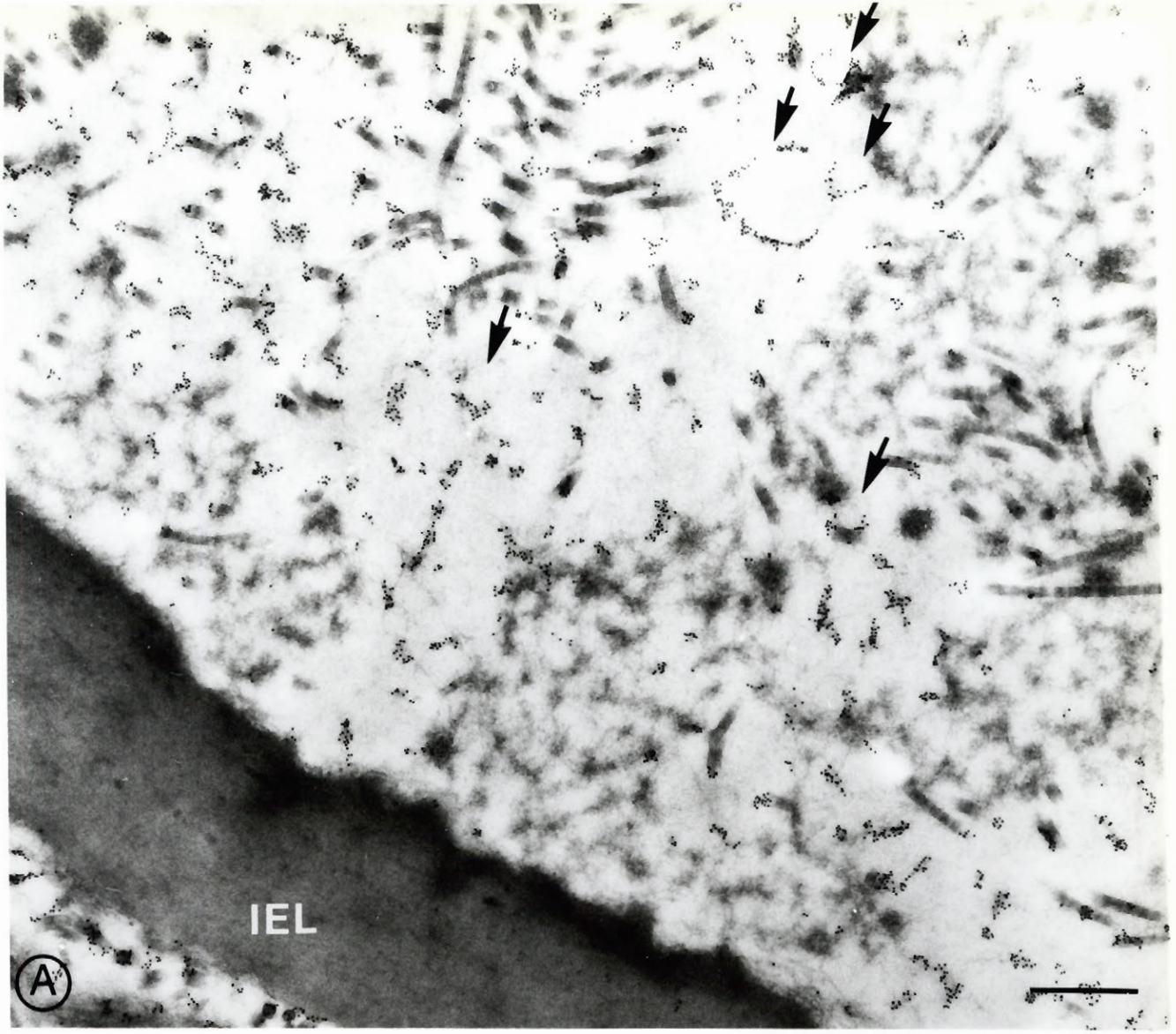
IEL
A

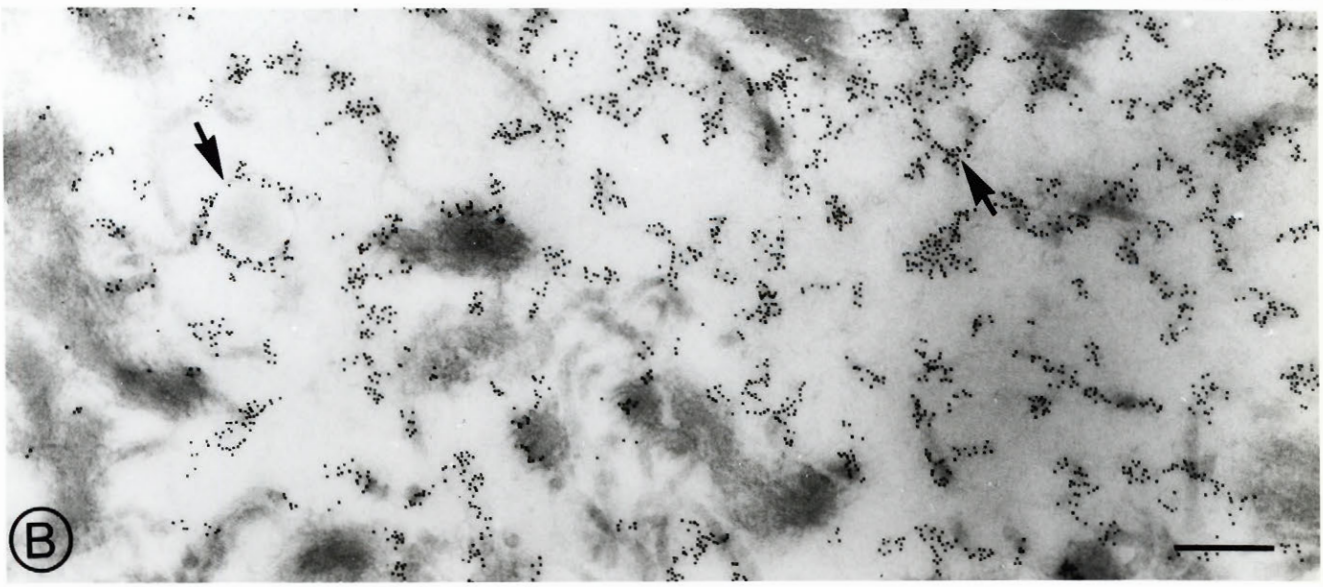
B

In the neointima covered by regenerated endothelium, the interstitial spaces were occupied by the large type of CS-PG (Fig. 5), similar to those found to be characteristic for the normal intima (ch. 3, Fig. 6). The high density of labelling and the arrangement displayed by these molecules generated the impression of extensive networks. Quite often, round profiles, presumably representing lipid, were found. Isolated lipid droplets appeared as if attached by strings in the otherwise open extracellular spaces.

As compared to the intima of normal aortas, the neointima of injured aortas contained considerable amounts of collagen. The massive collagen bundles were always accompanied by numerous clusters of collagen-associated CS-PG, and their presence was thus very prominent.

Fig. 5. Region covered by regenerated endothelium (E). Large CS-PG are present under the endothelium (A); and (B) around the smooth muscle cells (SMC). Extracellular vesicular structures (arrows), tentatively identified as lipid, are covered by CS-PG and appear as if attached by strings. x 25,000. Bar = 500 nm. L, lumen.

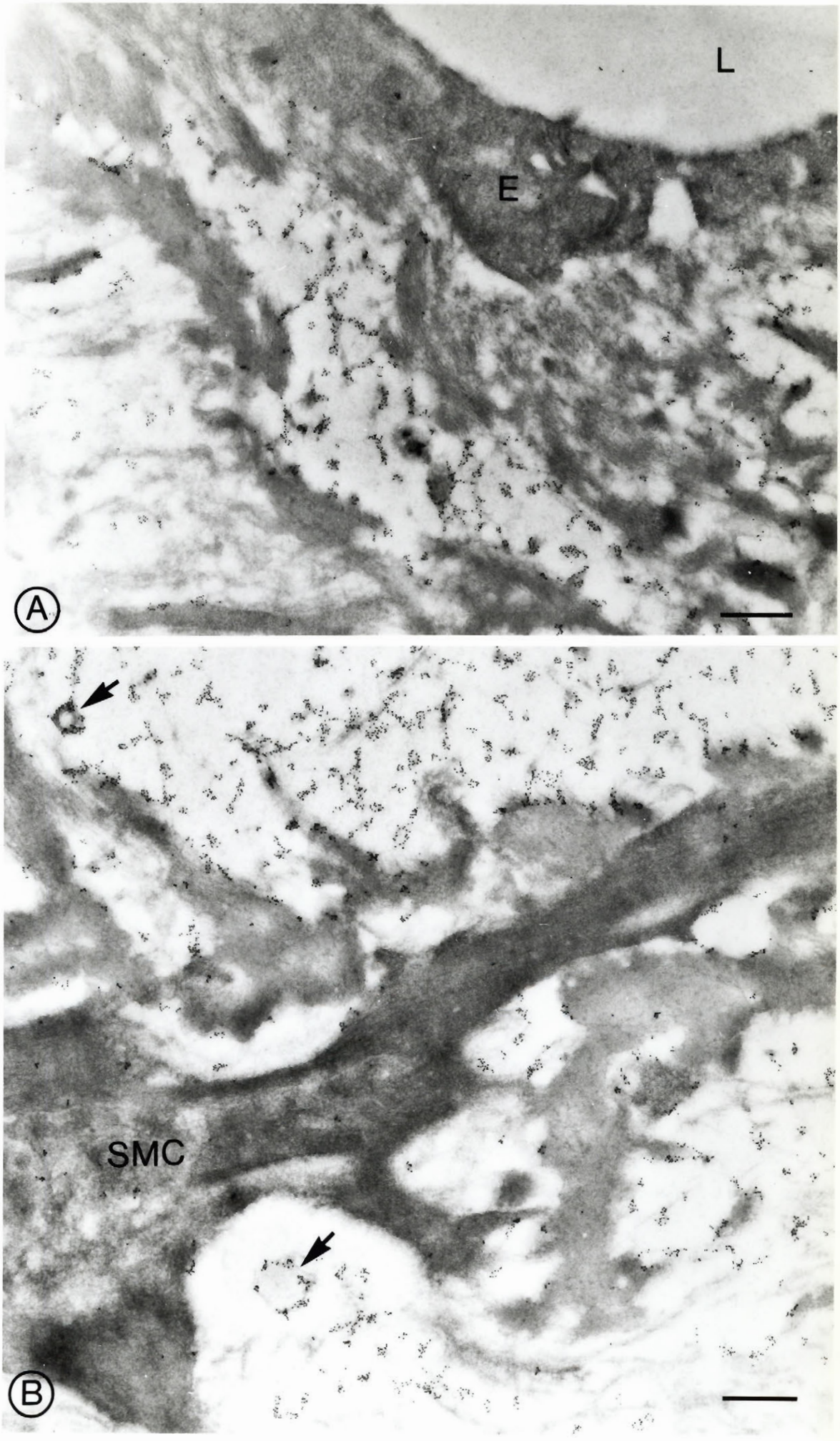
L
E
A
SMC
B

In the advanced lesions, the significant intracellular labelling of the large SMC of the synthetic type suggested an active production of CS-PG (Fig. 6). Their plasma membrane was frequently bordered by dense, CS-positive coats (Fig. 7). Many of the smooth muscle cells displaying the secretory phenotype were also containing lipid inclusions.

Gold particle strings appeared to have larger lengths that those detected previously in the normal aortas. An estimation made on linear strings yielded a length of 97.0 $\pm$ 13.8 ($n = 50$), value which was larger ($p < 0.05$) than the average length of gold particle strings previously measured in specimens of normal aorta (Galis et al., 1992).

Conspicuous extracellular deposits of small vesicular structures, recognized as lipid, were associated with vast interstitial areas of CS-PG accumulation (Fig. 8-9). In the areas of cellular necrosis, the surface of electron dense, vesicle-like structures was also frequently labelled by the anti CS-antibody. Isolated, large extracellular lipid inclusions were also found in the interstitial space of injured aortas (Fig. 10), and although often surrounded by collagen bundles, these did not appear to be directly involved in their accumulation.

Intracellular lipid was found in numerous cells of the lesions (Fig. 11). Many foam cells were recognized as being derived from SMC. The cells displaying lipid inclusion often possessed large vesicular organelles filled with CS-PG and typically, the two intracellular structures were disposed close to each other (Fig. 12).

Fig. 6. Large smooth muscle cell, containing lipid inclusions (L). Labelling of Golgi complex (G) and secretory vesicles (arrowheads), indicative of an active synthesis of CS-PG. x 42,200. Bar = 300 nm.

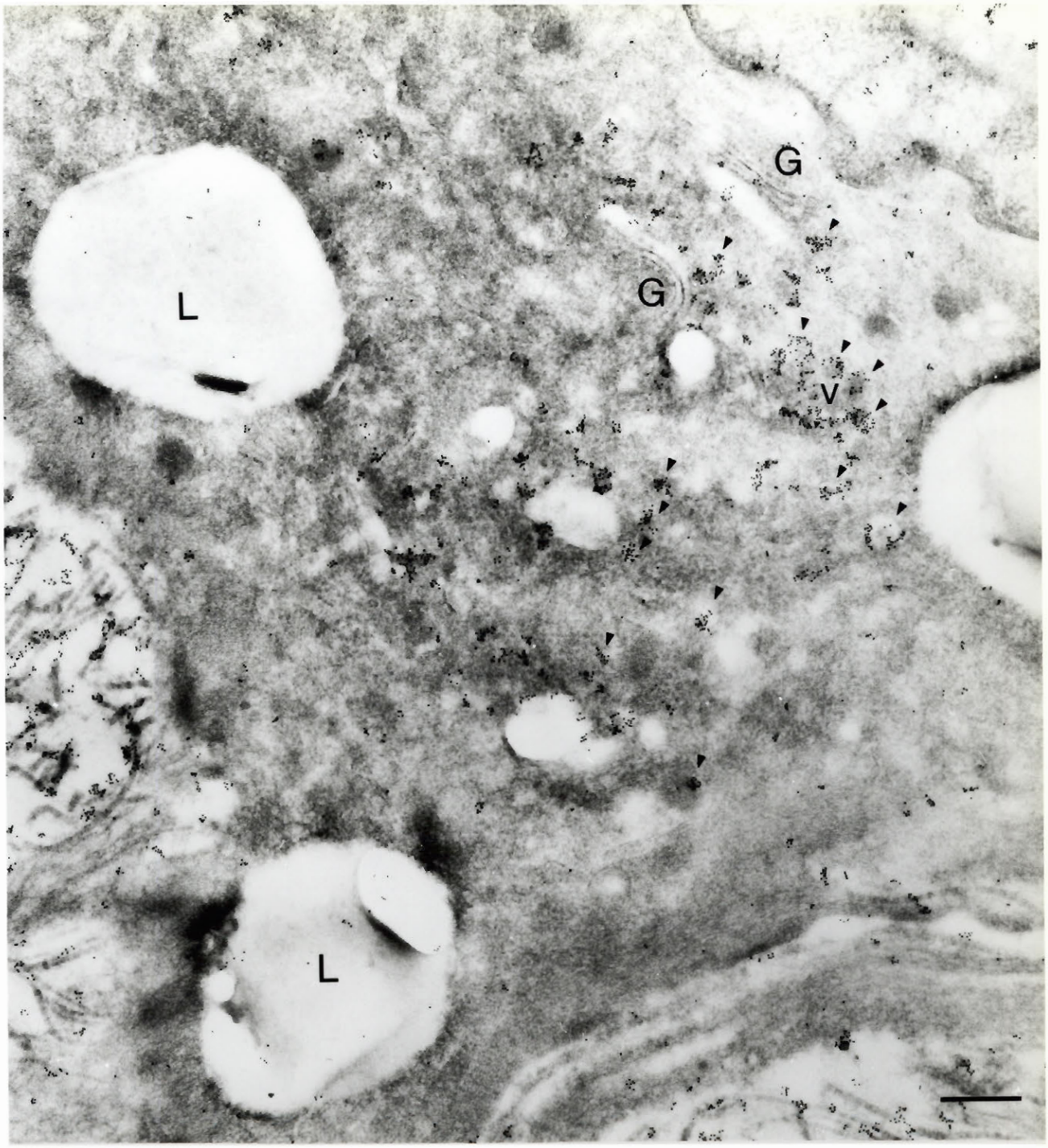
G
G
L
V
L

Fig. 7. Advanced lesion. Some of the apparent gold particle strings are circled. A. Pericellular CS-PG, labelling of the smooth muscle cell (SMC) process. x 35,500. Bar = 300 nm. B. Interstitial CS-PG. x 44,460. Bar = 300 nm.

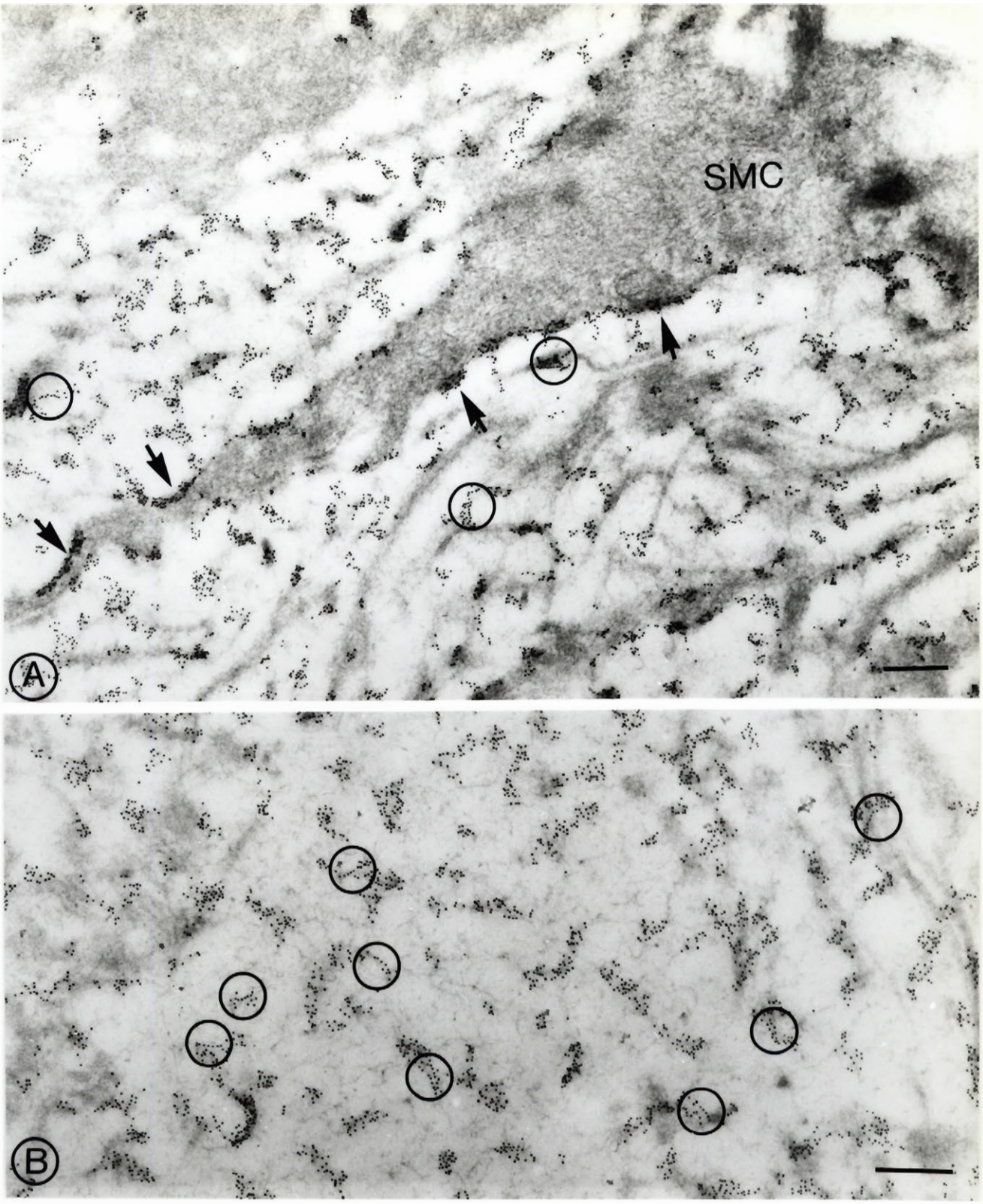
SMC
A
B

Fig. 8. Large accumulation of interstitial CS-PG. The gold labelling suggested round profiles (arrows), or spicules (arrowhead). An electron-lucent (thin arrows), and an electron-dense (thick arrows) type of vesicular structures are surrounded by CS-PG in the extracellular space, and respectively in areas of cellular necrosis. x 14,700. Bar = 1 μm.

Fig. 9. Higher magnification of the extracellular CS-PG accumulations. Round (arrows) or spicular (arrowhead) profiles are decorated by CS-PG. x 44,460. Bar = 300 nm.

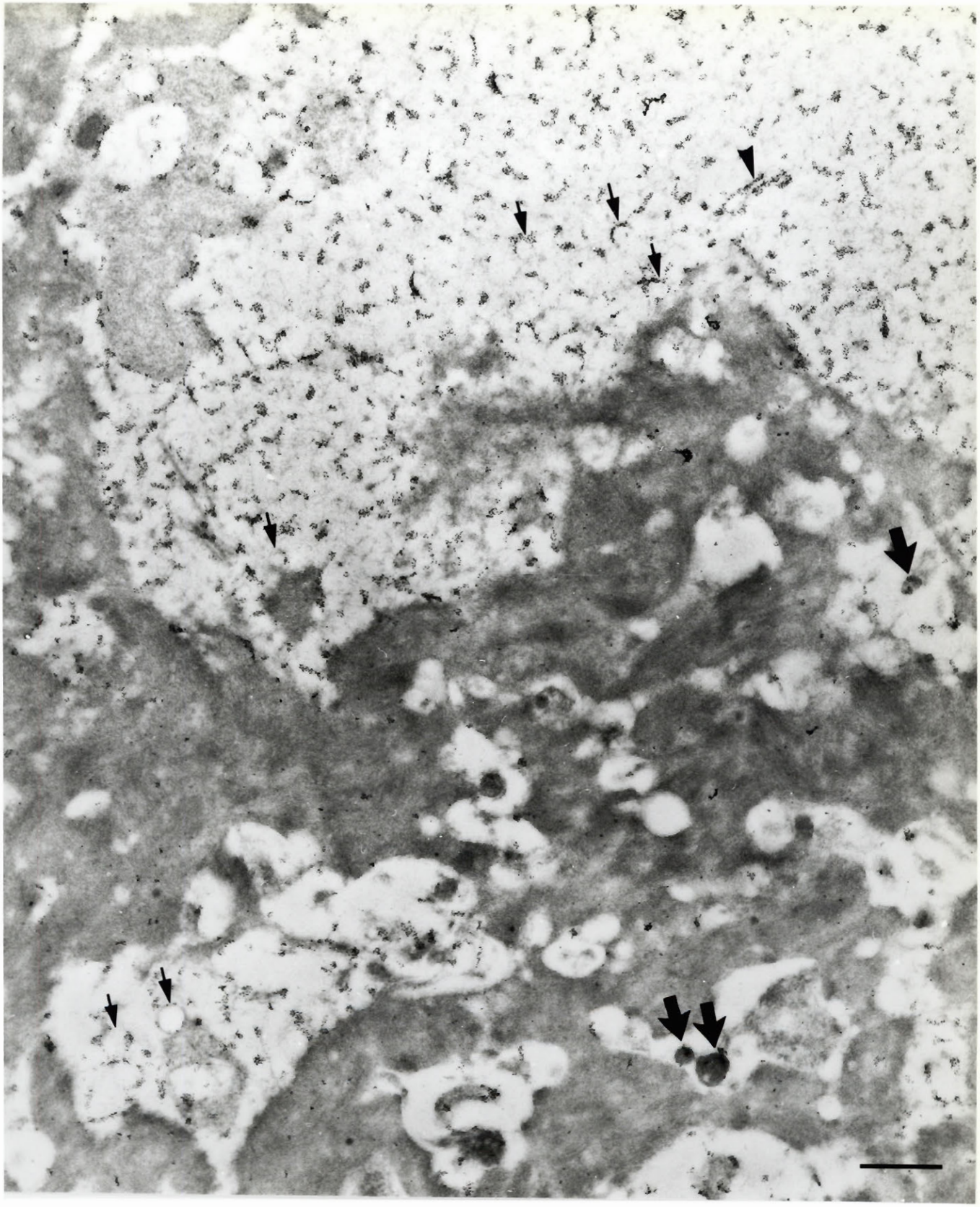

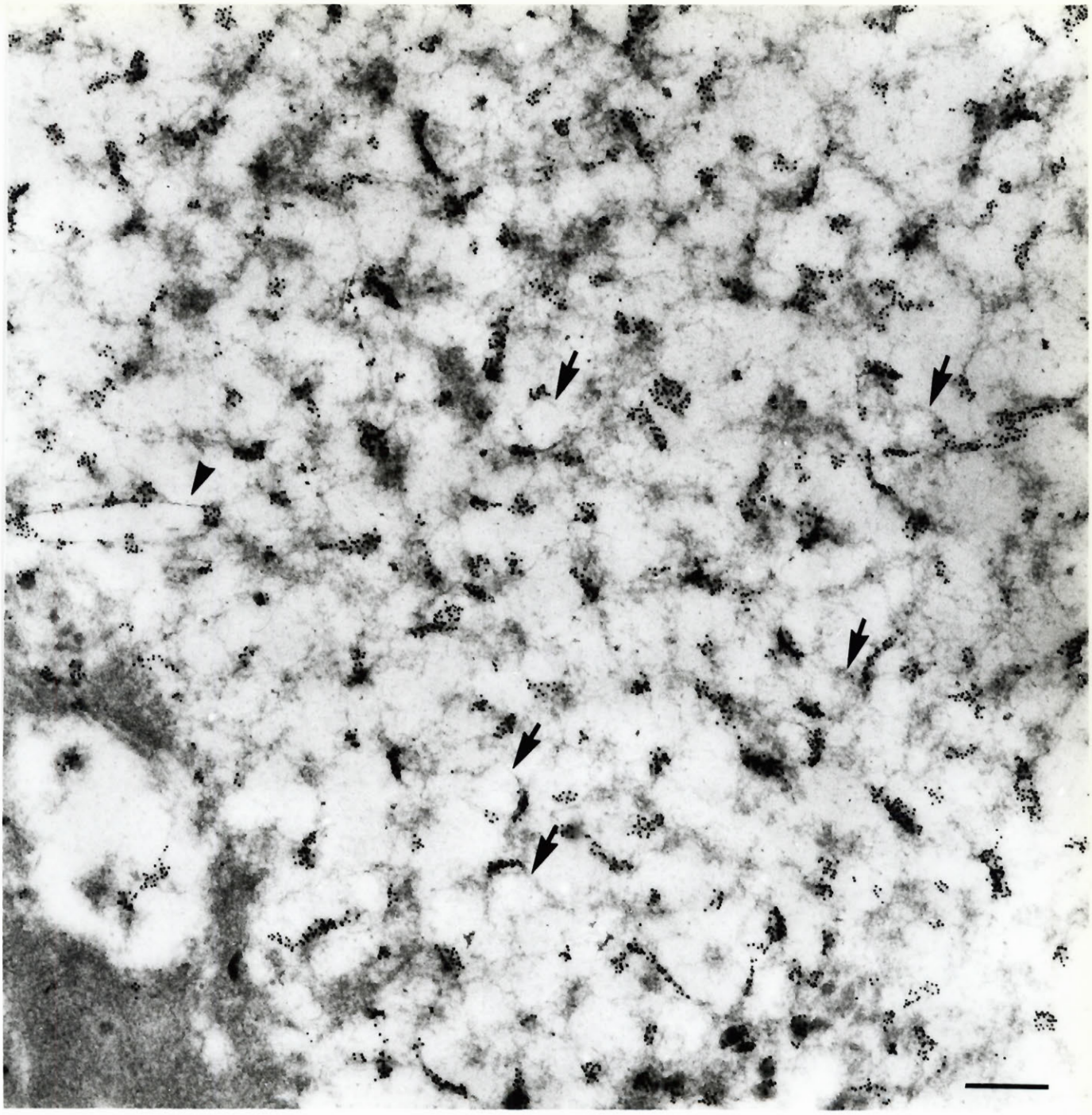

Fig. 10. CS-PG surrounding large lipid droplets, in the soluble extracellular matrix. Large intercellular space (A); and (B) close to a foam cell (FC). A, x 41,500. Bar = 300 nm; B, x 25,400. Bar = 500 nm.

Fig. 11. Extracellular (arrowheads), and respectively intracellular lipid (L) inclusions. Smooth muscle cell (SMC) of an advanced lesion. x 26,300. Bar = 500 nm.

Fig. 12. Close spatial relation between CS-positive intracellular vacuoles, and lipid inclusions (L) in a foam cell. x 22,230. Bar = 500 nm.

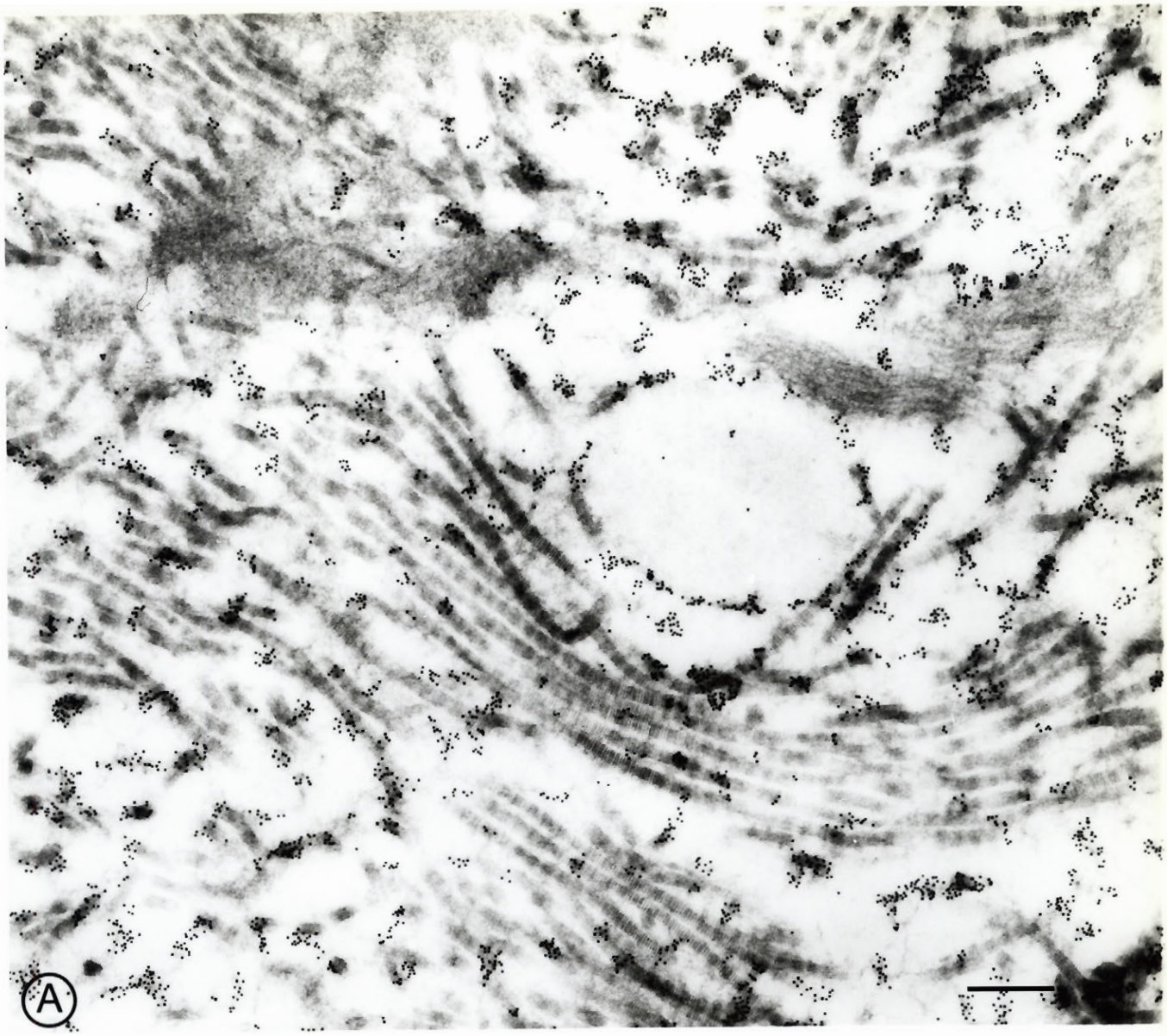
A

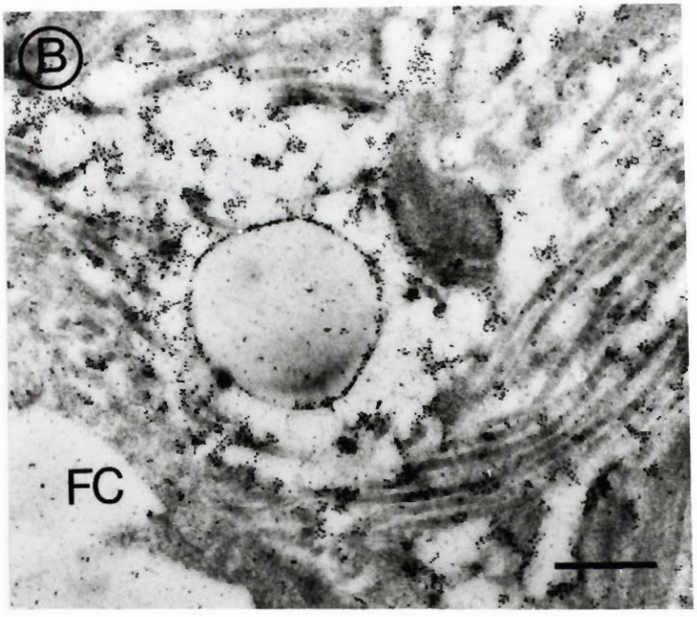
B
FC


L
L
L
SMC

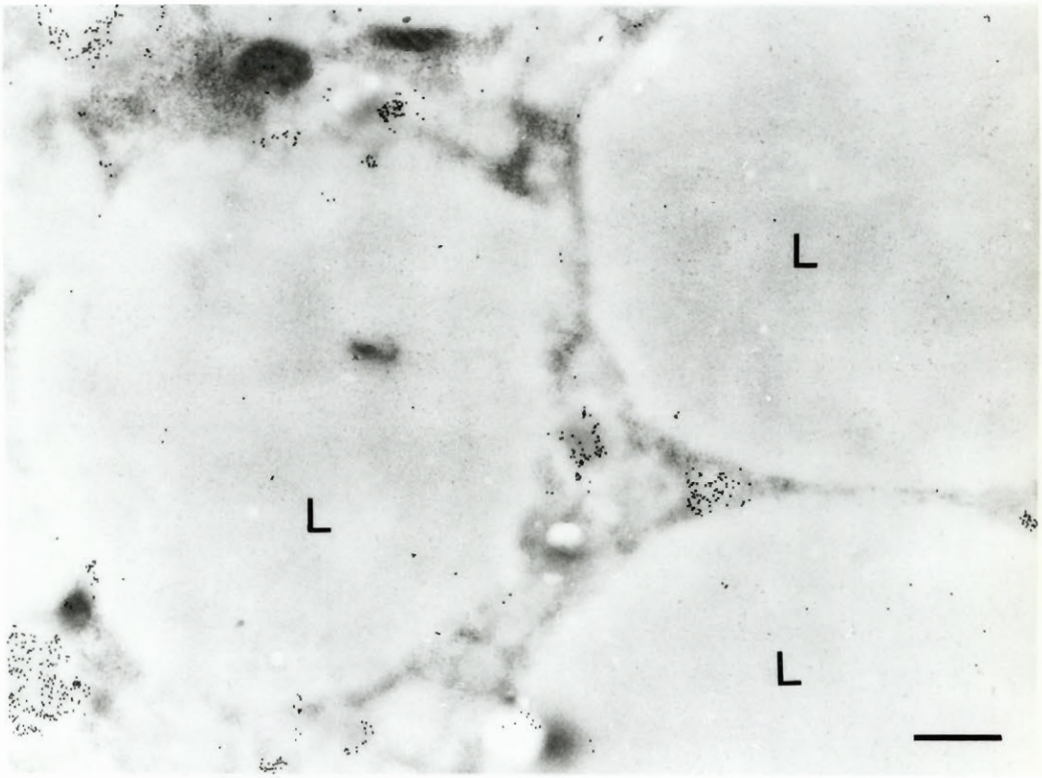
L
L
L

4.4. DISCUSSION

The main GAG moieties produced by normal arterial tissue of many species are of the CS type (Toledo and Mourao, 1980). In the normal rabbit aorta, we had previously detected that the great majority of CS-PG were concentrated in the innermost interstitial regions of the vessel wall. In the present study of the CS-PG distribution in balloon catheterized aortas, judging from the morphological characteristics of labelling, this type of PG appeared to be a major component of the vascular lesions. The thickened intima of injured aortas contained the largest share of the total aortic CS-PG, showing that the CS-PG were indeed associated with the aortic region which was most affected as an effect of the endothelial injury.

In the normal intima, the high quantity of CS-PG is probably related to the intricate interaction between endothelial and smooth muscle cells.

A recently described function for the extracellular matrix is to act as a specific, highly sensitive reservoir for the growth modulatory factors (Ruoslahti, 1989). In the case of injury, these factors would be liberated and become actively involved in the process of tissue regeneration and healing. A direct effect upon PG synthesis was found by Kahari et al. (1991), who reported that, besides a differential regulation of genes that code for the synthesis of various PG, TGFß induces fibroblasts to synthesize PG with longer GAG chains.

The healing of the aortas previously injured by endothelial removal, involves in fact many different processes. Both EC and SMC are bound to undergo migration and phenotypic modulation, processes closely influencing the synthesis of their extracellular matrix, which in turn affects the cell behaviour, and the high quantity of CS-PG in the areas covered by the regenerated endothelium could be correlated with these features of vessel repair. The migration of EC to cover the deendothelialized areas, and of SMC from the media into the intima, would depend on the inhibition of cell adhesion, and the CS moieties are known to inhibit adhesion of various other cells to their substrate (Harper and Reisfeld, 1983). Ruoslahti (1989) has proposed that this effect would be mediated

through CS-PG binding to fibronectin and masking the RGD sequences. A large CS-PG synthesized by fibroblasts was found to inhibit cell adhesion in vitro (Yamagata et al.,1989). Reid and Newman (1991) have recently reported that incorporation of CS into collagen gels facilitated the migration of human leukocytes. Kinsella and Wight (1986) also reported that wounding of endothelial cells increased the proportion of CS-PG synthesized, in comparison with the post-confluent cells, in which HS represented 80% of the synthesized sulfated PG.

Other aspects of the relation between active factors, e.g.: endothelial cell growth factor, heparin, TGFß, PDGF, and processes such as, in vitro proliferation of various cell types and the synthesis of extracellular matrix components, have been described (Chen et al., 1987; Madri et al., 1989; Battegay et al., 1990; Carey, 1991). Tan et al. (1989) reported that heparin, synthesized by EC, besides the effect upon the SMC proliferation, can modulate the content of their extracellular matrix, i.e. inhibit the synthesis of collagen, but stimulate the production of PG by the cultured SMC. This modulation of the extracellular matrix composition agrees well with the differences that were detected in this study between the ultrastructural morphology of the extracellular matrix, particularly in regard to CS-PG and collagen, in the neointima covered by the regenerated endothelium vs the regions lacking the endothelium. Lark and Wight (1986) found that collagen can in fact influence the SMC metabolism of PG, since the use of collagen gels as support to grow SMC in culture, caused the cells to both synthesize, and accumulate less chondroitin and heparan sulfate PG than SMC grown directly on plastic.

Besides EC and SMC, all other cells that have been implicated in the development of the atherosclerotic lesions can produce and secrete PG, among which CS-PG were consistently reported to be the major type of synthesized PG (Uhlin-Hansen et al., 1989; Steward et al., 1990; Nader, 1991). Conceivably, the blood borne cells could contribute directly to the total production of CS-PG in the injured aortas.

By using histochemical techniques, changes of the normal aortic sulfated PG had been previously detected in human atherosclerotic lesions (Völker et al., 1989), as well as in aortic lesions developed in experimental models of atherosclerosis (Wight and Ross, 1975; Moore and Richardson, 1985). In these studies, PG were detected through their

precipitation with various dyes, and as a result, several categories of granular precipitates were recognizable on EM, but in order to distinguish the possible nature of the molecules initially involved in the interaction, the effect of several specific enzymatic digestions of the tissue upon the staining had always to be assessed. A larger quantity of granules were usually detected in the aortic lesions. The most significant results were reported to be related to the granules supposedly contributed by CS-PG, which appeared to be more numerous, to have a larger size, and to be distributed preferentially in the same areas as the lipid accumulations.

In the present study, it was possible to detect solely the aortic CS-PG, by using a monoclonal antibody to the repetitive epitopes of the CS chains. The advantages of an unequivocal detection and of immunostaining of the tissue after embedding were combined. In this approach, the antibody did not alter the configuration of the CS-PG molecules, and had access to the entire thickness of the aortic wall. Due to the improved resolution of the immunogold labelling, we could find a reasonable explanation for the fact that in vascular lesions a larger size of chondroitinase ABC-susceptible precipitates had been shown by earlier studies. The linear strings of gold particles obtained by post-embedding detection appear to represent CS chains (Galis et al., 1992), and in injured aortas they were longer than those obtained by immunolabelling of normal aorta, suggesting that longer CS chains were present in the aortic lesions.

Since the presence of CS moieties was detectable also in intracellular sites, it was possible to see that the large, synthetic type of SMC (Thyberg et al., 1990) found in the advanced lesions of injured aortas were involved in a very active production of CS-PG, which would explain the large quantity of CS-positive material associated with their plasma membrane and secreted into the surrounding intercellular space. While various types of the extracellular CS-PG in injured aortas were reminiscent of those previously found in the normal aortas (Galis et al., 1992), the finding of conspicuous pericellular CS-positive material associated with the SMC of the lesions was new. In contrast, in the deendothelialized areas of our specimens, the synthetic activity went undetectable in the SMC of the innermost areas, in good concordance with their lack of CS-pericellular material, scarcity of extracellular CS-PG, and in fact with the overall different appearance

of these cells and their surroundings. Although at this point the meaning of this observation is not clear, different hypotheses could be put forward. Johansson et al. (1988) have demonstrated that in injured vessels the arterial SMC expressed specific antigens, and therefore it would be possible that the CS detected by us represent moieties of transmembrane proteins which were expressed by the SMC as a result of aortic injury. The specific expression of yet unidentified antigens, with a filamentous appearance, by the rabbit aortic SMC of atherosclerotic plaques, has been also reported (Desmoulière et al., 1990). On the other hand, as mentioned earlier, the amount of CS-PG could be directly related to the migration of the cells and their adhesiveness to the substrate.

In the extracellular space of the advanced lesions, CS-PG were frequently associated with the periphery of round, vesicle-like structures, presumed to represent lipid. It is possible that special properties of the CS-PG molecules or networks determine the immobilization of these structures, since the trapping effect was not detected in other densely packed extracellular material, such as the matrix of non-endothelialized regions. At least part of this effect might be related to the ionic interaction of CS-PG with the apo B moieties of the endogenous LP that typically accumulate in the advanced lesions (see ch. 2).

Numerous large CS-positive vacuoles were detected in SMC and in the lipid-filled cells of the neointima. In the latter, many of the vesicular structures were closely apposed to the lipid inclusions. Camejo et al. (1991) recently reported preliminary results indicating that the proliferating SMC produce in vitro a CS-PG of larger molecular weight than growth-arrested cells, and that this PG had higher affinity for LDL.

Based on the idea that the sulfated PG could form complexes with the LP, it was previously speculated that the foam cells could had also ingested PG (Berenson et al., 1985). However, to our knowledge, this is the first time that in situ loading of lipid-filled cells with CS-PG has actually been visualized. The finding of large intracellular CS-positive vacuoles in close relation with the intracellular lipid inclusions of foam cells, seems to support the hypothesis forwarded by the in vitro findings (Salisbury et al., 1985; Vijayagopal et al., 1985), that inside the arterial wall the CS-PG could directly contribute to the process of foam cell formation.

Our results bring new, specific evidence supporting the contribution of the aortic PG containing CS moieties in the development of the atherosclerotic lesions in an injury type of atherosclerosis.

4.5. REFERENCES

Alavi M.Z., and Moore, S. (1985). Glycosaminoglycan composition and biosynthesis in the endothelium-covered neointima of de-endothelialized rabbit aorta. Exp Mol Pathol, 42:389-400.

Battegay E.J., Raines, E.W., Seifert, R.A., Bowen-Pope, D.F., and Ross, R. (1990). TGF-ß induces bimodal proliferation of connective tissue cells via complex control of an autocrine PDGF loop. Cell, 63:515-524.

Berenson, G.S., Radhakrisnamurthy, B., Srinivasan, S.R., Vijayagopal, P., and Dalferes, E.R. (1985). Proteoglycans and potential mechanisms related to atherosclerosis. Am NY Acad Sci, 454:69-78.

Camejo, G., Hurt-Camejo, E., Fager, G., Rosengren, B., and Bondjers, G. (1991). Proliferating arterial smooth muscle cells's proteoglycans have higher affinity for low density lipoproteins than those from nonproliferating cells. Arteriosclerosis and Thrombosis, 11:1411a.

Camejo, G. (1982). The interaction of lipids and lipoproteins with the intercellular matrix of arterial tissue: Its possible role in atherogenesis. Adv Lipid Res, 19:1-53.

Camejo, G., Ponce, E., Lopez, F., Starosta, R., Hurt, E., and Romano, M. (1983). Partial structure of the active moiety of a lipoprotein complexing proteoglycan form human aorta. Atherosclerosis, 49:241-254.

Campbell J.H., Horrigan, S., Merrilees, M., and Campbell, G.R. (1990). Interactions between endothelium and other vascular structures and their abnormalities in diabetes. In Molinati, G.M., Barr, R.S., Belfiore, F., Porta, M. (eds.), Endothelial cell function in diabetic microangiopathy: problems in methodology and clinical aspects. Front Diabetes,

Basel, Karger, 9:108-117.

Carey, D.J. (1991). Control of growth and differentiation of vascular cells by extracellular matrix proteins. Annu Rev Physiol, 53:161-177.

Chen, J.K., Hoshi, H., and McKeehan, W.L. (1987). Transforming growth factor type ß specifically stimulates synthesis of proteoglycan in human adult arterial smooth muscle cells. Proc Natl Acad Sci USA, 84:5287-5291.

Desmoulière, A., Lamazière, J.M.D., and Larrue, J. (1990). Phenotypic expression of surface antigens of rabbit aortic smooth muscle cells in culture. Atherosclerosis, 85:25-35.

Galis, Z.S., Alavi. M.Z., and Moore, S. (1992). In situ ultrastructural characterization of chondroitin sulfated proteoglycans in normal rabbit aorta. J Histochem Cytochem, 40:251-263.

Harper, J.R., and Reisfeld, R.A. (1983). Inhibition of anchorage-independent growth of human melanoma cells by a monoclonal antibody to a chondroitin sulfate proteoglycan. J Natl Cancer Inst, 71:259-263.

Iverius, P.H. (1972). The interaction between human plasma lipoproteins and connective tissue glycosaminoglycans. J Biol Chem, 247:2607-2613.

Iverius, P.H. (1973). Possible role of the glycosaminoglycan in the genesis of atherosclerosis, In Porter, R., Knight, J., (eds.), Atherogenesis: Initiating factors, Ciba Foundation Symposium 12. Amsterdam, Associated Scientific Publishers, pp. 185-196.

Johansson, L., Holm, J., and Hansson, G.L. (1988). Smooth muscle cells express Ia antigens during arterial response to injury. Lab Invest, 58:310-315.

Kahari, V.M., Larjava, H., and Uitto, J. (1991). Differential regulation of extracellular matrix proteoglycan (PG) gene expression. J Biol Chem, 266:10608-10615.

Kinsella, M.G., and Wight, T.N. (1986). Modulation of sulfated proteoglycan synthesis by bovine aortic endothelial cells during migration. J Cell Biol, 102:679-687.

Lark, M.W., and Wight, T. (1986). Modulation of proteoglycan metabolism by aortic smooth muscle cells grown on collagen gels. Arteriosclerosis, 6:638-650.

Madri. J.A., Reidy, M.A., Kocher, O., and Bell, L. (1989). Endothelial cell behaviour after denudation injury is modulated by transforming growth factor-β_1 and fibronectin. Lab Invest, 60:755-765.

Merrilees, M.J., and Scott, L.J. (1985). Effects of endothelial removal and regeneration on smooth muscle glycosaminoglycan synthesis and growth in rat carotid artery in organ culture. Lab Invest, 52:409-419.

Moore, S, and Richardson, M. (1985). Proteoglycan distribution in catheter-induced aortic lesions in normolipaemic rabbits. Atherosclerosis, 55:313-330.

Nader, H.B. (1991). Characterization of a heparan sulfate and a peculiar chondroitin-4-sulfate proteoglycan from platelets. J Biol Chem, 266:10518-10523.

Radhakrishnamurthy B, Srinivasan, S.R., Eberle, K., Ruiz, H., Dalferes, E.R. Jr., Sharma, C, and Berenson, G.S. (1988). Composition of proteoglycans synthesized by rabbit aortic explants in culture and the effect of experimental atherosclerosis. Biochim Biophys Acta, 964:231-243.

Richardson, M., Gerrity, R.G., Alavi, M.Z., and Moore, S. (1982). Proteoglycan distribution in areas of differing permeability to Evans blue dye in the aortas of young

pigs. An ultrastructural study. Arteriosclerosis, 2:369-379.

Reid, G.G., and Newman, I. (1991). Human leucocyte migration through collagen matrices containing other extracellular matrix components. Cell Biol Int Rep, 15:711-720.

Robbins R.A., Wagner, W.D., Sawyer, L.M., and Caterson, B. (1989). Immunolocalization of proteoglycan types in aortas of pigeons with spontaneous or diet-induced atherosclerosis. Am J Pathol, 134:615-626.

Ruoslahti, E. (1989). Proteoglycans in cell regulation. J Biol Chem, 264:13369-13372.

Salisbury, B.G., Falcone, D.J., and Minick, C.R. (1985). Insoluble low-density lipoprotein-proteoglycan complexes enhance cholesteryl ester accumulation in macrophages. Am J Pathol, 120:6-11.

Steward, W.P., Christmas, S.E., Lyon M., and Gallagher, J.T. (1990). The synthesis of proteoglycans by human T lymphocytes. Biochim Biophys Acta, 1052:416-425.

Tan, E.M.L., Levine, E., Sorger, T., Unger, G.A., Nacobian, N., Planck, B., Iozzo, R.V. (1989). Heparin and endothelial cell growth factor modulate collagen and proteoglycan production in human smooth muscle cells. Biochim Biophys Res Commun, 163:84-92.

Toledo, O.M.S., and Mourao, P.A.S. (1980). Sulfated glycosaminoglycans in normal aortic wall of different mammals. Artery, 6:341-353.

Uhlin-Hansen, L., Eskeland, T., and Kolset, S.O. (1989). Modulation of the expression of chondroitin sulfate proteoglycan in stimulated human monocytes. J Biol Chem, 264:14916-14922.

Völker, W., Schmidt, A., and Buddecke, E. (1989). Cytochemical changes in a human arterial proteoglycan related to atherosclerosis. Atherosclerosis, 77:117-130.

Wight, T.N. (1989). Cell biology of arterial proteoglycans. Arteriosclerosis, 9:1-20.

Wight, T.N., Potter-Perigo, S., and Aulinskas, T. (1989). Proteoglycans and vascular cell proliferation. Am Rev Respir Dis, 140:1132-1135.

Wight, T.N. and Ross, R. (1975). Proteoglycans in primate arteries. I. Ultrastructural Localization and distribution in the intima. J Cell Biol, 67:660-674

Yamagata, M., Suzuki, S., Akiyama, S.K., Yamada, and K.M., Kimata, K. (1989). Regulation of cell-substrate adhesion by proteoglycans immobilized on extracellular substrates. J Biol Chem, 264:8012-8018.

CHAPTER 5

Selective extraction and alternative glycosaminoglycan moiety analysis of the sulfated proteoglycans synthesized by rabbit aorta[1]. Zorina S. Galis*, Misbahhudin Z. Alavi, and Sean Moore, Department of Pathology, McGill University, Montreal, Canada.

Running title: Selective proteoglycan extraction and glycosaminoglycan analysis

* For correspondence: Zorina Galis
Department of Pathology
McGill University
3775 University, Montreal
Que, Canada H3A 2B4
tel.: 514-398 7242, fax: 514- 398 7446

Subject category: purification of enzymes and proteins; or if possible - proteoglycan isolation and analysis

1. This work was supported by the Medical Research Council of Canada (MT 1065). ZSG receives a fellowship from Fonds pour la Formation de Chercheurs et Aide à la Recherche, Quebec, Canada.

5.1 ABSTRACT

We compared the molecular size distributions and glycosaminoglycan (GAG) compositions of the ^{35}S-metabolically labelled molecules extracted from normal rabbit aortic tissue by three different solutions containing urea, guanidine hydrochloride, or detergents. By using these different media, we found differences related not only to overall efficiency of the extraction, but also to the nature of the isolated sulfated proteoglycans (PG) extracted by each solution. A characteristic spectrum of ^{35}S-PG was consistently extracted by each solvent used for consecutive extractions of the tissue, either alone, or after another. The solution containing detergents was found to preferentially extract smaller, heparan sulfate-rich aortic PG, and to produced better yields for these molecules than the commonly used guanidine. We concluded that it was possible to selectively extract aortic PG types by alternatively using different types of extraction conditions. On the other hand, a larger variety of aortic ^{35}S-PG can be isolated from aortic tissue by the consecutive use of different solvents than by single extractions. An alternative method for the evaluation of the GAG distribution among different PG populations was also investigated by adsorbing gel filtration fractions to a support membrane. A simultaneous assessment of the GAG types in each fraction was possible through processing of the membrane. We found that in comparison with standard methods, the blotting method generated comparable information while being applicable directly after the chromatographic separation, using smaller quantities of sample and reducing the requirements of labour and laboratory equipment.

5.2. INTRODUCTION

A large variety of extracellular or cell-associated molecules (1,2) are grouped together as PG on the basis that all consist of a central core protein endowed with at least one unbranched carbohydrate GAG side chain. However, since the nature of the protein is variable and the glycosidic moieties vary widely in composition, number and size, different PG molecules can be extracted from one source (3). The GAG composition and PG properties of different tissues, such as the arterial wall, have been also shown to be modulated by different physiologic and pathologic conditions (4-6). While assays of the overall GAG composition of tissues are usually performed after delipidation and proteolytic digestion, therefore being less influenced by the method used for the GAG isolation, in the case of examining whole PG molecules present in a tissue, the results of the biochemical analysis depend largely on the conditions used for their extraction. We were interested in obtaining a preparation closely reflecting the variety of the PG molecules synthesized by the normal aortic wall. Currently, the use of high concentrations of guanidine hydrochloride (7) appears to be the method of choice for PG extraction from most sources (3), but Wiklund et al.(8) have found that 6 M urea to be more efficient than guanidine in extracting aortic PG. Therefore, we investigated in more detail the use of urea for extraction, by analyzing the properties of sulfated aortic PG that could be extracted with urea or guanidine, as well as of those extractable by using a detergent mixture. In addition, for the characterization of the GAG moieties present in the PG molecules separated by size distribution chromatography, we also tried to develop an easy way of obtaining the same kind of information, as that generated by the use of standard methods, but starting from smaller quantities of tissue extracts. Fractions from a single chromatographic run could be blotted on several support membranes and simultaneously analyzed by enzymatic treatments, immunostaining and autoradiography.

5.3. MATERIALS AND METHODS

The chondroitinase ABC (EC 4.2.2.4), chondroitinase AC (EC 4.2.2.5), heparinase III (E.C. 4.2.2.8), and anti-chondroitin sulfate (CS) monoclonal antibodies were from Sigma Chem Co. (St. Louis, MO), as well as other chemicals unless otherwise stated. Anti-mouse Ig/horseradish peroxidase (HRP) were from Amersham Canada Ltd. (Oakville, Ont). Blue dextran 2000 was from Pharmacia LKB Biotechnology (Uppsala, Sweden). Sepraphore-L cellulose acetate electrophoresis membrane was from Gelman Sciences Inc. (Ann Arbor, MI) and the nitrocellulose (NC) membrane from Bio-Rad Laboratories (Richmond, CA). $Na_2{}^{35}SO_2$, sulfate-depleted Dulbecco's modified Eagle's medium (DMEM), and Cytoscint scintillation cocktail were from ICN Biomedicals Canada, Ltd. (St. Laurent, Que).

5.3.1. Metabolic labelling. For the in vitro metabolic labelling of aortic PG, freshly harvested rabbit aortas were incubated separately in a controlled gaseous atmosphere (95% O_2 + 5% CO_2) at 37°C for 6 h, with 1 mCi $Na_2{}^{35}SO_4$ in sulfate-depleted DMEM supplemented with 10% fetal bovine serum. At the end of the incubation, the aortas were washed twice with cold sulfate-depleted medium, then with cold saline and the intimal-medial layers were peeled off and blotted dry. The intimal-medial tissue was weighed and evenly distributed for simultaneous extraction in three different extraction solutions.

5.3.2. PG extraction. After ice cold extraction solutions were added over the tissue (1 ml/100 mg), this was finely minced with scissors inside the vials, and extracted for 24 h at 4°C, on an orbital shaker. The tissue was pelleted by a 5 min centrifugation in a micro-centrifuge 235B (Fisher Scientific Ltd., Canada), the supernatants were collected, and fresh extraction media were added over the tissue. Similar procedures were used to re-extract the tissues up to three times, using for re-extraction the same solutions, or switching the extraction mixtures.

5.3.3. Extraction solutions. The following solution were used: A. 6 M urea, 1 M

NaCl; B. 20 mM Na phosphate buffer, pH 7.2, 300 mM Na chloride, 1% Na deoxycholate, 0.2% Na dodecyl sulfate, 2% Triton X-100, 0.2% Na azide (PBSTS); C. 4 M guanidine-HCl (GdnHCl) in 100 mM Tris-HCl, pH 8. In addition, all three solutions contained the following cocktail of protease inhibitors: 10 mM ethylenediaminetetraacetate (EDTA), 1 mM phenylmethylsulfonyl fluoride (PMSF), 5 mM benzamidine-HCl and 10 mM ϵ-aminocaproic acid.

5.3.4. PG characterization. Size distribution chromatography. The aortic extracts were chromatographed either directly, or after digestion with GAG specific enzymes. For gel filtration, the samples were dialysed overnight at 4°C against 100 mM Tris-HCl, pH 8 containing 0.5% Triton X-100, then redissociated by adding solid GdnHCL (to final 4 M) and injected into a Superose 6 HR 10/30 column connected to a FPLC System (Pharmacia LKB Biotechnology, Uppsala, Sweden). The column was equilibrated with 100 mM Tris-HCl, pH 8 containing 4 M GdnHCl and 0.5% Triton X-100. The void and the total volumes were determined using Blue dextran and $Na_2{}^{35}SO_4$ respectively. The flow rate used for separation was 0.2 ml/min, and 0.4 ml fractions of the inclusive volume were collected. Fractions were monitored for radioactivity by liquid scintillation counting of aliqouts using a LKB Wallac 1211 BetaRack instrument (Fisher Scientific Ltd., Canada). Aliquots of the gel filtration fractions obtained from the urea and PBSTS extracts were also blotted on NC membrane and processed as further described.

5.3.5. GAG composition of whole aortic extracts. GAG composition was determined after the proteolytic digestion of the extracts, previously dialysed against 100 mM Tris-HCl pH 8. These were incubated with papain (25:1 protein/enzyme, w/w) overnight at 37°C, in the presence of 5 mM cystine-HCl and 10 mM EDTA. The protein in the samples was precipitated with trichloroacetic acid (6% final concentration) and the supernatants were mixed with equivalent volumes of saturated Na acetate. GAG were precipitated overnight at -20°C by the addition of cold absolute ethanol (4:1), dried under nitrogen, then resuspended with distilled water, and applied to cellulose acetate membranes along with GAG standard mixtures for electrophoresis (5). The run was performed in a Semi-Micro electrophoresis chamber (Gelman Sci. Inc., Ann Arbor, MI) filled with 0.3 M cadmium acetate buffer, pH 4.1, at 4.5 mA/strip for 1 hr. The

cellulose membrane was stained with Alcian blue, then dried and exposed 7 days to X-ray film at -70°C for the detection of ^{35}S-GAG. Their composition was determined by the densitometric analysis of the autoradiographies using a Hoefer GS-300 scanning densitometer equipped with a computer GS-360 software (Hoefer Scientific Instruments, San Francisco, CA).

5.3.6. Distribution of sulfated GAG moieties. The distribution of various sulfated GAG types, as moieties of the PG molecules separated from each extract, was assessed by two methods.

(I). *Comparative size distributions of extracts before and after selective digestion with GAG lyases: chondroitinases ABC, AC, or heparinase III.* After incubation of aliquots with 100 mU enzyme/ml of 100 mM Tris-HCl, pH 8 at 37°C for 6 hr, solid GdnHCl was added, and then the digested samples were loaded on the Superose column.

(II) *Analysis of gel filtration fractions adsorbed on a support membrane.* 100 µl aliquots of the fractions obtained from both the urea and PBSTS extracts were applied in duplicates onto the same NC membrane using a slot-blot device (Bio-Rad Laboratories, Richmond, CA), thus generating two analogous parts for each blot. The slots of the blotting device were rinsed three times with 100 mM Tris-HCl, pH 8. Then the membranes were removed, allowed to dry, and cut into halves. Each two identical pieces were similarly processed. They were rehydrated and introduced in plastic bags filled with 50 mM Tris-acetate buffer, pH 8.0 (9). Chondroitinase ABC was added to one of the two bags (50 mU/ml), and both were incubated overnight at 37°C on an orbital shaker. At the end of the incubation, the membranes were washed with three changes of 10 mM Na phosphate, pH 7.2 containing 150 mM Na chloride, 0.05% Tween 20 (T-PBS), and 1% bovine serum albumin (BSA). In order to reveal the effect of the enzymatic treatment, some of the membranes have been dried and exposed to X-rays films for autoradiography, while others have been further incubated for 2 hr with an anti-chondroitin sulfate (CS) antibody diluted to 1/500 in T-PBS. The membranes were washed 3 x 5 min with T-PBS + 1% BSA, and incubated for 1 hr with 1/500 anti mouse Ig/HRP conjugate in T-PBS. The reaction was developed with diaminobenzidine (22 mg in 20 ml of PBS + 200 µl

1% cobalt chloride, and 10μl 30% hydrogen peroxide). For the evaluation of the results, the previously mentioned densitometric device was used to scan in the transmission mode the autoradiographic images of the blots, or in the reflection mode the immunostained blots.

5.4. RESULTS

5.4.1. Size distribution chromatography

Essentially two populations of ^{35}S-labelled PG could be separated from each extract of aortic intimal-medial tissue in the conditions chosen for size distribution chromatography (Fig.1A). A higher efficiency of extraction was obtained with urea than with guanidine, but the size distribution of ^{35}S-labelled PG isolated by either of them from the tissue was very similar. For instance, by the integration of the chromatographic profiles with an image analyzer (Videoplan Processing System, Kontron Bild Analyse, Germany), we estimated that in both urea and guanidine extracts, the sharp peak of high molecular weight ^{35}S-PG represented one third of the radioactive material, while the less homogenous population of sulfated PG forming the second, broader peak represented around 50% of the total area. In contrast with this molecular size distribution, the second peak of the PBSTS extract totalled around 80% of the ^{35}S-radioactivity of this sample.

5.4.2. Overall GAG composition

The GAG analysis (Fig. 1B) of the crude extracts obtained with 6 M urea or 4 M GdnHCl indicated that they contained predominantly chondroitin-4-sulfate and chondroitin-6-sulfate (which migrate in the same position on electrophoresis, so we designated both as CS), and smaller quantities of dermatan sulfate (DS) and heparan sulfate (HS). HS accounted for 25% to 38% of the total sulfated GAG in these extracts, while in the PBSTS extract it represented more than half.

Fig. 1. The characteristic chromatographic profiles (A) and GAG compositions (B) of the ^{35}S-metabolically labelled PG extracted by different solutions from the intimal-medial layers of normal rabbit aorta.

(A) Size distribution of newly synthesized sulfated PG obtained by gel filtration of various extracts in dissociating conditions on a Superose 6 HR 10/30 column.

(B) GAG electrophoresis. Autoradiographic image of cellulose acetate electrophoresis of ^{35}S-GAG isolated from the extracts obtained in: urea (1), PBSTS (2), and GdnHCl (3). (4) Alcian blue stained lane of the same cellulose membrane containing an electrophoretically separated GAG standard mixture. CS = chondroitin sulfate (both C-4-S and C-6-S), DS = dermatan sulfate, HS = heparan sulfate, HA = hyaluronic acid.

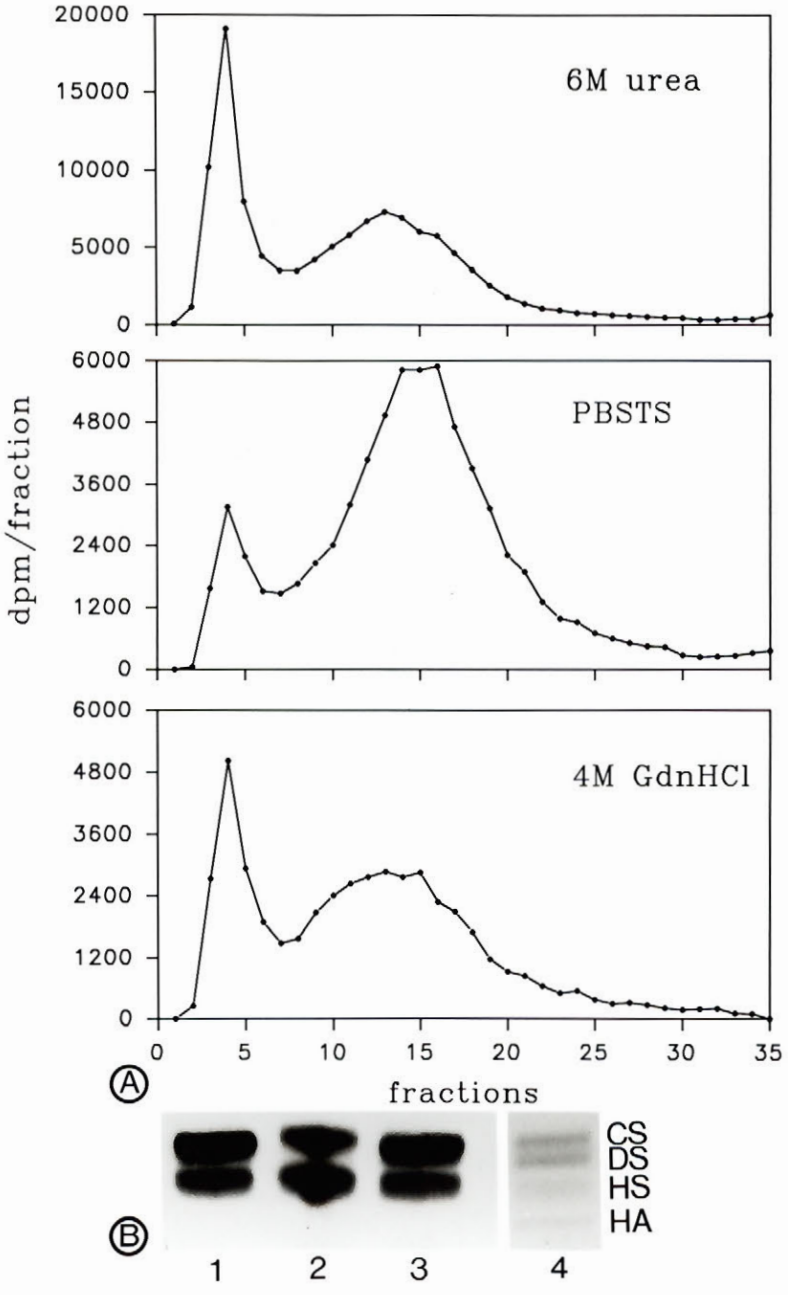
6M urea
PBSTS
4M GdnHCl
dpm/fraction
fractions
Ⓐ
Ⓑ
CS
DS
HS
HA
1
2
3
4

5.4.3. Effect of tissue re-extraction

We also analyzed the chromatographic profiles and the GAG compositions of the preparations obtained from the same sample by re-extraction when either the same, or a different solution was used (Fig. 2 A & B). In the case illustrated in Fig. 2 A, the reutilization of urea, analogous with an initial extraction, produced a balanced size distribution of 42% large molecular weight vs. 48% smaller ^{35}S-PG, and predominantly CS moieties. However, when after two extractions with urea, the solution was changed to PBSTS and a third reextraction of the same sample was conducted, 75% of the isolated ^{35}S-molecules were small PG, and this time mainly HS moieties were extracted from the tissue. This showed that if a different solution e.g. PBSTS was used for a subsequent extraction after an initial urea extraction, molecules endowed with distinct biochemical properties could be isolated from the same tissue sample. Parallel results were obtained when the samples were initially extracted with PBSTS, and then with urea (Fig. 2 B). It was concluded that the choice of a certain solution either for extraction or reextraction, even after another solution, would determine the nature of the sulfated PG molecules extracted from the aortic tissue. Specifically, the high molecular size sulfated PG were more efficiently extracted by urea used either in the first place, or for re-extraction either after urea, or PBSTS. Similarly, PBSTS extracted mainly lower molecular weight, HS-rich molecules either at an initial extraction or at subsequent re-extractions.

Fig. 2. The size distribution profiles and the GAG compositions of the ^{35}S-labelled PG obtained at successive reextractions of aortic tissue. The first and second extraction of each analogous sample was conducted in the same conditions (——), while for the third extraction the solutions were switched, and each sample was re-extracted in different

conditions (····). (A) Sample extracted the second time in urea (graph identified as "2 x urea"); and the third time in PBSTS ("2 x urea, 1 x PBSTS"). Inset. GAG electrophoresis. Autoradiographic image of the GAG isolated from the same sample at the second extraction by urea (lane 1), and at the subsequent third extraction by PBSTS (lane 2). Lane 3, Alcian blue-stained electrophoretic GAG standards simultaneously separated. (B). Sample consecutively extracted two times with PBSTS, "2 x PBSTS"; and the third time with urea, "2 x PBSTS, 1 x urea". Inset. Autoradiographic image of the GAG composition of corresponding extracts: the second PBSTS extract (lane 1), the third in urea (lane 2). Lane 3, GAG standards.

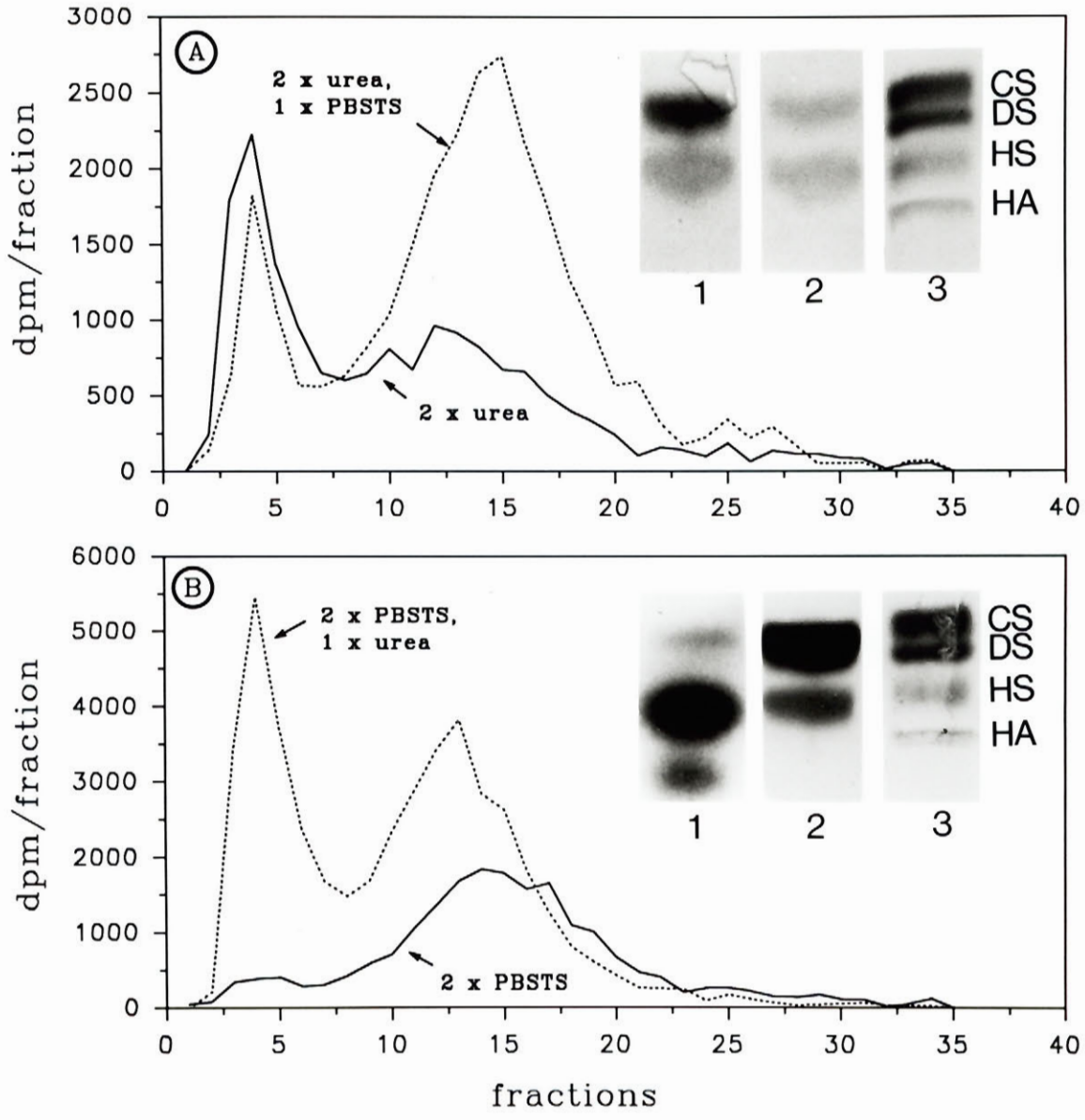
A
2 x urea,
1 x PBSTS
2 x urea
dpm/fraction
3000
2500
2000
1500
1000
500
0
0
5
10
15
20
25
30
35
40
CS
DS
HS
HA
1
2
3
B
2 x PBSTS,
1 x urea
2 x PBSTS
dpm/fraction
6000
5000
4000
3000
2000
1000
0
fractions

5.4.4. Distribution of GAG moieties

The allotment of the sulfated GAG moieties to PG of diverse molecular sizes was studied by two approaches.

(I) *Effect of a selective enzymatic digestion of the aortic extract prior to gel filtration.* The digestion of each of the three extracts with chondroitinase ABC produced an obvious reduction of the first peak amplitude, as exemplified in Fig. 3A for the urea extract. Overall bound ^{35}S-radioactivity in this sample was reduced to 50%, the first peak being especially affected. The second peak was also obviously diminished in the case of both urea and guanidine extracts, but much less so in the case of the PBSTS extract. The effect of the other enzymatic digestions supported the conclusion that the high molecular weight peak always contained C-4/6-S, while the second peak contained a mixture of DS, CS and HS in the urea/guanidine, or HS in the PBSTS extract.

(II) *Analysis of the gel filtration fractions immobilized on a support membrane.* Similar information was obtained by the alternative procedure involving the blotting of aliquots from successive fractions on the NC membranes. The X-ray films obtained by the exposure of the blots allowed the identification of the two peaks of ^{35}S-labelled molecules (Fig. 3B). The intensity of the lines corresponding to both the first and second peaks of the urea extracts were visibly reduced as a result of the incubation with chondroitinase ABC. For example, we estimated by densitometric analysis that, due to enzymatic digestion, the values of the optical density corresponding to the untreated NC membrane were reduced on average to $53.8 \pm 7.1\%$ ($n = 5$) for the fractions of the first peak, and respectively to $59.5 \pm 12.5\%$ ($n = 7$) for the second peak. In the PBSTS extract the intensity of the first peak was comparably diminished, while by averaging the decrease of individual fraction intensities in the second peak, this appeared to be much less affected ($87.2\% \pm 13.4\%$, $n = 7$). These estimations showed that the fractions adsorbed

to the NC membrane had been selectively affected by incubation with chondroitinase ABC and confirmed that by this method it was possible to distinguish the type of ^{35}S-GAG present in the fractions. In our conditions, an initial count of minimum 500 dpm per blotted aliquot was required for the assessment of the enzymatic treatment effect upon the intensity of the autoradiographic images of the blots.

Alternatively, the same distribution of the CS moieties was indicated on the blots by the anti-CS antibody, which stained the fractions forming the first peak of either urea or PBSTS, and the second peak of urea. The prior incubation of the blots with chondroitinase ABC practically abolished the immunostaining (data not shown).

Fig. 3. The distribution of sulfated GAG moieties in the urea extract, analyzed by two methods. (A) Size distribution chromatography of ^{35}S-labelled molecules before (——), and after (····) digestion with chondroitinase ABC. (B) Autoradiographic image of twin NC membranes on which identical aliquots of the chromatographic fractions of a similar urea extract were applied, top to bottom, # 2-8 on the left, and # 9-17 respectively on the right vertical row. The membrane on the right has been incubated with chondroitinase ABC (+), as described in the text.

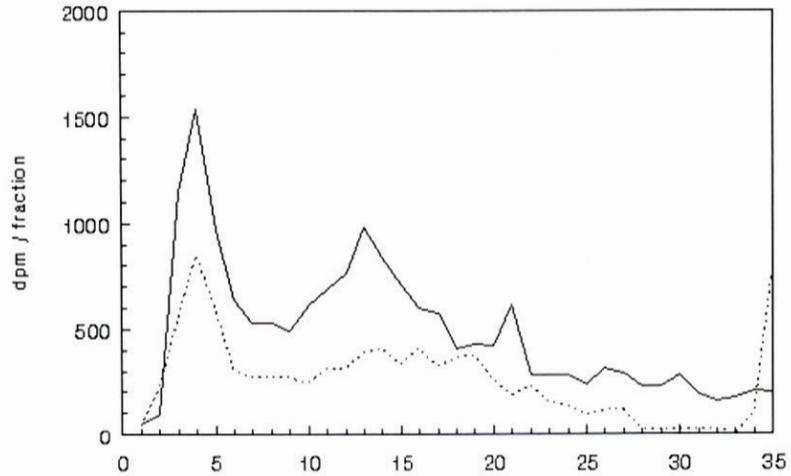
2000
1500
1000
500
0
dpm / fraction
0
5
10
15
20
25
30
35
fractions

Ⓐ

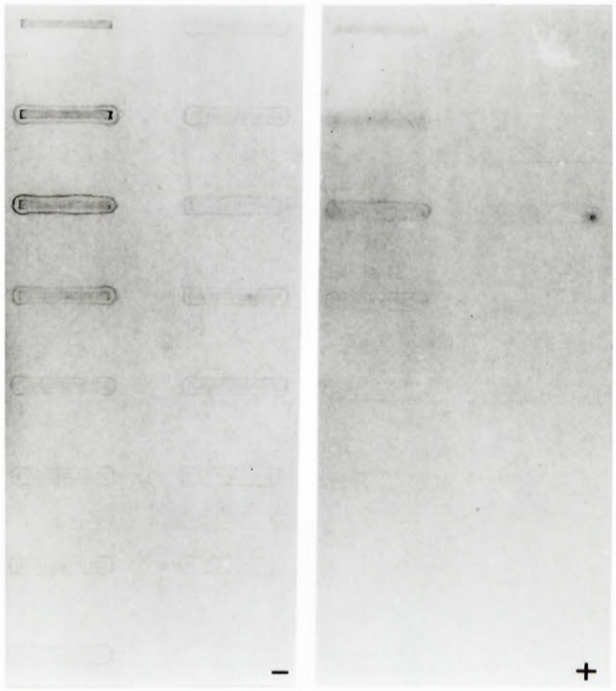
–
+

Ⓑ

5.5. DISCUSSION

The preparations obtained using three different solutions for extraction were afterwards equilibrated in the same buffer and analyzed by size distribution chromatography in the same conditions. The system selected for gel filtration allowed a good separation and recovery of all the samples. In spite of the disadvantage of a high UV absorbance, Triton X-100 was used in the elution buffer to maintain the solubility of the samples extracted with the detergent containing solution and to increase the recovery (3). The 100 mM Tris-HCl, pH 8 buffer was found to be an appropriate medium for the enzymatic digestions with chondroitinases, and with papain even in the presence of 0.5% Triton. The re-equilibration of the samples between different steps could be avoided by the consistent use of this buffer and simple addition of solid GdnHCl prior to chromatography.

5.5.1. Effect of the extraction medium upon the biochemical properties of aortic preparations

The choice of the method used for the extraction of PG will invariably influence the reported composition of the tissue. The guanidine and urea extraction of aortic tissues were found to result in preparations of sulfated PG with rather similar properties. In comparison, the detergent containing solution used for extraction, produced a high yield of HS-PG. The distinction was maintained even when one extractant was used after another, i.e. changing the solution used for re-extraction modified the characteristics of the ^{35}S-PG obtained from the same sample. This confirmed the capacity of urea and PBSTS for a selective isolation of PG molecules from the aortic tissues, and PBSTS solution might be useful for a preferential extraction of HS-rich PG. The HS has been previously reported to be the major GAG that remains unextracted from aortic tissue after a GdnHCl treatment (10), and the HS-PG are presumably more tightly bound in the cellular basement membrane or are cell-associated (1,6). In the case of tissue re-extraction by using a different solution, molecules less extractable in a previous solution supposedly

become mobilized, and the variety of the extracted sulfated PG could be increased by successive extractions in different conditions.

5.5.2. Assessment of the methods used for analyzing the distribution of GAG moieties

The GAG distribution among different PG populations separable by size chromatography has been commonly analyzed by two methods. One method is to perform separate gel filtration runs of the sample before and after digestion with specific enzymes, and to detect differences in the chromatographic profiles of the molecular size distribution. The release of small saccharidic residues by GAG enzymatic digestion of the sample decreases the quantity of the PG-associated radioactivity and reduces the molecular weight of the molecules, therefore displacing them in the chromatographic profile. This effect may significantly interfere with the individual assessment of the fractions most affected, such as digestion with chondroitinase ABC, which non-specifically attacks hyaluronic acid, the "backbone" of large aggregating PG. We examined the GAG distribution by both the standard method of several chromatographic runs and by an alternative method of simultaneously analyzing the immobilized fractions, and found that the latter produced comparable information. During this procedure, the GAG distribution was analyzed by blotting of the radioactive fractions obtained from the chromatographic separation, digestion of the blots, and autoradiography or immunostaining. In the standard method a larger quantity of sample is obviously necessary in order to perform the several runs required for the detection of the enzymatic digestion effect. This may not be a critical issue with some tissues, such as cartilage, which are readily available in sufficient quantities and contain important amounts of PG. In our experiments, we have been often confronted with problems related to the limited quantities of rabbit aortic tissue which contains rather small quantities of connective tissue, and therefore of sulfated PG. Therefore we found this method, which minimized the sample requirements, very useful. For the other, more elaborate standard procedure, the chromatographic fractions have to be individually processed, usually by dialysis, precipitation, and GAG electrophoresis, in order to obtain their GAG composition (3). In comparison with this method, the alternative blotting method still allows an individual

assessment of each fraction, without the rather complex handling of many separate samples. Actually, after a single chromatographic run, aliquots of the same fractions can be applied onto several membranes for various analyses aimed at an overall evaluation of the fraction content (i.e. radioactivity, GAG, protein), or for the more detailed assessment of the type of GAG moieties present in each fraction. We found that in spite of the high GdnHCl concentration and the presence of detergent, it was possible to process the blotted fractions directly after gel filtration by one, or by combinations of the following: enzymatic treatments with various enzymes digesting distinct GAG moieties, Alcian blue or protein staining, immunostaining, and autoradiography (when radioactive GAG were analyzed). We anticipate that other blotting supports, such as nylon membranes whose utility for an Alcian blue dot assay was previously described (11), could also be suitable for the enzymatic treatment procedures. The method may be used to analyze samples other than chromatographic fractions, being especially useful for samples that contain high salt concentration or detergents. The quantitative interpretation of the results obtained with the various methods of processing the immobilized fractions would require either a densitometric, spectrophotometric, or liquid scintillation counting analysis. However adequate information may be easily obtained from a simple visual inspection of the blots and/or autoradiographs; therefore the blotting method can be used efficiently with a minimum of equipment, i.e. in the absence of a beta counter, spectrophotometer, or densitometer.

5.6. REFERENCES

1. Ruoslahti, E. (1989) J. Biol. Chem. 264, 13369-13372.

2. Fransson, L.A. (1987) Trends Biochem. Sci. 12, 406-411.

3. Heinegard, D. and Sommarin, Y. (1987) in Methods in Enzymology (Cunningham, L.W., Ed), vol. 144, pp. 319-372, Academic Press, New York.

4. Radhakrishnamurthy, B., Srinivasan, S.R., Eberle, K., Ruiz, H., Dalferes, E.D.Jr., Sharma C., and Berenson, G.S. (1988) Biochim. Biophys. Acta 946, 231-243

5. Wagner, W.D., and Salisbury, B.G.J. (1978) Lab. Invest. 39, 322-328.

6. Wight, T.N. (1989) Arteriosclerosis 9, 1-20.

7. Sajdera, S.W., and Hascall, V.C. (1969) J. Biol. Chem. 244, 2384-2884.

8. Wiklund, O., Camejo, G., Mattsson, L., Lopez, F., and Bondjers G. (1990) Arteriosclerosis 10, 695-702.

9. Saito H., Yamagata T., and Suzuki S. (1968). J. Biol. Chem. 243, 1536-1542.

10. Salisbury, B.G.J., and Wagner, W.D. (1981). J Biol. Chem. 256, 8050-8057.

11. Buee, L., Boyle, N.J., Zhang, L., Delacourte, A., and Fillit, H.M. (1991) Anal. Biochem. 195, 238-242.

CHAPTER 6

CHARACTERIZATION OF SULFATED PROTEOGLYCANS EXTRACTED FROM INTIMAL-MEDIAL OR OUTER LAYERS OF NORMAL AND INJURED RABBIT AORTAS

6.1. INTRODUCTION

The obviously distinct morphology of different layers in a musculo-elastic artery underlines special biochemical characteristics and it is related to special physiological functions. It is widely recognized that the innermost region of the aorta is more prone be affected by different pathological events in atherosclerosis, in which the extracellular matrix could play an important part.

The characteristics of several vascular proteoglycans (PG), either synthesized by vascular cells in culture, or extracted from the intima of aorta, have been previously described by others (Oegema et al., 1979; Wight, 1989). The aortic composition in glycosaminoglycans (GAG), the saccharidic moieties of PG, was found to be altered in atherosclerosis and as a result of various experimental manipulations (Radhakrishnamurthy et al., 1988).

We have previously investigated by LM and ultrastructural immunocytochemistry, the distribution and the in situ characteristics displayed by PG containing CS moieties across the full width of the normal rabbit aorta (Galis et al., 1992). Based on size and patterns of associations, several types of CS-PG were distinguished in characteristic locations inside the aortic wall. The intima shared some common characteristics with the media, but the differences between the CS-PG of the intima and adventitia of normal aorta were striking. Traditionally, aortic PG have been extracted from the intimal-medial layers, and as far as we know, no previous studies reported the characteristics of the aortic PG extracted from the outer layer of the aorta. The differences suggested by immunocytochemistry were thought to merit further investigation of the possibility of distinguishing the biochemical attributes of sulfated PG contributing the distinctive properties of the extracellular matrix in these locations.

The matter of the visually suggested contrast between the aortic PG in the inner and outer layers of the normal aortic wall, was further pursued by comparing the biochemical characteristics of these molecules synthesized in vitro. For this purpose, the rabbit aorta was separated by peeling into two layers representing: the intima together with the inner and middle media on one hand, and the outer media and adventitia on the other hand. The size, type, and GAG composition of the sulfated PG synthesized in vitro by these two compartments of the aortic wall were analyzed.

The effect of this balloon catheter injury upon some of the normal characteristics of aortic CS-PG, as visualized by immunocytochemical detection, were described in a previous chapter (ch. 4). Since in the same type of experimental atherosclerosis, the endothelial injury was already reported to determine the modification of the GAG profile of the intimal-medial aortic layer (Alavi and Moore, 1985), in the present study, the emphasis was on the properties of the whole PG molecules. More specifically, we sought to examine the biochemical counterparts of the PG molecular, suggested by our previous morphological observations of injured aortas.

6.2. MATERIALS AND METHODS

The chondroitinase ABC (EC 4.2.2.4), chondroitinase AC (EC 4.2.2.5), and anti-chondroitin sulfate (CS) monoclonal antibodies were from Sigma Chem Co. (St. Louis, MO), as well as other chemicals unless otherwise stated. Sepraphore-L cellulose acetate electrophoresis membrane was from Gelman Sciences Inc. (Ann Arbor, MI). $Na_2{}^{35}SO_2$, sulfate-depleted Dulbecco's modified Eagle's medium (DMEM), and Cytoscint scintillation cocktail were from ICN Biomedicals Canada, Ltd. (St. Laurent, Que).

6.2.1. Sample collection and metabolic labelling. The aortic endothelium was selectively removed by balloon catheterization (Alavi and Moore, 1985). The biochemical procedures used in this study were established through a methodological investigation of PG extraction and analysis, and have been described before (§ 5.3) in detail. The freshly harvested normal or injured rabbit aortas were individually incubated for 6 h in culture dishes with $Na_2{}^{35}SO_4$ (1 mCi/ml of sulfate-free DMEM). The aortas were rinsed of

unincorporated $(^{35}SO_4)^{2-}$ with cold incubation medium, then the inner layer was peeled off. The intimal layer of the injured aorta was processed in toto, no attempt was made to separate the regions with a different macroscopic appearance. Small pieces of the two resulting layers were reserved for Epon embedding to verify their morphology, the rest of the tissue was extracted separately in the presence of protease inhibitors for 24 h at 4°C. Two different solutions, shown (§ 5.4) to extract different sulfated PG from rabbit aorta, were used. One solution contained 6 M urea and 1 M Na chloride, while the other contained 1% Na deoxycholate, 0.2% Na dodecyl sulfate, 2% Triton X-100 in 20 mM Na phosphate buffer, pH 7.2, 300 mM Na chloride, 0.2% Na azide (PBSTS). Both solutions contained protease inhibitors (§ 5.3.3). The supernatants were separated by centrifugation, dialysed, and subjected to evaluation of the GAG composition, as well as to analysis of size distribution of both the whole PG molecules, and of the GAG moieties.

6.2.2. GAG composition of crude extracts. The protein in the extracts was eliminated by digestion with papain and trichloroacetic acid precipitation (§ 5.3.5). The GAG were precipitated overnight in cold (-20°C) absolute ethanol, the pellets were dried under nitrogen, resuspended in water. ^{35}S-GAG were separated by cellulose acetate electrophoresis, visualized by autoradiography, and estimated by densitometry of the X-ray films.

6.2.3. Size distribution of PG. Whole ^{35}S-PG molecules were separated on a Superose 6 HR 10/30 column (Pharmacia, Uppsala, Sweden) in dissociative conditions, using 4 M GdnHCl and 0.5% Triton X-100 in 100 mM Tris-HCl buffer, pH 8.0. The fractions were assayed for radioactivity by liquid scintillation counting, and for the identification of the GAG moieties by the blotting method earlier described (§ 5.3.6).

6.2.4. Size distribution of GAG moieties. The size of the GAG moieties present in various extracts was examined after their digestion with papain. The samples equilibrated in the running buffer, i.e. 100 mM Tris-HCl, pH 8, containing 4 M GdnHCl and 0.5% Triton X-100, were separated by gel filtration on a HR 16/50 column packed

with Sephadex G 100, attached to a FPLC System (Pharmacia Biotechnology, Uppsala, Sweden) at 0.5 ml/min. The void and the total volume were determined with Blue dextran, and $(^{35}SO_4)^{-2}$ respectively. 1.5 ml fractions of the inclusive volume of the column were collected and their radioactivity was assayed by liquid scintillation.

6.3. RESULTS

The microscopic examination of the tissue, showed that the inner layer peeled from aorta contained the whole intima and two thirds of the media, and the tissue that remained after peeling encompassed the outer media and the adventitia. Consequently, the intima and adventitia were present in different preparations, and although both extracts contained parts of the media, for the sake of simplicity, these preparations were designated as normal intima (NI), and normal adventitia (NA) respectively. The inner tissue from the injured aorta was called injured intima (II). The outer layer of the injured aorta was analyzed as well, but since it closely resembled its normal counterpart, i.e. NA, no further mention of this tissue was found to be necessary.

6.3.1. Sulfated PG of the inner and outer normal aorta

The sulfated PG extracted by urea from NI and NA were separated by size distribution chromatography into two main populations (Fig.1).

In the urea extract, the NI contained a significant proportion of high molecular weight ^{35}S-PG, as indicated by the sharp, prominent peak which eluted first from the column. The second, broader peak represented several species of sulfated PG of lower molecular weights. Both chromatographic peaks were diminished by a previous digestion with chondroitinase ABC (see Fig.2, previous chapter) and were positively identified with an anti-CS antibody (data not shown).

In identical conditions of separations of NA urea extract, two main populations of PG were obtained. The position of the first peaks of NA and NI were identical, however, in NA the percentage of large molecules, represented by the area of the first peak divided by the total radioactivity incorporated into ^{35}S-PG, was smaller than in NI. It was concluded that although large molecules of comparable sizes were present in both preparations, they comprised different proportions of NI or NA. As compared to the second peak of NI, the position of elution for the second peak of NA was shifted with five fractions, clearly indicating a reduced molecular weight of the small sulfated PG of NA. These small molecules made up most of the total radioactivity incorporated in PG.

If, prior to its loading on the column for gel filtration, the NA was digested with chondroitinase ABC, which destroys the two isomers of CS and dermatan sulfate (DS) (formerly called CS A, C, and respectively B), the chromatographic profile of NA was practically effaced (Fig. 1B).

The GAG analysis of crude urea extracts showed that the GAG composition clearly differed in the extracts obtained form the inner or outer layers (Fig. 1, inset). Half of the sulfated GAG moieties synthesized de novo by NI were CS, and NI contained also heparan sulfate (HS) in comparable amounts. In contrast, in NA, DS clearly predominated, representing around 70% of the total sulfated GAG.

The ^{35}S-PG molecules extracted by the detergent solution from either NI or NA (Fig. 2) demonstrated more similarity than the urea extracts, both in regard size distribution profile and GAG composition. The detergent extracts also comprised two populations of PG, mostly lower molecular weight PG molecules. Both detergent extracts of NI and NA contained CS and HS, the percentage of HS being greater in the inner regions (Fig. 2A, inset). The digestion with chondroitinase ABC prior to size chromatography, showed that in contrast to the peak of high molecular weight molecules, destroyed by the enzyme, the major peak was largely resistant to this enzyme, showing that it was contributed mainly by HS-PG (Fig.2B).

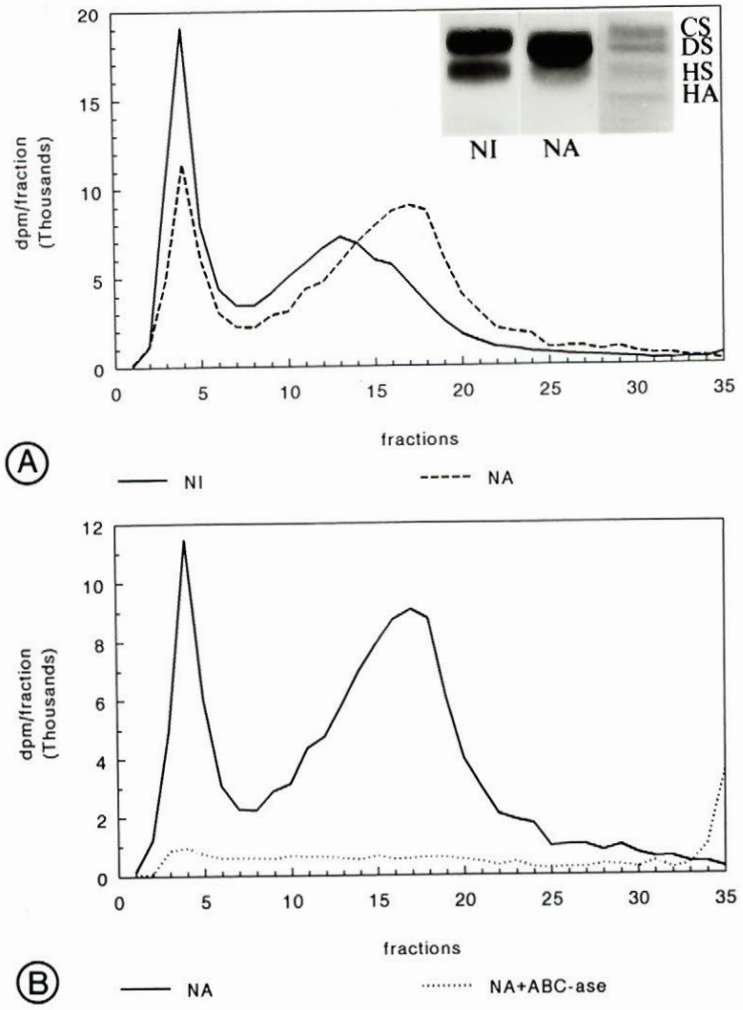

Fig. 1. ^{35}S-PG extracted with urea from the inner and outer regions of normal aorta. A. Size distribution chromatography of whole PG molecules (Superose 6 HR 10/30 column). Two main population of molecules were separated from NI and NA. Inset. ^{35}S-GAG composition of the extracts. Differences in the content of NI and NA, as revealed by autoradiographic image of GAG electrophoresis. Dermatan sulfate accounts for most of the ^{35}S-GAG synthesized by the outer regions (NA). Electrophoretic GAG standards: CS, chondroitin sulfate 6 and 4 together; DS, dermatan sulfate; HS, heparan sulfate; HA, hyaluronic acid. B. Effect of chondroitinase ABC digestion upon the chromatographic profile of the NA extract.

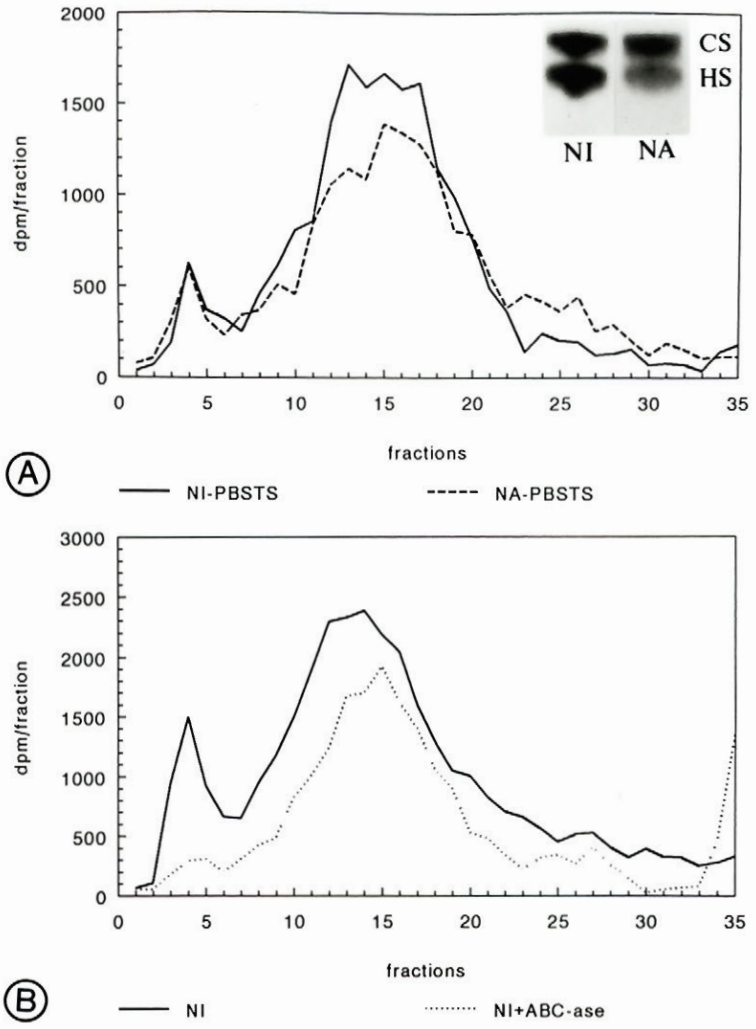

Fig. 2. ^{35}S-PG extracted with a solution containing a detergent mixture from the inner (NI) and outer region (NA) of normal aorta. A. Size distribution chromatography of whole PG molecules. Inset. ^{35}S-GAG composition of the detergent extracts. GAG content of NI and NA, as revealed by autoradiographic image of GAG electrophoresis. Both extracts contained CS and HS. The percentage of HS is smaller in NA. B. Effect of chondroitinase ABC digestion upon the chromatographic profile of a detergent extract obtained from NI. The first peak was eliminated, while the second peak was only slightly affected.

6.3.2. Sulfated PG of injured aorta

The molecules extracted by urea from the inner layers of the injured aortas also had also a bimodal size distribution profile (Fig. 3). As compared to the corresponding preparation of normal aorta, in II the radioactive material was typically redistributed between the two peaks, that is the relative area of the first peak was reduced, while the that of the second peak was increased, indicating that the injured aorta contained a higher proportion of small sulfated PG. At the same time, both the first and the second peaks were broader, the PG-associated radioactivity starting to increase slightly earlier than the peaks of NI. These changes suggested that each of the two PG populations extracted from the lesioned tissue contained a fraction of sulfated PG with higher molecular weights than those synthesized by the normal aorta.

The distribution of ^{35}S-GAG among the PG populations was assessed by the effect of chondroitinases AC/ABC upon the distribution profile (Fig. 3B). Chondroitinase AC, which digests C-6-S and C-4-S, but not DS, preferentially affected the first peak. Both peaks were visibly diminished by digestion with chondroitinase ABC (Fig.3B). The remaining radioactivity presumably represented the presence of HS moieties.

We did not detect obvious differences between the size distribution profiles or the GAG compositions of the molecules extracted with detergent from NI or II (data not shown).

6.3.3. Size of the sulfated GAG moieties in normal and injured aorta

The three GAG samples, obtained from the urea extracts of different aortic tissues were separated in identical conditions and their peaks eluted in different fractions, demonstrating that they had distinct molecular sizes (Fig. 4). In the two preparations obtained from normal aorta, the majority of the NI ^{35}S-GAG chains were clearly longer than those extracted from NA. Nevertheless, the longest chains of sulfated GAG were extracted from the injured aorta, as showed by the earliest elution from the column of the GAG contained in II. As in the case of the whole PG molecules, the rapid increase in the peak radioactivity and its slight asymmetry, suggested that only part of the chains were

longer than normal.

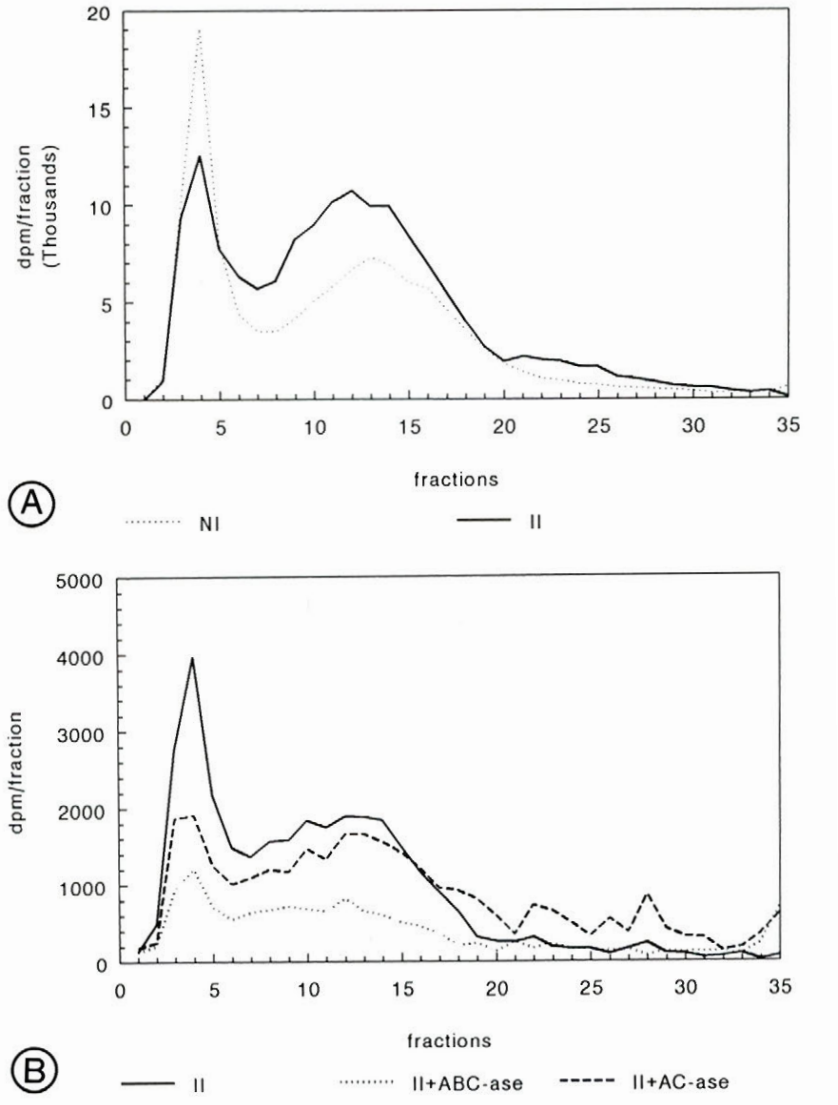

Fig. 3. Size distribution chromatography of ^{35}S-PG extracted by urea from the inner region of injured aorta (II). A. Comparison with the inner normal aorta (NI). B. Distribution of the GAG moieties as determined by digestion with specific GAG enzymes. The first peak was significantly affected by digestion with chondroitinase AC, the effect of chondroitinase ABC was more extensive.

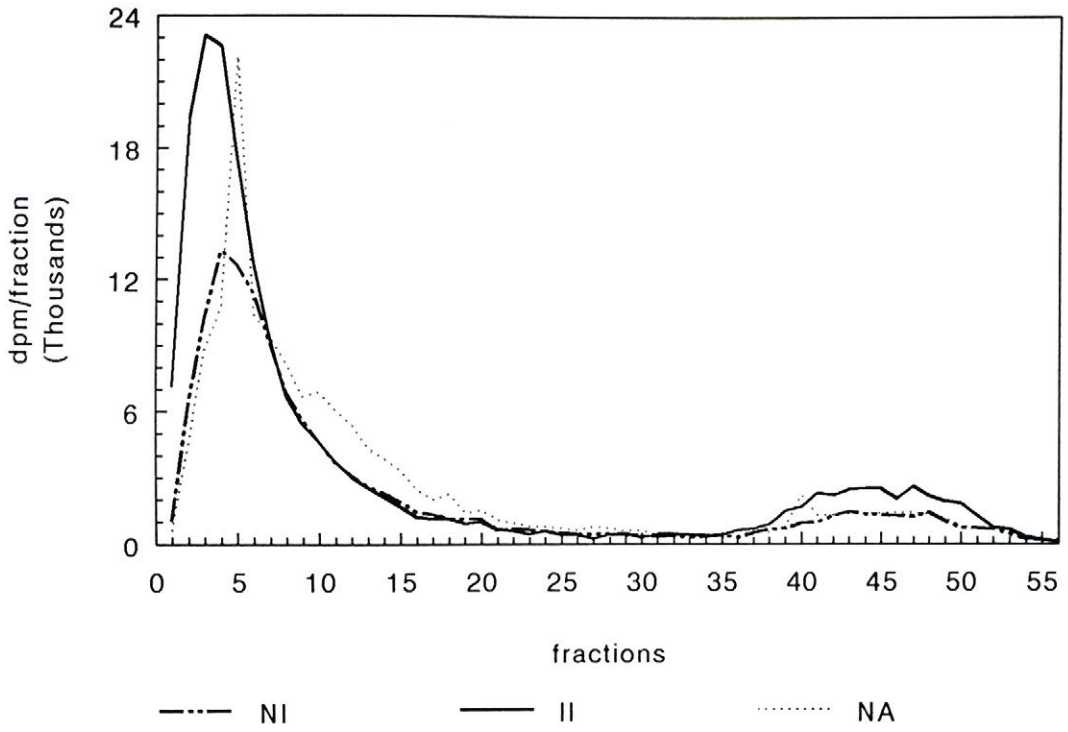

Fig. 4. Size distribution chromatography of ^{35}S-GAG moieties obtained by papain digestion from urea extracts of inner (NI) and outer (NA) regions of normal aorta, and the neointima of injured aorta (II). Separation on a HR 16/50 Sephadex G100 column.

6.4. DISCUSSION

The biochemical characteristics of vascular PG have been often studied (reviewed by Wight, 1989). These molecules were typically extracted with GdnHCl from the intimal-medial tissue of many species (Oegema et al., 1979), or from the cell layers and media of cultured vascular cells (Rauch et al., 1986; Kinsella and Wight, 1988; Lindblom et al., 1989). Additional data have been obtained from many morphological observations of different aortic tissues (Volker et al, 1987; Wight, 1989). However, probably due to the restricted penetration of different chemical agents used for visualization of PG, the studies typically reported the observations made on PG detected over areas usually limited at a single layer of aorta. As a result of these earlier studies, it is largely accepted that three main types of sulfated PG, containing HS, CS or DS moieties respectively, are synthesized in the aorta. The CS-PG have been described to be the main PG produced by smooth muscle cells and to be localized in the interstitial matrix, while small DS-PG are produced both by SMC and fibroblasts and associate with the collagen. Endothelial cells (EC) produce mainly HS-PG, which are major components of the basement membrane; some are associated with elastin (Volker et al., 1987), and other types of HS-rich molecules are expressed on the surface of EC (Kinsella and Wight, 1988).

By using an immunogold post embedding approach which allowed a high resolution of detection over the entire thickness of normal rabbit aorta, we have previously found that several types of PG that contained CS chains could be detected in different locations throughout the aortic wall (Galis et al., 1992). The normal intimal layers contained mainly large CS-PG molecules capable of forming extensive networks. The main type detected in the media was associated with the collagen fibres, while in the adventitia the labelling was strikingly sparse.

We therefore decided to search for the biochemical support of the differences detected by the in situ investigation of aortic PG. In the present study, we compared some of the biochemical characteristics of the sulfated PG extracted from the inner or outer layers of normal aorta, and found them to be distinct. We should however note that, for

the biochemical approach the aorta could be separated by peeling only in two layers. Portions of the media were consequently distributed between the two preparations, and probably attenuated the real differences between the innermost and outermost regions. Nevertheless, the data obtained by analyzing the sulfated PG synthesized by the inner or outer normal aorta, confirmed that there are many differences between these molecules in the two locations.

CS has been recognized as the main type of sulfated aortic GAG, but we intended to get a broader, unbiased biochemical image of the sulfated PG of aorta, and therefore tried to obtain and analyze a larger variety of ^{35}S-PG. The tissues were extracted with two different solutions, which were found to mobilize sulfated PG from different pools of the aortic tissue (§ 5.4). The urea extract of the inner layers contained a high proportion of large CS-PG, while the extract of the outer layers contained mainly small PG rich in DS. These findings support the marked differences found by the immunocytochemical detection of the CS-PG in these two regions, using a monoclonal antibody which recognizes the two isomeric forms of the CS, C-6-S and C-4-S, but not DS. The second populations of smaller CS-positive PG extracted by urea from NI, was most likely related to the CS-PG that were seen associated with the collagen, and which were probably derived mainly from the medial tissue. This supposition would also fit with the finding of an increased proportion of the smaller CS-PG in the urea extract of the injured intima, in which the extracellular volume occupied by the collagen, and consequently collagen-associated CS-PG, was visibly increased.

In the outer region, the small DS-PG formed the predominant peak extracted by urea. This finding is in good agreement with the fact that in vitro, the smooth muscle cells synthesize besides CS-PG also small DS-PG, and the DS-PG are the main product of cultured fibroblasts (Wight, 1989; Rauch et al., 1986). On human aortic sections, by using a monoclonal antibody to a DS-containing PG, Sobue et al. (1988) showed the staining of the adventitia.

The extraction with a detergent solution yielded sulfated PG containing a high content of HS and CS moieties. The HS-PG are known to be resistant to the extraction with GdnHCl, and Radhakrishnamurthy et al. (1988) have proposed a scheme for their

isolation from the aortic tissue involving the use of several consecutive enzymatic digestions. We have suggested the use of a detergent mixture (§ 5.5.1), which selectively isolates the HS-PG from the rabbit aorta. These PG were not extracted neither by GdnHCl or urea and had similar molecular weights in the two layers of aorta. Typically, the cell-associated PG have CS and HS chains (Ruoslahti, 1988; David et al., 1989), and in vitro the EC produce mainly cell-associated HS-PG (Lindblom et al., 1989). The sulfated PG extracted by detergent from the two preparations were of similar sizes and could have been associated with the cellular surface, basement membranes, or elastin in the various layers. The higher percentage of HS in the inner layer as compared with the outer layer, might be due to the presence of the endothelium, the major HS-PG producer in the aorta, and/or to more elastin, a larger number of cells, and the associated basement membranes, contained in the inner layer.

Due to the numerous physiological functions of PG, the differences revealed between the sulfated PG in the inner or outer regions of normal aorta, have potentially important implications. These versatile molecules are important determinants of the extracellular matrix composition and architecture, as well as of cell regulation. They may influence the viscoelastic and permeability properties of the blood vessel, therefore the characteristic sulfated PG detected in different locations of the aorta are likely to contribute to the local properties of the layers.

The in vitro interactions of PG with different proteins in general (Ruoslahti and Yamaguchi, 1991), and with lipoproteins (LP) in particular (Mourao et al., 1981; Srinivasan et al.,1988, Wilkund et al., 1990), are mediated through their GAG moieties. Whether dependent on specific sequences of the GAG chains, or being primarily a charge-dependent interaction, its strength would be influenced by the type, charge, size, and number of the GAG chains. These properties are altered in atherosclerosis, as well as numerous other pathological conditions (Kennedy, 1976).

The present comparative analysis of the size of the sulfated PG in injured aorta showed mainly two aspects. First, the population with small molecular weights, forming the second peak of the chromatographic distribution, accounted for a larger percentage of total ^{35}S-PG. This might be related to a larger number of collagen-associated PG. As

we have previously detected by immunocytochemistry (ch. 3), a PG containing CS chains is closely associated with the collagen fibrils, and a DS-PG was previously shown by others to accompany collagen. Both these PG contain sulfated moieties, and could therefore contribute to increase the proportion of small PG. Another converging argument is that atherosclerotic aortas reportedly contain more DS (Stevens et al., 1976).

The second observation was that the extracts of injured intima contained a fraction of sulfated PG and GAG with molecular weights higher than normal. Our previous morphometric measurements of the gold labelling patterns, suggested that longer CS chains might be present in the neointima of balloon-catheterized aortas (§ 4.3.2), and the present comparative biochemical data obtained by size distribution chromatography of the PG molecules and GAG moieties, extracted from normal or injured aortas, were found to agree with this observation. Wagner et al. (1986) also described the properties of a PG extracted from human atherosclerotic lesions, and proposed that this might contain fewer, but longer CS side chains. Radhakrishnamurthy et al. (1988) studied the PG synthesized in vitro by explants of aorta derived from hypercholesterolemic rabbits, and hypothesized from their results that the differences found in comparison with the PG of normal aorta might be due to longer CS chains. In the same model of endothelial injury, van der Heiden et al. (1988) inferred from calculations of their results that GAG chains might be longer in injured aortas. The conditions used for liquid chromatography in the present study, have actually determined differences between the molecular weights of the sulfated GAG moieties. The injured intima synthesized sulfated chains with higher molecular weights, which in the case of the unbranched structure of GAG could be only due to an increased chain length. Again, the particular composition of the tissue in a vascular location, as well as the individual molecular structure of the PG, would bear on their interactions with LP inside the aortic wall. The larger sulfated PG isolated from injured intima could conceivably have altered properties, such as a modified affinity for LP in the aortic lesions.

6.5. REFERENCES

Alavi, M.Z., and Moore, S. (1985). Glycosaminoglycan composition and biosynthesis in the endothelium-covered neointima of de-endothelialized rabbit aorta. Exp Mol Pathol, 42:389-400.

David, G., Lories, V., Heremans, A., Van Der Schueren, B., Cassiman, J.J., Van Der Berghe, H. (1989). Membrane associated chondroitin sulfate proteoglycans of human lung fibroblasts. J Cell Biol, 108:1165-1175.

Galis, Z.S., Alavi, M.Z., and Moore, S. (1992). In situ ultrastructural characterization of chondroitin sulfate proteoglycans of normal rabbit aortas. J Histochem Cytochem, 40:251-263.

Kennedy, J.K. (1976). Chemical and biochemical aspects of the glycosaminoglycans and proteoglycans in health and disease. Adv Clin Chem, 18:1-97.

Kinsella, M.G., and Wight, T.N. (1988). Structural characterization of heparan sulfate proteoglycan subclasses isolated from bovine aortic endothelial cell cultures. Biochemistry, 27:2136-2144.

Lindblom, A., Carlstedt, I., and Fransson, L.A. (1989). Identification of the core proteins in proteoglycans synthesized by vascular endothelial cells. Biochem J, 261:145-153.

Mourao, P.A.S., Pillai, S., and Di Ferrante, N. (1981). The binding of chondroitin 6-sulfate to plasma low density lipoprotein. Biochim Biophys Acta, 674:178-187.

Oegema, T.R., Hascall, V.C., and Eisenstein R. (1979). Characterization of bovine aorta proteoglycan extracted with guanidine hydrochloride in the presence of protease

inhibitors. J Biol Chem, 254:1312-1318.

Radhakrisnamurthy, B., Srinivasan, S.R., Eberle, K., Ruiz, H., Dalferes, E.R. Jr., Sharma, and Berenson, G.S. (1988). Composition of proteoglycans synthesized by rabbit aortic explants in culture and the effect of experimental atherosclerosis. Biochim Biophys Acta, 964:231-243.

Rapraeger, A., Jalkanen, M., Endo, E., Koda, E., and Bernfield, M. (1985). The cell surface proteoglycan from mouse mammary epithelial cells bears chondroitin sulfate and heparan sulfate glycosaminoglycans. J Biol Chem, 260:11046-11052.

Rauch, U., Glossl, J., and Kresse, H. (1986). Comparison of small proteoglycans from skin fibroblasts and vascular smooth-muscle cells. Biochem J, 238:465-474.

Ruoslahti, E. (1989). Proteoglycans in cell regulation. J Biol Chem, 264:13369-13372.

Ruoslahti, E. and Yamaguki, Y. (1991). Proteoglycans as modulators of growth factors activities. Cell, 46:867-869.

Sobue, M., Nakashima, N., Fukatsu, T., Nagasaka, T., Katoh, T., Ogura, T., and Takeuchi, J. (1988). Production and characterization of monoclonal antibody to dermatan sulfate proteoglycan. J Histochem Cytochem, 36:479-485.

Srinivasan, S.R., Vijayagopal, P., Eberle, K., Dalferes, E.R., Radhakrishnamurthy, B., and Berenson, G.S. (1988). Low density lipoprotein binding affinity of arterial wall isomeric chondroitin sulfate proteoglycans. Atherosclerosis, 72:1-9.

Stevens, R.L., Colombo, M., Gonzales, J.J., Hollander, W., and Schmid, K. (1976). The glycosaminoglycans of the human artery and their changes in atherosclerosis. J Clin Invest, 58:470-481.

Toledo, O.M.S., and Mourao, P.A.S. (1980). Sulfated glycosaminoglycans in normal aortic wall of different mammals. Artery, 6:341-353.

van der Heiden, R., Hatton, M.W.C., and Moore, S. (1988). Extraction and analysis of glycosaminoglycans from intima-media of single rabbit aortae: effect of balloon catheter de-endothelialization on the content and profile of glycosaminoglycans. Atherosclerosis, 73:203-213.

Volker, W., Schmidt, A., and Buddecke, E. (1987). Mapping of proteoglycans in human arterial tissue. Eur J Cell Biol, 45:72-79.

Wagner, W.D., Salisbury, B.G.J., and Rowe, H.A. (1986). A proposed structure of chondroitin 6-sulfate proteoglycan of normal and adjacent atherosclerotic plaque. Arteriosclerosis, 6:407-418.

Wight, T.N. Cell biology of arterial proteoglycans. Arteriosclerosis. 9:1-20.

Wilkund, O., Camejo, G., Mattsson, L., Lopez, F., and Bondjers, G. Cationic polypeptides modulate in vitro association of low density lipoprotein with arterial proteoglycans, fibroblasts, and arterial tissue. Arteriosclerosis, 10:695-702.

CHAPTER 7

IMMUNOCYTOCHEMICAL DETECTION OF ENDOGENOUS APOLIPOPROTEIN B AND CHONDROITIN SULFATE PROTEOGLYCANS IN THE ADVANCED LESIONS INDUCED BY ENDOTHELIAL INJURY IN AORTAS OF NORMOCHOLESTEROLEMIC RABBITS

7.1. INTRODUCTION

The extracellular arterial proteoglycans (PG) are considered major factors implicated in the accumulation of lipoproteins (LP) in the atherosclerotic lesions. Besides observations correlating the contents in endogenous LP and glycosaminoglycan (GAG) of human aortas, or of aortas of hypercholesterolemic animals (Falcone et al., 1984; Hoff and Wagner, 1986; Yla-Herttuala et al., 1987), most of the pertaining evidence came from in vitro studies.

The high affinity of various GAG and PG for LP has been recognized for a long time (Bihary-Varga et al., 1964; Iverius, 1972; Camejo et al., 1975), and it has been extensively analyzed (for review see Berenson et al., 1988), constituting a key argument for this hypothesis. Another important step toward building the case against the extracellular PG, was the reporting of the isolation of complexes containing LP and mucopolysaccharides, the old name of GAG, from the fatty streaks of human aorta (Srinivasan et al., 1972). The complexes formed in vitro between LP and aortic PG have been shown to induce the accumulation of lipid in peritoneal macrophages (Salisbury et al., 1985; Vijayagopal et al., 1985) and in human macrophages (Hurt-Camejo et al., 1990).

In this study, starting from many pieces of evidence accumulated during the years, and based on our own previous immunocytochemical observations relating the distribution of CS-PG and of apo B in injured aortas, we tried to reveal the in situ relation between these components in the advanced lesions triggered by endothelial injury.

7.2. MATERIAL AND METHODS

The monoclonal anti-chondroitin sulfate antibody and the anti-mouse IgM conjugated with 10 nm colloidal gold (αIgM-Au_{10}) were from Sigma Chem Co (St. Louis, MO). The goat anti-apo B antibody was raised and characterized, as previously described (ch. 2). The donkey anti-mouse coupled with fluorescein isothiocyanate (FITC) and the donkey anti-goat coupled with tetramethyl-rhodamine isothiocyanate (TRITC), were developed for multiple labelling by Jackson Immunoresearch Laboratories, and are distributed by Bio/Can Scientific Inc. (Mississauga, Ont). The protein A conjugated to colloidal gold of 20 nm diameter (PA-Au_{20}), kindly provided by Dr. L. Ghitescu from Departement d'Anatomie, Université de Montreal, was prepared according to Ghitescu and Bendayan (1990). OCT embedding medium was from Miles (Elkhart, IN), and Lowicryl K4M from JB EM Services (Dorval, Que).

7.2.1. Tissue samples. The aortic tissues were obtained from New Zealand rabbits injured by balloon catheterization, as previously described (ch. 2). Frozen sections were obtained from full circumference aortas and directly embedded in OCT, while for EM, the injured tissue was divided according its macroscopic appearance, fixed in 4 % paraformaldehyde + 0.5 % glutaraldehyde in 100 mM Na phosphate, pH 7.4, and separately processed by low temperature embedding in Lowicryl K4M (Bendayan, 1984). Consecutive thin sections of Lowicryl embedded tissue were collected on nickel grids covered with carbonated parlodion. For the double EM immunocytochemistry, thin section were also collected on grids lacking the backing parlodion film.

7.2.2. Double immunofluorescence. Freshly cut frozen sections of 5 μm were collected on poly-L-lysine coated slides and allowed to dry overnight at room temperature. The sections were rehydrated with 50 mM Tris-HCl, pH 7.6 for 10 min, then incubated at 37°C for 30 min with a mixture of the primary antibodies, diluted in the same buffer to 1/50 the anti-CS, and respectively to 1/10 the anti-apo B. Slides were

rinsed 2 x 10 min with Tris, then simultaneously incubated with the secondary antibodies, both diluted to 1/100 in Tris. The sections were rinsed with Tris (3 x 10 min), and mounted with 90% glycerine in Tris-HCl, pH 8.6. The specificity of the primary antibodies were previously confirmed (see ch.2 & 3). For the control of the secondary antibodies, the sections were directly incubated with the fluorescent-tagged antibodies, either separately, or mixed together. The possible cross reactions were tested by incubation with switching of the secondary antibodies, i.e. anti-CS monoclonal followed by anti-goat/TRITC, respectively anti-apo B polyclonal IgG followed by anti-mouse IgM/FITC. For orientation, from each group of sections, one was stained with Mayer's haematoxylin.

7.2.3. EM immunocytochemistry

Single antigen detection. Consecutive grids were processed for the detection of apo B and CS-PG in an attempt to obtain similar areas labelled for each of the antigens. The same procedure of immunostaining was used for all grids, irrespective of the immunoreagents. The grids were incubated for 2 h in the primary antibody, washed 3 x 5 min with 10 mM phosphate buffered saline, pH 7.3, incubated with the appropriate gold immunoconjugate for 30 min, and finally washed 3 x 5 min with distilled water. The immunoreagents were diluted with PBS as follows: 1/50 anti-apo B from a 2.5 mg/ml isolated IgG fraction, 1/200 anti-CS ascites fluid, 1/5 αIgM/Au_{10}, and PA-Au_{20} with optical absorption A_{520} = 1.0.

Double gold immunocytochemistry. The two antigens were detected by incubating consecutively the two faces of the grids, as proposed by Bendayan (1982). Apo B was detected on the face on which the thin sections were applied, using the anti-apo B, followed by the PA-Au_{20} gold conjugate. The grids were washed and dried, then CS-PG was detected by floating the grid on face two, in the anti-CS monoclonal and respectively, the αIgM-Au_{10} conjugate. The procedures used for incubation of each face were otherwise similar to those used for single antigen detection. After labelling the two

faces, the grids were counterstained with uranyl acetate and Reynold's lead citrate, covered with parlodion, and carbonated.

The controls for these procedure included the omission of the primary antibodies on one of the faces, or on both.

7.3. RESULTS AND DISCUSSION

Numerous data point towards the direct involvement of sulfated PG in the sequestration of LP in the atherosclerotic lesions.

The most direct previous evidence of the in situ association between LP and PG was the extraction of their respective complexes from human fatty streaks. The extraction of LP-PG complexes from aortic tissue, while being very suggestive of their mutual affinity, does not constitute by itself a proof of their association in situ. The affinity of sulfated PG for LP is so great, that PG are able to selectively precipitate LP particles from solutions in the presence of other proteins. Therefore, one could always argue that PG might have not been in a complex with the LP ad initio, but they became associated during the procedure of extraction.

While the study of the in vitro interaction studies has obvious advantages, allowing the manipulation and evaluation of the effect of different factors, it is inevitably subjected to the limitations common to this type of experiments. There would always be the question of selecting the right conditions for the incubations, the objective selection of the partners to be studied, and the lack of many other elements which might substantially influence their interaction in vivo.

Therefore we decided to examine the relation between LP and sulfated PG by detecting them in situ. The distribution of CS-PG and endogenous apo B was analyzed in the aortic lesions triggered by an endothelial injury, in normocholesterolemic conditions. The present study represents in fact the first in situ detection of the endogenous LP containing apo B and of CS, the PG moiety most suspected to bind LP in the vascular lesions.

7.3.1. Double immunofluorescence

In the sections of normal aorta, the highest signal produced by apo B was detected over the endothelial layer and in the subendothelial space (Fig. 1). The CS-PG was concentrated in the extracellular intimal space beneath.

In the thickened neointima (Fig. 2), the luminal front was clearly labelled, but this

time most obvious was the apo B presence in the space between the aortic endothelium and the internal elastic lamina. Positive cellular contours were suggested by the TRITC fluorescent staining. A dense, punctated staining was revealed deeper inside the lesions. The FITC signal for CS-PG was stronger in the luminal and basal areas of the thickened lesions due to apparently confluent patches. Otherwise, the whole neointima contained CS-PG.

Fig. 1 (top). Frozen section of normal rabbit aorta. Double immunofluorescence: green (FITC) fluorescence detects CS-PG, red (TRITC) fluorescence labels endogenous apo B. Areas of overlapping labelling appear as orange. Apo B is concentrated in the innermost areas of aorta, while the highest density of CS-PG is distributed over the extracellular space of the entire intima. The elastic laminae display endogenous fluorescence with both FITC and TRITC filters. L = lumen of aorta, IEL = internal elastic lamina. Original magnification x 250.

Fig. 2 (bottom). Distribution of apo B and CS-PG in an obviously thickened lesion covered by regenerated endothelium (same original magnification as Fig. 1). Neointima of an injured aorta, frozen section stained by double immunofluorescence. Apo B, detected with rhodamine, is concentrated over the regenerated endothelium, marks the contour of cellular profiles, and forms a fine, punctated pattern in the middle of the lesion. The CS-PG forms an interlaced background throughout the lesion, the extensive networks of CS-PG are most visible in the inner and basal area of the neointima. Although the regional intensity of the staining is different for the two antigens in the lesion, the two colours are nicely interspersed in all locations.

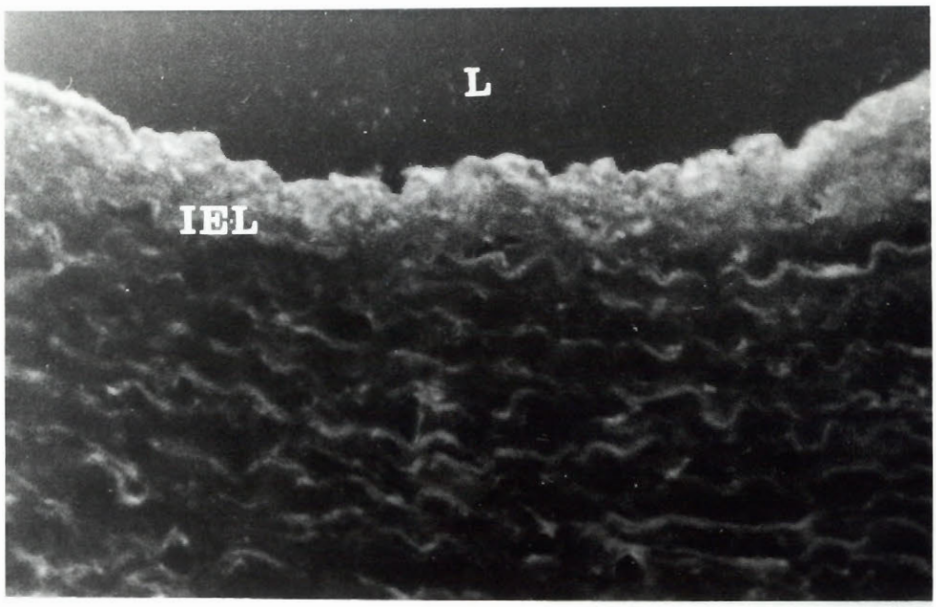
L
IEL

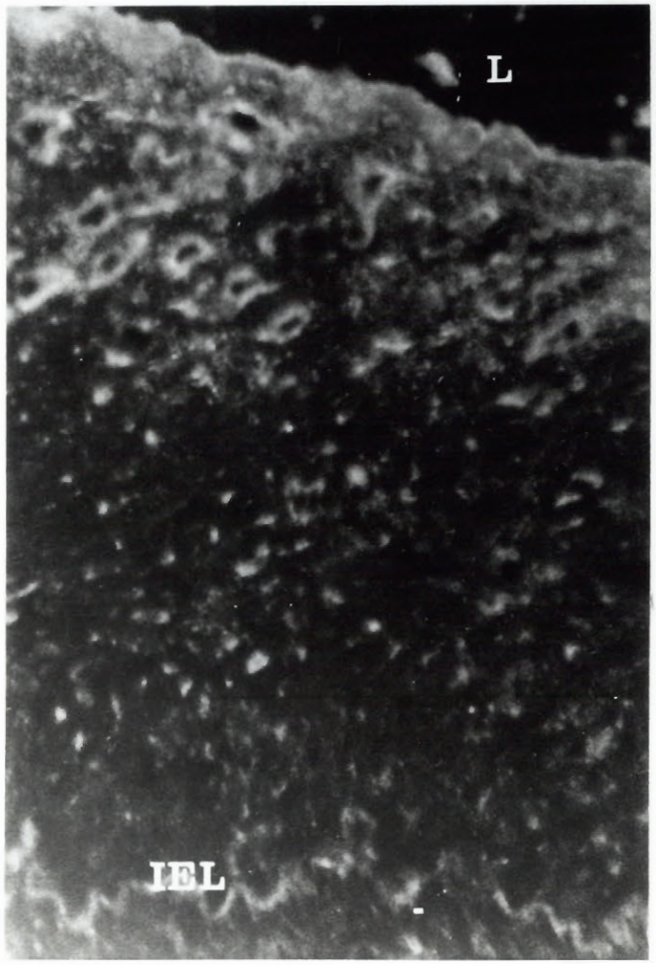
L
IEL

Fig. 3. Immunofluorescent detection of apo B and CS-PG in a frozen section of an advanced lesion (lumen of aorta is at left). Original magnification x 250. (top). Numerous bright spots and contours, some of which were identified as cells, were visible in red fluorescence (detecting apo B). (middle). CS-PG staining occasionally displayed brighter spots, but typically was more diffuse, and suggested confluent structures. (bottom). Simultaneous detection of apo B and CS-PG. CS-PG are creating a lacework in which the apo B-positive structures appear embedded.

Fig. 4. Higher magnification of Fig. 3. The two colours are associated with the contour of many labelled structures, some of which are pointed by arrows. Original magnification x 400.

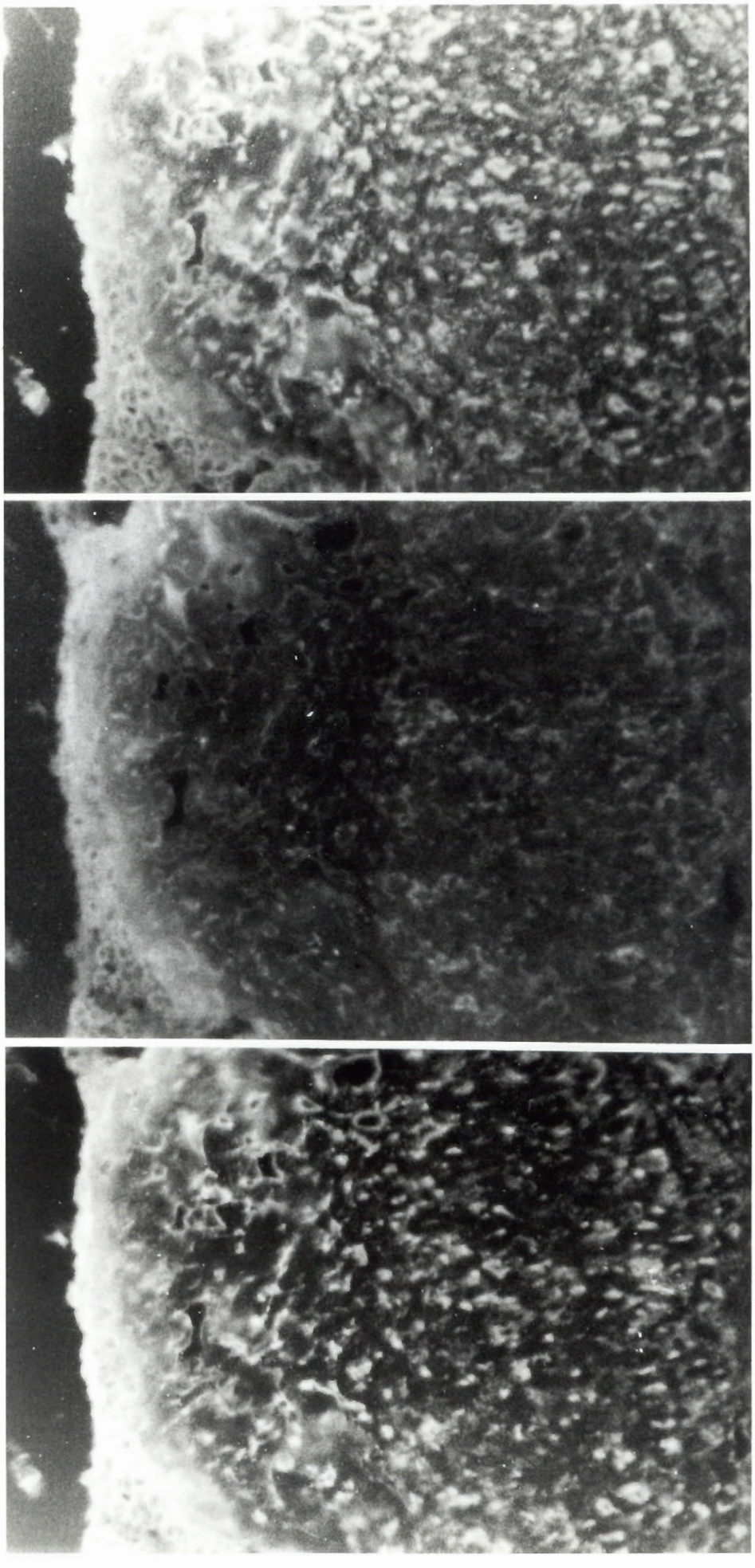

7.3.2. Ultrastructural detection of apo B and CS-PG

First, apo B and CS-PG were detected by the separate incubation of consecutive sections of injured aortas, and the labelling of similar areas was compared. From the previous experiments, described in chapters 2 and 4, the general patterns of distribution for the two antigens was known. Both apo B and CS-PG have the tendency to accumulate in the extracellular and intracellular space of the advanced lesions. The purpose of these experiments was to generate specimens resembling as close as possible. Although it is difficult to identify the same ultrastructures in different specimens, it was reasonably easy to find areas bearing a close similarity and to analyze the ultrastructural pattern of labelling for the two antigens. Then, the two antigens were simultaneously visualized by detection on the same thin section using colloidal gold conjugates of two different sizes. Both the intensity of the contrast, and the density of labelling were reduced in these conditions, due to technical problems discussed further.

Two main types of associations were detected in the advanced lesions.

Extracellular accumulations

The prominent extracellular accumulations of small lipid droplets were found in the regions where the networks of large CS-PG were also present (Fig. 5 A & B). The correlation between apo B and CS-PG was strengthened by the observation that intercellular regions fully occupied by other components of the extracellular matrix, such as by the collagen bundles, did not contain apo B accumulations. Isolated lipid particles, positive both for apo B and CS-PG were noticed close to the periphery of collagen fibrils (Fig. 6).

The relation between a certain type of aortic CS-PG, characteristic for the interstitium of the intimal layer (Galis et al., 1992), and the sites of the most significant depositions of apo B was also suggested by double gold EM immunocytochemistry (Fig. 7).

Fig. 5. Ultrastructural immunocytochemical detection of (A) endogenous apo B and, respectively (B) aortic CS-PG, in the advanced lesions induced by endothelial injury. Areas bearing a close resemblance on two consecutive sections, marked with stars. Apo B and CS-PG were detected in similar locations (arrowheads). x 43,000. Bar = 300 nm.

Fig. 6. Immunocytochemical detection of (A) apo B, and (B) CS-PG in the injured aorta. Isolated round structures positive both for apo B and CS-PG, in the vicinity of collagen fibrils. The structures appear as if attached by strings (arrows). x 43,000. Bar = 300 nm.

Fig. 7. Simultaneous detection of apo B and CS-PG in the extracellular space of an advanced lesion, by double gold immunocytochemistry. The two antigens were detected on the two faces of the same grid, based on the use of gold immunoconjugates of two different sizes; apo B is labelled by colloidal gold of 20 nm, while CS-PG is labelled by the smaller gold particles, of 10 nm. Frequently the two markers are associated (large arrows), at the edge of slightly darker, vesicle-like profiles. The two antigens were nevertheless found isolated as well, as indicated by the small arrows. x 43,000. Bar = 300 nm.

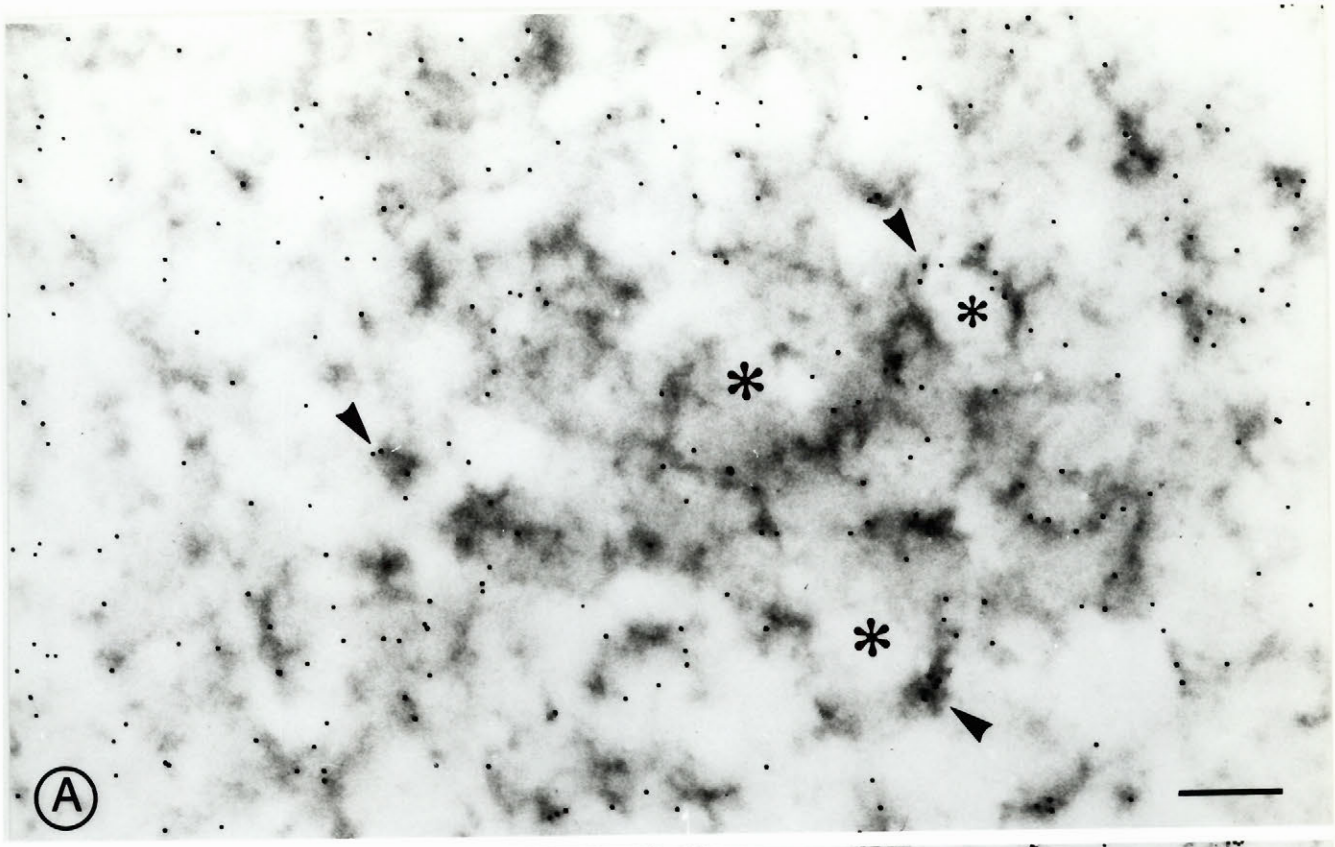
A

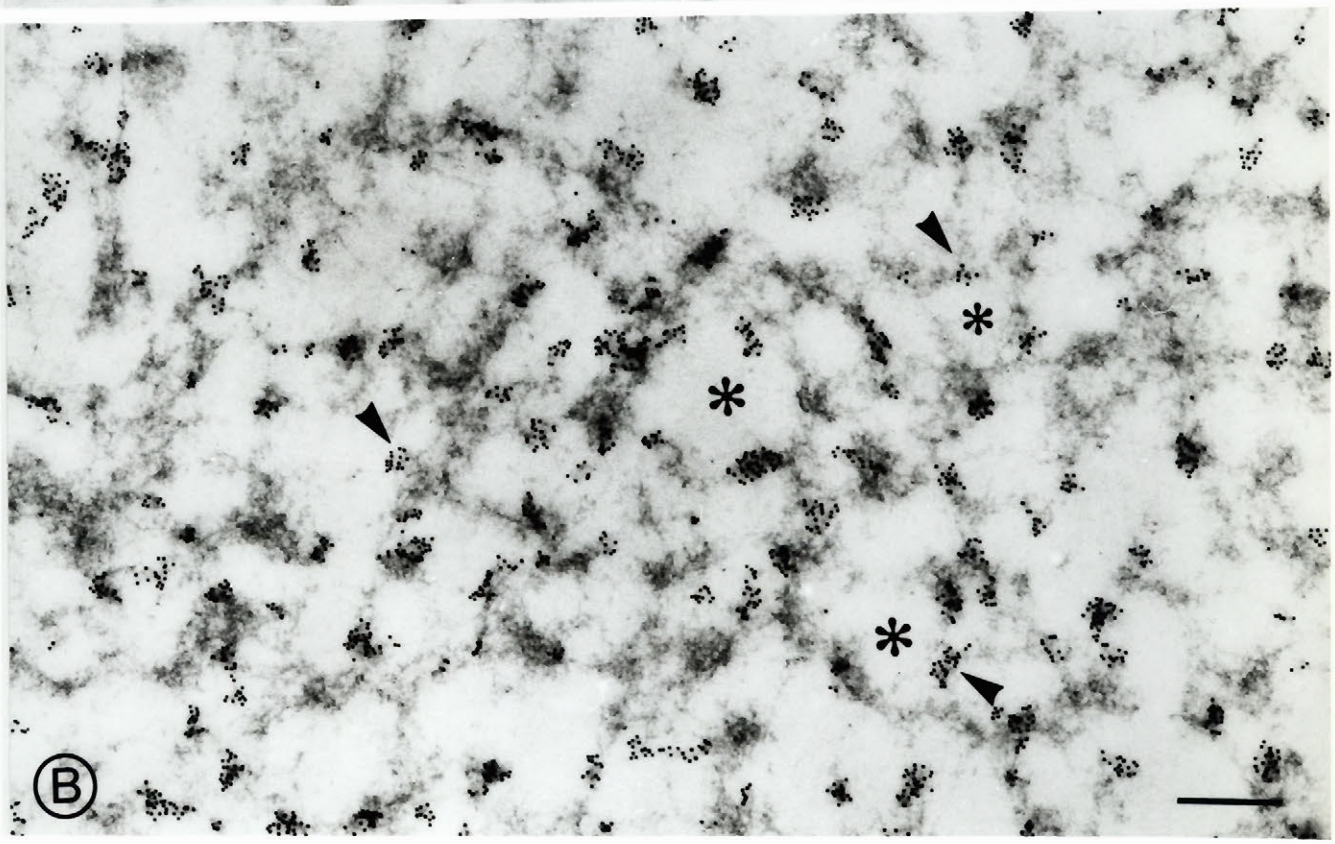
B

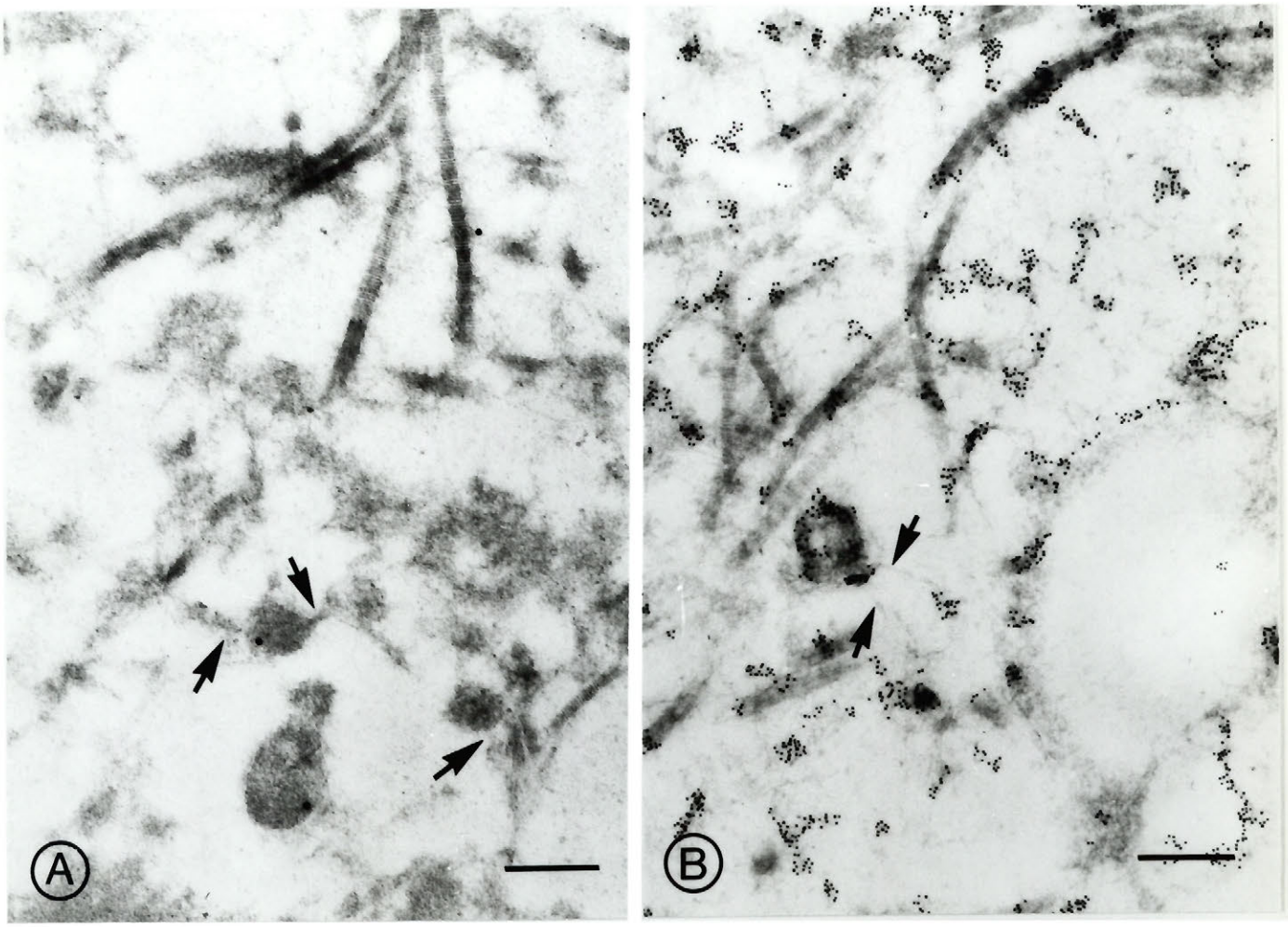
A
B

Endogenous apo B and CS-PG detected either on consecutive thin sections, or by using a procedure for their simultaneous visualization, were found in the same extracellular and intracellular sites. We should note however that, since the appropriate preservation of the antigenicity of both apo B and CS, did not allow the use of lipid contrasting agents for embedding, the quality of the contrast was affected. In addition, the methods used for the double detection have their own limitations. Correlating exactly the ultrastructural features on consecutive sections can be sometimes very difficult. Alternatively, the quality of the sections used for double labelling was under that of other specimens that we had usually obtained by post-embedding immunogold. The initial lack of the carbonated parlodion film backing, in order to keep the two faces of the sections accessible for immunolabelling, made the sections used for the simultaneous visualization of the two antigens were very friable and their contrast was poorer. The decrease in the immunocytochemical signal could be related to a restricted access of the immunoreagents through the mesh of the grid, due to a high superficial tension of the liquid. The immunostaining after the embedding, can only detect those antigenic epitopes that are exposed at the surface of the section. Since the embedded structures are randomly positioned in regard to the plane of sectioning, it is obvious that the probability of exposing simultaneously two related antigens is low. However, since the dual labelling permitted the frequent visualization of both labels closely apposed, suggesting that apo B and CS-PG interact inside the vascular lesions.

The extracellular CS-PG could determine the sequestration of LP particles, either by individual ionic interactions, or due to the evident organization of the PG networks in the interstitial spaces, through molecular sieving and steric hindrance. The direct accumulation of LP from plasma was suggested by the high density of apo B detection in the advanced lesions developed in the areas covered by regenerated endothelium.

Earlier studies by Smith et al. (1967), have shown that the lipid content of the fine extracellular droplets of human fatty streaks bears close resemblance with the serum lipids. Similar extracellular deposits of small lipid particles were found in the human atherosclerotic plaques (Guyton and Klemp, 1989). Mora et al. (1989) have detected apo

B-positive deposits in the aortas of hypercholesterolemic rabbits. From the analysis of the chemical composition of the lipid particles extracted from the human lesions, Chao and colleagues (1990) suggested that the small type could be derived from the aggregation of plasma LP sequestered in the vessel wall. The interaction of LP with C-6-S was previously found to modify the conformation of the apo B, to reduce the thermal stability, and to increase its susceptibility to proteolysis (Camejo et al., 1991).

We think that the CS residues, by masking the positive domains of apo B could reduce the mutual repulsion between the LP particles and contribute to their coalescence in the extracellular space.

Intracellular associations

Another visible compartment where apo B and CS-PG were often colocalized, was inside the foam cells of the lesions (Fig. 8). Since both apo B and CS-PG appeared to have been internalized by the same lipid-filled cells, and because they were often detected in close apposition, at the level of the plasma membrane and in the intracellular organelles, it seems possible that their uptake could have been simultaneous. Two groups (Salisbury et al., 1985; Vijayagopal et al., 1985) have independently reported that the PG-LP complexes triggered the formation of foam cells in vitro. Initially, the presence of the negative PG molecules in the LP-PG complexes was thought to stimulate a non-specific pinocytosis.

More recently, Vijayagopal et al. (1988, 1991) showed that, although the uptake of LP-PG complexes in the mouse peritoneal macrophages does not depend on the apo B/E receptor, and the uptake has the features of a receptor-mediated endocytosis. However, Orekhov et al. (1989) reported that the LDL complexed with CS, heparan sulfate or hyaluronic acid did not induce the accumulation of cholesterol/cholesterol esters in human SMC and macrophages, while incubation with LDL in the presence of various other preparations, including latex beads, caused the formation of foam cells. In addition, in they found that HDL, if present in large insoluble complexes, could determine a significant cellular accumulation of cholesterol.

Fig. 8. Simultaneous visualization of endogenous apo B (large gold particles) and CS-PG (small gold particles). Double immunogold on Lowicryl section of injured aorta. Apo B and CS-PG are frequently associated in the extracellular space (EXC) as depicted by the large empty arrows, at the level of the foam cell (FC) plasma membrane (arrows), and inside intracellular organelles (arrowheads). x 41,500. Bar = 300 nm. Inset. Detail of labelling. The close spatial relation between the two antigens, suggests the possibility of a simultaneous uptake by the foam cells in the lesions. x 59,250. Bar = 200 nm.

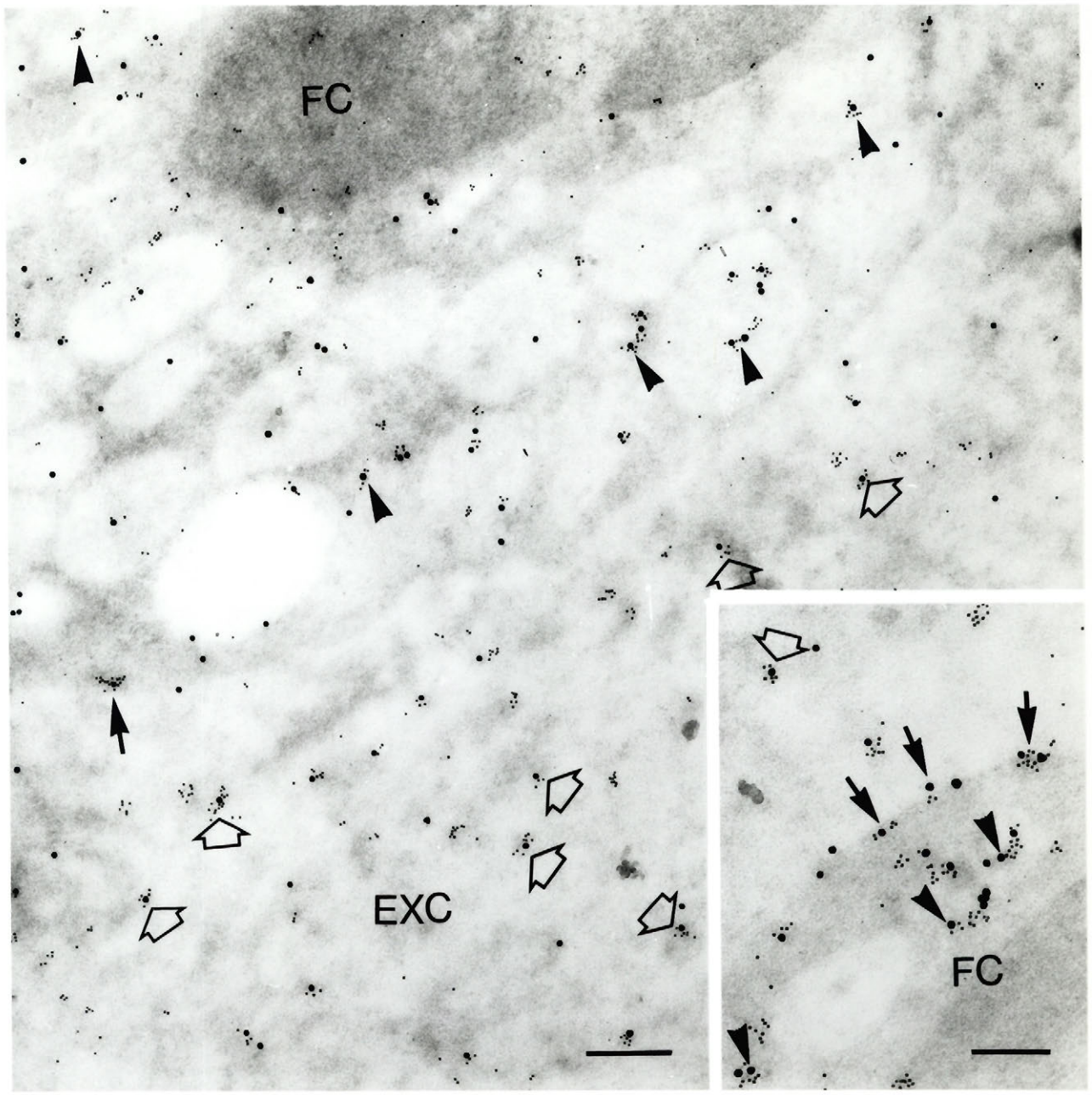
FC
EXC
FC

According to the results of the latter study, it seems that phagocytosis of very large particles, of various provenance, containing LP plays an important role in foam cell formation. We interpret the failure of the LDL-CS complexes to increase the intracellular cholesterol, as being most probably due to the fact that only GAG moieties were used for incubation, and their results could be in fact another argument advocating the importance of the whole PG molecule in the interaction with the LP and the subsequent foam cell formation. Although it is the GAG side chains of the PG that bind the apo B positive sites of LP, by themselves these moieties have poor complexing capacity (Berenson et al., 1985; Steele et al., 1987), therefore the generation of insoluble complexes, which trigger in vitro the transformation of monocytes/macrophages into foam cells, depends probably on the presence of intact PG molecules. The presence of PG in association with apo B-containing LP could determine the lipid loading of the cells by various mechanisms, e.g. blocking of the apo B cluster containing positively charged amino acids abolishes the interaction with the apo B receptor (Young, 1989), and LP could be taken up by the cells through a pathway which is no longer down-regulated, as in the classical case of the LDL receptor. PG could also modify the susceptibility of the LP contained in the complexes to lysosomal degradation.

Both partners are likely to contribute in the process of LP accumulation in the arterial wall in pathologic conditions. Only the influence of the aortic tissue properties upon the interaction with the endogenous LP have been addressed in the present investigation of an injury model of atherosclerosis. In the human lesions, there is a strong possibility that the individual characteristics of the LP particles also contribute to the variability of the interaction with the aortic components. The effect of hypercholesterolemia and the possible modification of the LP were extensively examined and reviewed (Steinberg, 1987). The in vitro affinity of cellular (St. Clair et al., 1986), or extracellular components (Alavi et al., 1991) of aorta were found to be increased for LP isolated from the sera of hypercholesterolemic animals. It is interesting to note that LDL are very heterogenous (Rudel et al., 1986), and different subclasses of LP were detected in normal human plasma (Krauss and Burke, 1982). The difference in the degree of affinity manifested by the extracellular or cellular elements for various subfractions of

LDL particles could be responsible for the heterogeneity of their atherosclerotic potential (Wagner et al., 1989; Hurt-Camejo et al., 1990).

REFERENCES

Alavi, M.Z., Galis, Z., Li, Z., and Moore, S. (1991). Dietary alterations of plasma lipoproteins influence their interactions with proteoglycan enriched extracts from neointima of normal and injured rabbit aorta. Clin Invest Med, 14:419-431.

Bendayan, M. (1984). Protein A-gold electron microscopic immunocytochemistry: Methods, applications and limitations. J Electron Microsc Tech, 1:243-270.

Bendayan, M. (1982). Double immunocytochemical labelling applying the protein A-gold technique. J Histochem Cytochem, 30:81-85.

Berenson, G.S., Radhakrishnamurthy, B., Srinivasan, S.R., Vijayagopal, P., and Dalferes, E.D. (1985). Proteoglycans and potential mechanisms related to atherosclerosis. Am NY Acad Sci, 454:69-78.

Bihary-Varga, M., Gergely, J., and Gero, S. (1964). Further investigations on complex formation in vitro between aortic mucopolysaccharides and ß-lipoproteins. J Atheroscl Res, 4:106-109.

Camejo, G., Hurt, E., Wilkund, O., Rosengren, B., Lopez, F., and Bondjers, G. (1991). Modifications of low-density lipoprotein induced by arterial proteoglycans and chondroitin-6-sulfate. Biochim Biophys Acta, 1096:253-261.

Camejo, G., Lopez, F., Vegas, H., and Paoli, H. (1975). The participation of aortic proteins in the formation of complexes between low density lipoproteins and the intima-media extracts. Atherosclerosis, 21:77-91.

Chao, F.F., Blanchette-Mackie, E.J., Chen, Y.J., Dickens, B.F., Berlin, E., Amende,

L.M., Skarlatos, S., Gamble, W., Resau, J.H., Mergner, W.T., and Kruth, H. S. (1990). Characterization of two unique cholesterol-rich lipid particles isolated from human atherosclerotic lesions. Am J Pathol, 136:169-176.

Falcone, D.J., Hajjar, D.P., and Minick, C.R. (1984). Lipoprotein and albumin accumulation in reendothelialized and deendothelialized aorta. Am J Pathol, 114:112-120.

Ghitescu, L., and Bendayan, M. (1990). Immunolabeling efficiency of protein A-gold complexes. J Histochem Cytochem, 38:1523-1530.

Guyton, J.R., and Klemp, K.F. (1989). The lipid-rich core region of human atherosclerotic fibrous plaques. Prevalence of small lipid droplets and vesicles by electron microscopy. Am J Pathol, 134:705-717.

Hoff, H.F., and Wagner, W.D. (1986). Plasma low density lipoprotein accumulation in aortas of hypercholesterolemic swine correlates with modifications in aortic glycosaminoglycan composition. Atherosclerosis, 61:231-236.

Hurt-Camejo, E., Camejo, G., Rosengren, B., Lopez, F., Wiklund, O., and Bondjers, G. (1990). Differential uptake of proteoglycan-selected subfractions of low density lipoprotein by human macrophages. J Lipid Res, 131:1387-1398.

Krauss, R., and Burke, D.J. (1982). Identification of multiple subclasses of plasma lipoproteins in the normal subjects. J Lipid Res, 23:97-104.

Iverius, P.H. (1972). The interaction between plasma lipoproteins and connective tissue glycosaminoglycans. J Biol Chem, 247:2607-2613.

Mora, R., Lupu, F., and Simionescu, N. (1989). Cytochemical localization of ß-lipoproteins and their components in successive stages of hyperlipidemic atherogenesis

of rabbit aorta. Atherosclerosis, 79:183-195.

Orekhov, A.N., Tertov, V.V., Mukhin, D.N., Koteliansky, V.E., Glukhova, M.A., Frid, M.G., Sukhova, G.K., Khashimov, K.A., and Smirnov, V.N. (1989). Insolubilization of low density lipoprotein induces cholesterol accumulation in cultured subendothelial cells of human aorta. Atherosclerosis, 79:59-70.

Rudel, L.L., Parks, J.S., Johnson, F.L., and Babiak, J. (1986). Low density lipoproteins in atherosclerosis. J Lipid Research, 27:465-474.

Salisbury, B.G., Falcone, D.J., and Minick, C.J. (1985). Insoluble LDL-proteoglycan complexes enhance cholestryl ester accumulation in macrophages. Am J Pathol, 120:6-11.

Smith, E.B., Evans, P.H., and Downham, D. (1967). Lipid in the aortic intima. The correlation of morphological and chemical characteristics. J Atheroscler Res, 7:171-186.

Srinivasan, S.R., Dolan, P., Radhakrishnamurthy, B., and Berenson, G.S. (1972). Isolation of lipoprotein-acid mucopolysaccharide complexes from fatty streaks of human aortas. Atherosclerosis, 16:95-104.

St. Clair, R.W., Randolph, R.K., Jokinen, M.P., Clarkson, T.B., and Barkat, H.A. (1986). Relationship of plasma lipoproteins and the monocyte-macrophage system to atherosclerosis severity in cholesterol-fed pigeons. Arteriosclerosis, 6:614-626.

Steele, R.H., Wagner, W.D., Rowe, H.A., and Edwards, I.J. (1987). Artery wall derived proteoglycan-plasma lipoprotein interaction: Lipoprotein binding properties of extracted proteoglycans. Atherosclerosis, 65:51-62.

Viajayagopal, P., Srinivasan, S.R., Radhakrishnamurthy, B., and Berenson, G.S. (1991). Studies on the mechanism of uptake of low density lipoprotein-proteoglycan complex in

macrophages. Biochim Biophys Acta, 1092:291-297.

Viajayagopal, P., Srinivasan, S.R., Jones, K.M., Radhakrishnamurthy, B., and Berenson, G.S. (1985). Complexes of low density lipoprotein and arterial proteoglycan aggregates promote cholesteryl ester accumulation in mouse macrophages. Biochim Biophys Acta, 837;251-261.

Wagner, W.D., Edwards, I.J., St. Clair, R.W., and Barkat, H. (1989). Low density lipoprotein interaction with artery derived proteoglycan: the influence of LDL particle size and the relation to atherosclerosis susceptibility. Atherosclerosis, 75:49-59.

Yla-Herttuala, S., Solakivi, T., Hirvonen, J., Laaksonen, H., Mottonen, M., Pesonen, E., Raekallio, J., Akerblom, H.K., and Nikkari, T. (1987). Glycosaminoglycans and apolipoproteins B and A-I in human aortas. Chemical and immunological analysis of lesion-free aortas from children and adults. Arteriosclerosis, 7:333-340.2

Young, S.G. (1989). Recent progress in understanding apolipoprotein B. Circulation, 82:1574-1594.

CHAPTER 8

OVERALL CONCLUSIONS

The interaction of apo B with the normal aorta is thought to hold a key to the development of the atherosclerotic lesions. Smith reported that, over the entire range of plasma LP concentrations assayed in human subjects, the LDL concentration found in the interstitial fluid of the normal human intima was twice as much as in the serum (Smith, 1990). The explanation proposed for this unexpectedly high intima/serum ratio, higher than for any other plasmatic protein, was that the internal elastic lamina selectively retains the LP which penetrate the aorta. The highest concentration of LDL was foreseen to develop between this barrier and the basement membrane of the endothelial cells.

Indeed, by morphometric analysis of the immunocytochemical detection of endogenous apo B in normal aorta, a relatively high density was found in the subendothelial space, but the highest concentration was measured over the endothelial layer itself. In order to explain these values and the numerous endothelial vesicles that contained apo B, it would be reasonable to suppose that the endogenous LP containing apo B cross actively, supposedly in both ways, this cellular layer. The elastic lamina might contribute to restrain the inward movement of LP, since no detectable amounts were found in the media. Nevertheless, several factors might contribute to determine the apo B distribution, since the confinement of the apo B distribution around the blood vessels of the vasa vasorum, also permeable to apo B and lacking a visible restrictive layer, was noticed.

In the injured aortas, although the distribution varied according to the morphological characteristics of the region, some consistent relations were found. The high values of apo B in the intima were associated with the presence of an endothelial layer. The role of the endothelium in this process could be much more complex, but the following seem very likely. The endothelium could regulate the quantity of the LP containing apo B inside the aortic wall, by both actively bringing them inside, and by restricting their free backward flow into the lumen, that seems to occur in the regions lacking an endothelial layer. In addition, during the passage through the endothelium, this

could modify the LP, rendering them less recognizable for the reverse transport into the lumen of the aorta or/and more susceptible to become involved in interactions with the aortic wall environment, which could be also altered in pathologic conditions. There are several candidates for this sequestration effect, such as the fibrinogen/fibrin degradation products, elastin (Smith, 1991), collagen (Hoover et al., 1988), and the PG. From the results obtained in the experiments described earlier in this thesis, we suggest that the following aspects regarding the aortic CS-PG might be significant in direct relation with the apo B accumulations in injured aorta.

In the normal rabbit aorta, three main types of CS-PG were distinguished by ultrastructural immunocytochemistry, of which two were associated with the collagen fibrils. The CS-PG, which were not found in the company of other extracellular matrix components, seemed capable of forming extensive molecular networks by homophyllic associations only in the intima. The significant differences found between the inner and the outer layer of aorta regarding the type, the size, and the molecular associations of CS-PG, most likely participate in creating differences in the structure and properties of the extracellular matrix in different areas of the aorta. The many implications of the relation between the matrix and the cells embedded in it, have already been discussed in the previous chapters. The characteristic composition and organization of the extracellular PG would likely influence the local properties of the blood vessel itself, such as vascular permeability, tensile strength, and elasticity. The CS sulfate lattices have the capacity to resist water flow (Comper, 1990), a property which could determine the restriction of macromolecular movement in interstitial spaces rich in CS. In contrast, the presence of CS moieties enhance the cellular migration through collagen gels. The combination of these two properties appears relevant in atherogenesis, where LP particles accumulate, while cells are thought to migrate from media through the aortic intima, which was found to be preferentially endowed with CS-PG.

In the injured aortas, variations of the normal morphological and biochemical properties of the sulfated PG were found. The wide extracellular spaces of the neointima covered by a regenerated endothelium were occupied by large associations of interstitial CS-PG. The interstitial space of the intimal thickening in the regions that remained

deendothelialized, was crowded instead with collagen and other fibrous structures, while the CS-PG were very scarce and were mostly collagen-associated CS-PG. The large intimal CS-PG type is likely synthesized by SMC, and maybe also by EC, but at any rate the presence of endothelium appeared to be crucial. We would interpret these observations as another expression of the complex interaction that takes place in aortic intima between the endothelium and the SMC. Depending on their own state, the EC produce in vitro either growth stimulatory, or inhibitory factors which modulate the SMC phenotype, and both the GAG synthesis and the uptake of ß-VLDL were increased in vitro by incubation of SMC with EC-conditioned culture medium (Campbell et al., 1990). The endothelium could also control the type of PG synthesized in situ by SMC. In addition, the presence of the endothelium might restrict the release of PG molecules into the blood stream, contributing to the difference between the CS distribution in the areas persistently deendothelialized or covered by regenerated endothelium (Alavi and Moore, 1985).

It might be significant that we could recognize by EM immunocytochemistry that rather deep inside the thickened intima of the persistently deendothelialized areas, not far above the internal elastic lamina, patches of the interstitial CS-PG were present, and they usually contained some lipid. It was concluded that these CS-PG represented remnants of the initial intimal extracellular matrix over which the SMC have proliferated and produced their new extracellular matrix. The observation was considered important because it provided a reasonable explanation for the reversed pattern of apo B distribution in the extracellular space of the deendothelialized regions, where the deep interstitial space was more densely labelled than the inner space of the myointimal thickening. In the regions where the endothelium was regenerated, the large confluent CS-PG networks were also re-created in the inner areas. Their presence in the injured aortas was associated with the extracellular and intracellular accumulation of apo B. Although it is not yet clear why the LP do not become trapped in normal conditions, one might speculate that the biochemical properties of the partners involved in the interaction might be altered in the injured aortas. For instance, we found biochemical and ultrastructural evidence that the injured aortas produced PG with longer GAG chains. These are liable to change the

structure of individual PG molecules and implicitly their individual biochemical properties, but may also affect the characteristics of the supramolecular sieve formed in the extracellular space of the neointima. There are therefore reasons to believe that the apo B-containing LP become trapped mainly in the extensive extracellular CS-PG meshworks, since little lipid was found in the intercellular areas occupied with collagen or other components of the extracellular matrix. Although these regions appeared satiated with an intricate extracellular matrix, and contained many CS moieties of the collagen-associated PG, they did not seem to sequester significant quantities of LP. A possible explanation for these observed differences, that would still fit the hypothesis that the CS moiety is crucial in the interaction with the apo B molecule, is that these PG are more sparsely distributed and tightly bound to collagen, being allowed only a restricted interaction with apo B. Meanwhile, in the soluble extracellular matrix the LP particles could drag isolated CS-PG, until their movement is completely restrained, and/or become stuck in the dense networks, which might be less penetrable and have a higher negative charge density than the collagen bundles.

An important physicochemical property of concentrated solutions of polysaccharides is that they amplify the electrostatic interactions with the positive groups of other proteins because the concentration of the typical inhibitors, i.e. ionic electrolytes such as NaCl, is lowered in their presence (Comper, 1990). By reducing the quantity of the competing counterions and/or by shielding the positive charges of the LP particles, the presence of extracellular CS-PG could conceivably abolish their mutual repulsion, cram them together in restricted spaces, contribute to their accumulation, and probably their coalescence with formation of larger lipid droplets. Therefore, contributing to the development of atherosclerotic lesions, may be, not only the individual properties of the molecules, known to interact in vitro with the LP, but also their typical in vivo supramolecular organization and distribution in the aortic wall.

In the advanced lesions, another visible location of the CS-PG was inside the lipid-laden cells, many of which were recognized as SMC, and in those presumed to be macrophages and neutrophils. The closeness between the intracellular lipid inclusions and the numerous CS-filled vacuoles, as well as the detection of apo B and CS colocalized

inside the same lysosomes, showed that both were avidly taken up by these cells, and suggested that their uptake might be related. It has been previously shown that the in vitro complexing of LP with aortic PG induces the formation of foam cells. The mechanism is still not clear, but in macrophages it appears to rely on a new protein G-coupled receptor for modified LP (Vijayagopal, 1991). It remains to be demonstrated if a similar receptor is expressed by the SMC, detected in the present study to be loaded in situ with apo B and CS-PG, in the lesions of the injured aortas. An interesting observation was that the SMC displaying the synthetic phenotype, in contrast with the SMC of the normal intima, often had the plasma membrane decorated by a CS-positive rim, which could have been contributed by proteins either spanning, or closely associated with their plasma membrane. It is currently known that growth factor receptors and receptors for the extracellular matrix contain CS chains, and the presence of CS has also recently been associated with the processes of cellular adhesion and motility. At this point it would be difficult to asses the role of the pericellular CS detected in the SMC of the neointima, but it could be speculated that they might be related to the phenotypic modulation of the SMC and could have implications for the properties and functions of SMC in the vascular lesions.

As stated by Munro and Cotran (1988), any theory regarding atherogenesis must provide a reasonable justification for the proliferation of SMC, the presence of the lipid in most lesions, the typical location of the atherosclerotic lesions, and the impact of risk factors. The aortic wall healing, triggered by an experimental mechanical injury to the endothelium, determines the appearance of vascular lesions, which contain the same elements as human atherosclerotic lesions. The lipid, demonstrated to originate from the circulating endogenous LP, was caused to accumulate in the extracellular space and inside cells of injured aortas, in conditions of normal levels of plasma cholesterol. The CS-PG seemed to be directly involved in these processes due to their relation with cell migration, proliferation, and interaction with apo B-containing LP. The typical location of the aortic atherosclerotic lesions was very well correlated with the presence of the regenerated endothelium and with the preferential distribution of CS-PG within the aortic intima.

The hypercholesterolemia was found to produce endothelial dysfunction (Pritchard

et al., 1991), to increase the affinity of aortic PG extracted from injured aortas for plasma LP (Alavi et al., 1991), and to exacerbate the effect of endothelial injury (Minick et al., 1979). Age, hypertension, and hemodynamic factors alter the properties of the endothelium (Huttner et al., 1982), and increase the sulfated PG content of the aorta (Richardson et al., 1988).

These observations suggest that endothelial injury, which does not necessarily have to be overtly expressed (Gimbrone, 1986; Ryan, 1986), can independently determine the initiation of atherosclerotic lesions, and the sulfated PG of the arterial wall play an important part in this process.

REFERENCES

Alavi, M.Z., Galis, Z., Li, Z., and Moore, S. (1991). Dietary alterations of plasma lipoproteins influence their interactions with proteoglycan enriched extracts from neointima of normal and injured rabbit aorta. Clin Invest Med, 14:419-431.

Alavi, M.Z., and Moore, S. (1985). Glycosaminoglycan composition and biosynthesis in the endothelium-covered neointima of de-endothelialized rabbit aorta. Exp Mol Pathol, 42:389-400.

Comper, W.D. (1990). Extracellular matrix interactions: Sulfation of connective tissue polysaccharides creates macroion binding templates and conditions for dissipative structure formation. J Theor Biol, 145:497-509.

Campbell, J.H., Horrigan, S., Merrilees, M., Campbell, G.R. (1990). Endothelial-smooth muscle cell interactions. In: Interactions between endothelium and other vascular structures and their abnormalities in diabetes. Molinati,G.M., Bar, R.S., Belfiore, F., and Porta, M. (eds.). Endothelial cell function in diabetic microangiopathy: Problems in methodology and clinical aspects. Front Diabetes, Basel, Karger, 9, pp 108-117.

Gimbrone, M.A. Jr. (1986). Endothelial dysfunction and the pathogenesis of atherosclerosis. In: Fidge, N.H., and Nestel, P.J. (eds), Atherosclerosis VII, Elsevier, Amsterdam, pp.367-369.

Huttner, I., Costabella, P.M., De Chastonay, C., and Gabbiani, G. (1982). Volume, surface, and junctions of rat aortic endothelium during experimental hypertension: a morphometric and freeze fracture study. Lab Invest, 46:489-504.

Hoover, G.A., Mc Cormick, S., and Kalant, N. (1988). Interaction of native and cell-modified low density lipoprotein with collagen gel. Arteriosclerosis, 8:525-534.

Mininck, C.R., Stemerman, M.B., and Insull, W. (1979). A role of endothelium and hypercholesterolemia in intimal thickening and lipid accumulation. Am J Pathol, 95:1131-1158.

Munro, M., and Cotran, R. (1988). The pathogenesis of atherosclerosis: Atherogenesis and inflammation. Lab Invest, 58:249-261.

Pritchard Jr., K.A., Tota, R.R., Lin, J.H.C., Danishefsky, K.J., Kurilla, B.A., Holland, J.A., and Stemerman, M.B. (1991). Native low density lipoprotein. Endothelial cell recruitment of mononuclear cells. Arteriosclerosis and Thrombosis, 11:1175-1181.

Richardson, M., Hatton, M.W.C., and Moore, S. Proteoglycan distribution in the intima and media of the aortas of young and aging rabbits: an ultrastructural study. Atherosclerosis., 71:243-256.

Ryan, U. (1986). The endothelial surface and responses to injury. Fed Proc, 45:101-108.

Smith, E.B. (1990). Transport, interactions and retention of plasma proteins in the intima: the barrier function of the internal elastic lamina. Eur Heart J, 11 (suppl):72-81.

Vijayagopal, P., Srinivasan, S.R., Radhakrisnamurthy, B., and Berenson, G.S. (1991). Studies on the mechanism of uptake of low density lipoprotein-proteoglycan complex in macrophages. Biochim Biophys Acta, 1092:291-297.